

# IN-LAKE NUTRIENT PROCESSING IN TE WAIHORA/LAKE ELLESMERE

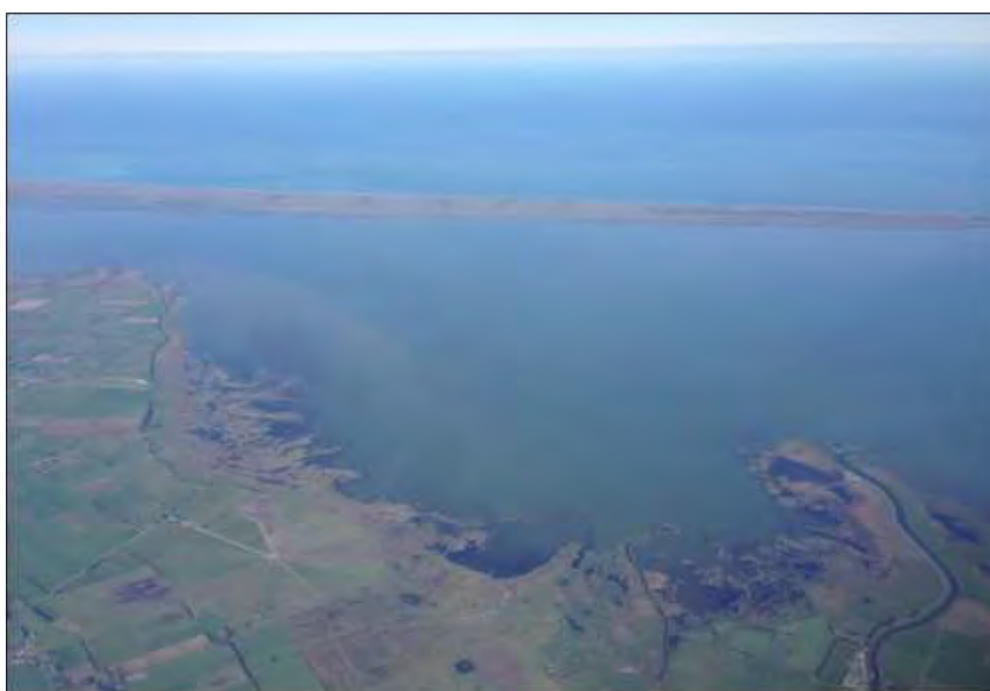
---

Prepared by: Marc Schallenberg<sup>1</sup> and Josie Crawshaw<sup>2</sup>

For: Environment Canterbury and Whakaora Te Waihora

<sup>1</sup> *Department of Zoology, University of Otago, Dunedin*

<sup>2</sup> *Department of Marine Science, University of Otago, Dunedin*



*Looking south over Te Waihora/Lake Ellesmere, showing Kaitorete Spit in the distance, the Selwyn River/Waikirikiri estuary to the right, the Aririra/L2 estuary on the centre right, and the Greenpark Sands to the left.*

----- July 2017 -----

# EXECUTIVE SUMMARY

---

Te Waihora/Lake Ellesmere is one of the most eutrophic lakes in New Zealand. Our study undertook to determine the extent to which in-lake nutrient processing could mitigate or contribute to the nitrogen and phosphorus availability to phytoplankton in the lake.

We examined how nutrient dynamics in the lake related to the timing of phytoplankton blooms as recorded in ECAN's water quality monitoring dataset. Phytoplankton blooms occurred mostly in spring and summer and were irregular, occasionally lasting more than 1 year. Sudden increases in dissolved reactive phosphorus, nitrate and ammonium concentrations often preceded the blooms and these nutrients were sometimes depleted from the water column during the blooms. The analysis confirmed the findings of other studies indicating that nitrogen and phosphorus availability is related to phytoplankton growth and biomass in the lake.

We undertook a variety of studies to understand oxygen dynamics in the lake because oxygen concentrations, particularly near the sediment-water interface, can influence the processes of denitrification and internal phosphorus release from the lake bed.

We observed transient periods of anoxic bottom waters at the mid-lake site, but only during summer and autumn. Sediment oxygen demand was greater at the deeper sites where sediments were finer in texture and had higher porosity and organic matter content. Oxygen penetration depths in the sediment were highly variable, even within study sites, and this was mostly attributable to the effects of burrowing infauna, which facilitate the irrigation of the sediments. Based on our analysis, sediment organic matter concentration, grain size, depth and infauna density all affected the oxygenation of the lake bed and potentially influenced biogeochemical processing of nutrients in the lake.

Although we weren't able to measure direct phosphorus release from *in situ* sediments, we measured the amounts of redox-exchangeable P in the sediments at 18 sites. In addition, we chemically extracted different fractions of P from the sediments at these sites. Sediment at most sites released P into porewaters under anoxic conditions. It appeared that the iron- and manganese-bound fractions of P

were the main fractions that released bound P under anoxic conditions. However, other fractions may also be important at certain sites and the supply of P via the mineralisation of organic matter by microbes is also likely to be important in supplying P for release to the water column. We also found that most sediments released small amounts of N under anoxic conditions. Our oxygen studies indicated that anoxic releases of P and N are most likely to occur in summer and autumn, when external loading to the lake of these nutrients is low and the ambient concentrations of these nutrients in the water column of the lake may be low enough to limit the growth of phytoplankton. Thus, the internal loads, while relatively small, have the potential to be important in supplying phytoplankton with available forms of N and P during times when external inputs of nutrients to the lake are limited.

The extremely high external loads of nitrate to the lake have the potential to be converted to inert nitrogen gas via denitrification – a microbial ecosystem service that could remove substantial amounts of N from the system. We measured rates of denitrification in sediment samples from 18 sites, in the laboratory after additions of both nitrate and glucose (optimal conditions). We also designed and deployed customised enclosures for *in situ* measurements of denitrification, which we deployed in different seasons at a subset of sites.

Both sets of measurements showed that the denitrification rate in the lake sediments was highly variable, both spatially and temporally. We were unable to measure *in situ* nitrate conversion during winter, indicating that cold winter temperatures inhibited the microbial conversion of nitrate to N<sub>2</sub>. This inhibition occurs at a time when nitrate loads to the lake are greatest, indicating that external nitrate input and in-lake denitrification are temporally decoupled. Sites with the highest rates of denitrification were on the northern and eastern margins of the lake. The availability of carbon sources (organic matter) stimulated the conversion of nitrate to N<sub>2</sub>, as did the addition of glucose in the laboratory experiments, showing that the availability of labile carbon in the sediments influences denitrification rates.

Large episodic inputs of nitrate from the tributaries to the lake occur in winter. We studied the fate of similar pulses of nitrate to our enclosures. The nitrate added to

enclosures was rapidly taken up by phytoplankton, indicating that direct inputs of nitrate are mostly unavailable for denitrification. Measured rates of nitrate conversion to N<sub>2</sub> gas in summer were consistent with rates of denitrification reported in other aquatic ecosystems. Most of the nitrate was depleted from the enclosures over the 48 h experiments, however, high rates of uptake by phytoplankton resulted in the conversion of only around 10% (on average) of the nitrate added to the enclosures to N<sub>2</sub>. Unfortunately, we were unable to measure the long-term cycling of organic N (e.g., nitrate taken up by phytoplankton) and this pool of N may also contribute to denitrification in the lake after the senescence and settling of phytoplankton cells to the lake bed. Further study would be required to quantify all possible pathways of denitrification in the lake.

This research demonstrates that internal nutrient loading and denitrification contribute to nutrient processing and cycling in Te Waihora/Lake Ellesmere and thereby influence nutrient availability to phytoplankton. The findings of this report contribute to an updating of the Te Waihora/Lake Ellesmere dynamic ecological model (Norton *et al.* 2014; Dada *et al.* 2016), which is being used to test future land use and climate change scenarios for the lake. Our findings also support many of the pathways and actions outlined by the Selwyn Waihora Zone Committee. Actions in the catchment to reduce nitrogen, phosphorus and fine sediment losses to the lake are likely to reduce nitrogen and phosphorus availability to phytoplankton in the lake both by reducing the external loads but also by reducing nutrient availability due to in-lake processing. All four lake interventions of interest to the Selwyn Waihora Zone Committee (water level management, phosphorus legacy management, restoration of macrophytes and wetland development) are also likely to affect in-lake nutrient processes in ways which will reduce nutrient (re)cycling and availability to phytoplankton. Te Waihora/Lake Ellesmere is one of the most eutrophic lakes in New Zealand and while in-lake interventions to reduce nutrient availability to phytoplankton are likely to provide some benefits, returning the lake back to a condition where improved water clarity supports both macrophyte beds and more diverse aquatic communities ultimately depends on successful reduction of the external nutrient loads to the lake.

# CONTENTS

---

Executive Summary .....	2
Contents .....	5
List of Figures.....	7
List of Tables .....	10
Acknowledgements .....	12
1 Introduction.....	13
A flipped lake and the role of ecological feedbacks.....	13
Internal nutrient cycling .....	15
Analysis of phytoplankton blooms in Te Waihora.....	16
2 Spatial variation in sediment characteristics in Te Waihora/Lake Ellesmere .....	21
Introduction.....	22
Methods .....	23
Findings .....	26
Conclusions.....	39
3 Sediment oxygen dynamics in Te Waihora/Lake Ellesmere.....	40
Introduction.....	41
Methods .....	43
Findings .....	47
Conclusions.....	70
4 Sediment Nutrient Pools and Fluxes Under Conditions of Anoxia.....	71
Introduction.....	72
Methods .....	74
Findings .....	77
Discussion and Conclusions.....	85
5 Denitrification in the sediments of Lake Ellesmere/Te Waihora .....	88
Introduction.....	89
Methods .....	92
Findings .....	95
Discussion and conclusions .....	117
6 Summary of N and P dynamics in Te Waihora/Lake Ellesmere and relevance for management .	120
The relationship between nutrient and phytoplankton dynamics .....	121
The role of denitrification in nitrogen cycling .....	124
The potential for internal P loading .....	128
Relevance of findings for management .....	131

References.....	134
7 Appendix A: Spatial sediment survey.....	145
Site GPS Locations .....	145
Site sediment characteristics .....	145
Site physico-chemical conditions .....	149
8 Appendix B: Oxygen dynamics .....	150
Oxygen profiles summer 2015 .....	150
Oxygen profiles winter 2015 .....	152
Oxygen profiles summer 2016 .....	154
9 Appendix C: Denitrification .....	157
Long-term nitrate pulse analysis .....	157
Methods .....	160
In situ nitrate conversion experiment – Supplemental data.....	166

# LIST OF FIGURES

---

Figure 1.1. The theoretical pathways of degradation and restoration in a lake ecosystem dominated by internal ecological feedback mechanisms and by non-linear responses to pressures. X indicates the approximate position of Te Waihora/Lake Ellesmere in this scheme. The difference between the two tipping points shows the effects of different feedbacks operating to stabilise the lake in either of its two stable states. Adapted from Scheffer (2004). .....	14
Figure 1.2. Environment Canterbury’s chlorophyll a data from 1992 to 2013, with periods of phytoplankton blooms identified. Vertical shaded bars indicate winter seasons. ....	16
Figure 2.1. Location of the 18 sampling sites and the main inflow tributaries.....	23
Figure 2.2. Water depths (m) at the 18 sites in April 2013 (A) and April 2014 (B).....	26
Figure 2.3. Maps of sediment grain size at the 18 sites, in April 2013 (A = clay %, C = silt %, E = sand %) and April 2014 (B = clay %, D = silt %, F = sand %). ....	28
Figure 2.4. The relationship between sediment grain size fractions (sand, silt, clay %) and sediment porosity. 2014 survey data. ....	29
Figure 2.5. Maps of sediment characteristics measured in April 2013 (A = porosity ( $\text{kg m}^{-2}$ ), C = redox potential (mV), E = organic matter ( $\text{kg m}^{-2}$ )) and April 2014 (B = Porosity ( $\text{kg m}^{-2}$ ), D = Redox potential (mV), F = organic matter ( $\text{kg m}^{-2}$ )). ....	33
Figure 2.6. Principal component analysis showing correlations among variables and the distribution of the sites in relation to the two main gradients in sediment characteristics.....	33
Figure 2.7. Empty chironomid tubes remaining long after inhabitation in a sediment core. No chironomids were found in the core which was collected in April 2014, after a prolonged period of high salinity affected the lake. ....	34
Figure 3.1. Ecosystem engineering by sediment infauna, influencing benthic nitrogen cycling in aquatic ecosystems by deepening the zone of oxygen penetration into the sediment (modified from Stief (2013)). ....	42
Figure 3.2. Range of sediment dissolved oxygen ( $\text{mg L}^{-1}$ ) depletion rates at the sites and oxygen depletion in lake water. Sediment samples were 1 mL of sediment diluted in 300 mL of sterile water. Site E13 had the lowest rate, E3 had the median rate and E2 had the maximum rate of depletion in the lake. The experiment was run near the in situ temperature at the time of sampling ( $12^\circ\text{C}$ ). ....	47
Figure 3.3. Sediment biological and chemical oxygen demand ( $\text{mg O}_2 \text{mL}^{-1} \text{h}^{-1}$ at $12^\circ\text{C}$ ) at the 18 sites, ranked from lowest to highest total oxygen demand.....	48
Figure 3.4. Ordination diagram of a principal components analysis on the correlation matrix of sediment variables from 18 sites in Te Waihora/Lake Ellesmere. See Table 3.2 for definitions of variable names. Circles and numbers represent sites.....	50
Figure 3.5. Temperature, dissolved oxygen ( $\text{mg L}^{-1}$ ) and salinity (ppt) dynamics at the mid-lake site from June 2015 to June 2016. The blue line is data from 30 cm below the lake surface. The red line is data from 50 cm above the lake bed. The green line is salinity (interrupted due to sensor malfunction). ....	51
Figure 3.6. Number of severe oxygen depletion events over the measurement period at the mid-lake site. Data are shown both as the number of events as well as the number of days during which such events occurred.....	52
Figure 3.7. The maximum durations of deoxygenation events of various severities and the total percentage of time events of various severities were recorded over the study period.....	53
Figure 3.8. Temperature, dissolved oxygen ( $\text{mg L}^{-1}$ ) and salinity (ppt) dynamics at the Taumutu site measured from June 2015 to June 2016. The blue line is data from 30 cm below the lake surface. The red line is data from 50 cm above the lake bed. The green line is salinity. ....	55

Figure 3.9. Frequency plot showing the % frequency distributions of all the wind data (15 minute intervals) from the mid lake site as well as the frequency distributions for winds recorded at the times of oxygen depletion events of various severities. Data cover the study period (se Fig. 3.5 and Fig. 3.8). ..... 56

Figure 3.10. Sediment oxygen penetration depth measured by oxygen micro-sensors across multiple sites and seasons. Error bars are standard errors. The lack of a bar means DO penetration depth was not measured at that site during that season..... 57

Figure 3.11. The effect of sediment porosity on oxygen penetration depth (mm) at the time of the three sampling campaigns..... 58

Figure 3.12. Relationships between oxygen penetration depth (mm) and the density of oligochaetes in winter and summer 2015. .... 64

Figure 3.13. The effect of benthic infauna burrows on sediment oxygen microprofiles. A = oxygen profiles unaffected by bioturbation, B = two oxygen profiles unaffected by bioturbation, while profile replicate B crossed through an infaunal burrow increasing oxygen penetration in the deeper sediment layers. .... 65

Figure 3.14. A schematic diagram of the effects of temperature on dissolved oxygen concentration and denitrification. Taken from (Veraart et al. 2011). + and – indicate the direction and strength of relationships. .... 66

Figure 3.15. Principal components analysis showing correlations among variables in summer 2015. Clay, Silt and Sand indicate the percentage composition of sediment particles in the indicated size classes. OM indicates sediment organic matter concentration ( $\text{mg m}^{-2}$ ). P. ant indicates the density of the snail, *Potamopyrgus antipodarum*. P. exc indicates the density of the amphipod, *Paracorophium excavatum*. Oligo indicates the density of oligochaetes. Diff O2 indicates the oxygen penetration depth. Codes and circles refer to sites and replicates (replicate a, b or c). .... 67

Figure 3.16. Principal components analysis showing correlations among variables in winter 2015. See Fig. 3.15 for explanation of symbols and labels. Axes 1 and 2 explained 63% and 19% of the total variation in the data, respectively..... 68

Figure 3.17. Principal components analysis showing correlations among variables in summer 2016. Nereidae indicates the density of polychaetes. Chiro indicates chironomid density. Oligo indicates oligochaete density. Redox indicates sediment redox potential. See Fig. 3.15 for explanation of other labels and symbols. .... 69

Figure 4.1. Correlation between metal oxyhydroxide-bound P ( $\text{mg m}^{-2}$ ) and redox-exchangeable P ( $\text{mg m}^{-2}$ ).  $r = 0.48$ ,  $N = 16$ ,  $P = 0.078$ . The blue line is the 1:1 line. .... 80

Figure 4.2. Map of sediment redox-exchangeable P expressed as a daily rate of release ( $\text{mg m}^{-2} \text{d}^{-1}$ ).. 80

Figure 4.3. Map of sediment metal oxyhydroxide-bound P concentration ( $\text{mg m}^{-2}$ ). .... 81

Figure 4.4. Sediment P geochemistry by site. Redox-exchangeable P is expressed as a release rate in  $\text{mg P m}^{-2} \text{d}^{-1}$ . P concentration is in  $\text{mg m}^{-2}$ . In panel A, data for site E8 was unavailable and in panels B to D, data for site E17 were unavailable. .... 82

Figure 4.5. Daily N release rates from anoxic sediments ( $\text{mg N m}^{-2} \text{d}^{-1}$ ), measured over 36 h incubations. .... 85

Figure 4.6. Map of anoxic N release rates calculated over 36 h incubations ( $\text{mg m}^{-2} \text{d}^{-1}$ ). .... 85

Figure 5.1. Mid-lake nitrate concentrations from 1993-2013. ECAN data..... 90

Figure 5.2. Study sites. Blue circles indicate the sites of in situ denitrification measurements. .... 92

Figure 5.3. In situ core enclosure deployed in the lake bed. A = bottom section of core structure pushed into the sediment, with flexible polyethylene tubing running up to rigid cylinders at top, B = lids at the top of the enclosures, showing the sampling ports. \*Note photos are taken from setup in Tomahawk Lagoon (Dunedin), as the underwater visibility was too poor in Te Waihora/Lake Ellesmere to photograph the deployed cores..... 93



Figure 5.4. Spatial contour plots showing the denitrification potential in different treatments. (A) nitrate amended. (B) carbon and nitrate amended and (C) the effect of carbon addition (+C+N response minus +N response). The data were collected in April 2014. .... 95

Figure 5.5. Seasonal denitrification rates ( $\mu\text{mol N m}^{-2} \text{ h}^{-1}$ ) measured in Lake Ellesmere across three sites in three different seasons. Summer 2016 rates were not measured at site 5 due to rough lake conditions. Each circle indicates a rate measurement for each core. .... 99

Figure 5.6. Nitrate conversion rates ( $\mu\text{mol N m}^{-2} \text{ h}^{-1}$ ) across seven sites in the summer seasons (March 2015 and January 2016). Each circle indicates the rate for a core. Note the break in the y-axis. .... 100

Figure 5.7. Time series of  $\text{N}_2$  produced ( $\mu\text{mol N L}^{-1}$ ) in three sets of enclosures in summer 2015 (March). Error bars show the standard error for each of the 4 replicates at each site. .... 103

Figure 5.8. Nitrate concentrations measured in enclosures over time in summer 2015 (March) (A), winter 2015 (Aug) (B), and summer 2016 (Jan) (C). Standard errors are shown. .... 104

Figure 5.9. Nitrogen dynamics during the enclosure experiments at site 19 in summer 2016. A -  $^{29}\text{N}_2$  gas production ( $\mu\text{mol L}^{-1}$ ). B - Ammonium concentrations. C – Nitrate concentrations. Dark shading indicates night; no shading indicates daylight hours. .... 107

Figure 5.10. The sediment grain size fractions - sand (63-2000  $\mu\text{m}$ ), silt (2-63  $\mu\text{m}$ ) and clay (0-2  $\mu\text{m}$ ). Data is from the enclosure cores in summer 2016, with the exception of site 5 which was measured in summer 2015. .... 108

Figure 5.11. Densities of the three most abundant infauna species (individuals  $\text{m}^{-2}$ ) collected from the enclosure cores. A = the mud snail *Potamopyrgus antipodarum*, B = the amphipod *Paracorophium excavatum*, and C = the annelid worm family, *Oligochaeta*. Standard errors are shown. 'n' indicates the invertebrates were not found at that time. .... 111

Figure 5.12. A sediment sample from Te Waihora/Lake Ellesmere showing oxidised zones around chironomid burrows. .... 112

Figure 5.13. Scatter plots comparing the different denitrification measurements: +N = DEA nitrate amended, +C+N = DEA carbon and nitrate amended, S15 = summer in situ 2015 nitrate conversion rate, S16 = summer in situ 2016 nitrate conversion rate. .... 113

Figure 7.1. Spatial patterns of surface salinity (A), surface temperature (B), total nitrogen (C), total phosphorus (D), dissolved  $\text{NO}_2^- + \text{NO}_3^-$  (E), dissolved reactive phosphorus (F), and  $\text{NH}_3$  (G), across the 18 sites in Lake Ellesmere in April 2014. .... 149

Figure 8.1. Sediment oxygen microprofiles measured at site E5 in summer 2015. .... 150

Figure 8.2. Sediment oxygen micro-profiles measured at site E2 in summer 2015. .... 150

Figure 8.3. Sediment oxygen micro-profiles measured at site E6 in summer 2015. .... 151

Figure 8.4. Sediment oxygen micro-profiles measured at site E6 in winter 2015. .... 152

Figure 8.5. Sediment oxygen micro-profiles measured at site E2 in winter 2015. .... 152

Figure 8.6. Sediment oxygen micro-profiles measured at site E5 in winter 2015. .... 153

Figure 8.7. Sediment oxygen micro-profiles measured at site E1 in summer 2016. .... 154

Figure 8.8. Sediment oxygen micro-profiles measured at site E3 in summer 2016. .... 154

Figure 8.9. Sediment oxygen micro-profiles measured at site E2 in summer 2016. .... 155

Figure 8.10. Sediment oxygen micro-profiles measured at site E6 in summer 2016. .... 155

Figure 8.11. Sediment oxygen micro-profiles measured at site E14 in summer 2016. .... 156

Figure 8.12. Sediment oxygen micro-profiles measured at site E19 (Hart's Creek estuary) in summer 2016. .... 156

Figure 9.1. Frequency of nitrate concentration pulses ( $\text{mg L}^{-1}$ ) from measurements taken between 1993 and 2013. Data is split into measurements taken at the two sites, mid-lake and at the mouth of the Selwyn River. .... 157

Figure 9.2. Long-term nitrate concentration data (mg L<sup>-1</sup>) taken at the ECAN mid-lake site and at the Selwyn River mouth. Black dotted line indicates 0.3 mg L<sup>-1</sup> marking the spike definition. Black circles show the maximum peak within the seasonal sustained high concentrations ..... 159

## LIST OF TABLES

---

Table 1.1.1. Factors correlated with bloom formation and collapse in Te Waihora/Lake Ellesmere. Data analysed were supplied by ECAN. The pre-bloom period examined was 30 days. NH <sub>4</sub> – ammonium. NO <sub>3</sub> – nitrate, DRP – dissolved reactive phosphorus. Turbidity/Salinity indicates whether these factors appeared to be related to the bloom. A question mark indicates that uncertainty exists about the connection to the blooms.....	18
Table 1.1.2. Times that available nutrients were correlated with phytoplankton blooms in Te Waihora out of 14 identified blooms (see Table 1.1). .....	19
Table 2.1. Pearson correlation analysis of variation in the sediment variables between the two years (2013 and 2014). *** = p<0.001, ** = p<0.01, * = p<0.05.....	29
Table 2.2. Pearson correlation matrix showing pairwise relationships among the 2013 sediment variables. *** = p<0.001, ** = p<0.01, * = p<0.05.....	31
Table 2.3. Pearson correlation matrix showing pairwise relationships among the 2014 sediment variables. *** = p<0.001, ** = p<0.01, * = p<0.05.....	31
Table 3.1. Total (TOD), chemical (COD) and biological (BOD) oxygen demand at 18 sites and in the water column of Te Waihora/Lake Ellesmere. Rates for sediment are in mg O <sub>2</sub> mL <sup>-1</sup> h <sup>-1</sup> . Rates for the lake water are mg O <sub>2</sub> L <sup>-1</sup> h <sup>-1</sup> . *rate is for whole lake water. ....	48
Table 3.2. Pearson correlation matrix focusing on the relationships between total sediment oxygen demand (TOD), biological oxygen demand (BOD) and chemical oxygen demand (COD) and other sediment characteristics. Bolded correlation coefficients are statistically significant (P < 0.05). .....	49
Table 3.3. Sediment characteristics in the cores in which oxygen penetration depth was measured, showing site averages and standard errors across sampling campaigns. NA indicates variables were not recorded. ....	59
Table 3.4. Pearson correlation matrix for data collected in summer 2016 in cores in which oxygen penetration depth (Diff O <sub>2</sub> ) was measured. *** = p<0.001, ** = p<0.01, * = p<0.05. P.ant – density of <i>Potamopyrgus antipodarum</i> ; P.exc – density of <i>Paracarophium excavatum</i> ; Olig – density of oligochaetes; Chiro – density of chironomids; Neridae – density of Nereidae.....	61
Table 3.5. Pearson correlation matrix for data collected in summer 2015 in cores in which oxygen penetration depth (Diff O <sub>2</sub> ) was measured. *** = p<0.001, ** = p<0.01, * = p<0.05. P.ant – density of <i>Potamopyrgus antipodarum</i> ; P.exc – density of <i>Paracarophium excavatum</i> . ....	62
Table 3.6. Pearson correlation matrix for data collected in winter 2015 in cores in which oxygen penetration depth (Diff O <sub>2</sub> ) was measured. *** = p<0.001, ** = p<0.01, * = p<0.05. P.ant – density of <i>Potamopyrgus antipodarum</i> ; P.exc – density of <i>Paracarophium excavatum</i> . ....	63
Table 4.1. Solvents and inferred P fractions extracted according to the modified (Psenner et al. 1988) protocol. ....	75
Table 4.2. Sediment P geochemistry at the 18 sites. REP rate is the daily rate of dissolution of redox-exchangeable P and REP is the total extracted redox-exchangeable P, calculated from 36 h incubations. DLB is the dissolved and loosely-bound fraction. MOB is the metal oxyhydroxide-bound fraction. AB is the aluminium-bound fraction. OB is the organic fraction. CB is the calcium-bound fraction.....	78
Table 4.3. Pearson correlation coefficients between fractions of P (measured by sequential extraction) and redox-exchangeable P (the difference in pore water P concentration between anoxic and oxic	

sediments). The cumulative P fractions begin with loosely-bound + dissolved P and add each fraction until all fractions have been summed. .... 79

Table 4.4. Anoxic N releases and release rates calculated from 36 h incubations. .... 84

Table 5.1. Pearson’s correlation matrix showing the relationships between the denitrification potential measured in Ellesmere summer 2014, and the associated sedimentary variables. \* =  $p < 0.05$ , \*\* =  $p < 0.01$ , \*\*\* =  $p < 0.001$ . .... 97

Table 5.2. Measured physiochemical variables taken during in situ nitrate conversion experiments... 98

Table 5.3. Mean (+/- standard errors) sediment characteristics from cores enclosed in the in situ denitrification experiments (measurements taken from 2016 sampling with exception of site 5, which was from summer 2015). .... 102

Table 5.4. Nitrate uptake rates in the first 24 h (due to depletion of nitrate around 24 hours) during the in situ nitrate conversion experiments in summer 2015, winter 2015 and summer 2016. .... 105

Table 5.5. Pearson correlation matrix showing the relationships between the denitrification rates recorded in summer 2016 and sediment variables. \* =  $p < 0.05$ , \*\* =  $p < 0.01$ , \*\*\* =  $p < 0.001$ . .... 109

Table 5.6. Previously published denitrification rates measured in aquatic ecosystems using a type of in situ enclosure. .... 115

Table 5.7. The nitrogen budget of the in situ enclosures using summer 2016 data (except site 5 which is 2015 summer data)..... 116

Table 6.1. Summary of findings of studies linking nutrient availability to phytoplankton biomass and production in Te Waihora/Lake Ellesmere..... 123

Table 6.2. Relevance of findings of the present study to lake restoration pathways and actions identified by the Selwyn Waihora Zone Committee (SW ZIP 2013)..... 132

Table 7.1 GPS locations of the 18 sediment coring sites around Lake Ellesmere. Locations are in NZGD 2000..... 145

Table 7.2. Sediment characteristics of the 18 sampled sites in Lake Ellesmere in 2013. .... 146

Table 7.3. Sediment characteristics of the 18 sampled sites in Lake Ellesmere in 2014. .... 147

Table 7.4. Presence/absence of invertebrate species recorded in sediment cores at 18 sites in Lake Ellesmere in 2014. A cross indicates presence..... 148

Table 9.1. Frequency of nitrate concentration pulses ( $\text{mg L}^{-1}$ ) from measurements taken between 1993 to 2013, showing the seasons they occurred in. Data is split into measurements taken at the two sites, mid-lake and at the mouth of the Selwyn River..... 158

Table 9.2. Ambient dissolved nutrient concentrations ( $\text{NO}_3^-$ ,  $\text{NH}_4^+$ , DRP) at the time of the three in situ denitrification experiments (summer 2015, winter 2015 and summer 2016). .... 166

Table 9.3. Pearson correlation matrix showing the relationships between the denitrification rates recorded in summer 2016, and sedimentary characteristics and invertebrate species. \* =  $p < 0.05$ , \*\* =  $p < 0.01$ , \*\*\* =  $p < 0.001$ . .... 167

## ACKNOWLEDGEMENTS

---

We thank our colleagues Dave Kelly (Cawthron Institute), David Hamilton (Waikato University), Keith Hamill (RiverLakeFen Ltd) and Candida Savage (University of Otago) for stimulating discussions and their enthusiasm and support for this work. We thank Alex Ring (Environment Canterbury) for collecting and sharing ECAN's in-lake sensor data and providing interesting insights on the data. Ari Santoso (University of Waikato) kindly ran denitrification enzyme assays and provided helpful reports on the data. We are very grateful to Sorrel O'Connell-Milne, Cameron Schallenberg, Stéphanie Roosa, Matthew Highton, Dave Kelly and Moritz Lehmann for field assistance. Julie Clark (Otago Geography Dept.) and Nicky McHugh (Otago Zoology Dept.) provided valuable assistance with chemical analyses. We also thank Leigh-Anne Jeffris for accommodation at her Lake House and ECAN for accommodation at Taumutu. The primary funder for this research was ECAN, Whakaora Te Waihora and the Central Government Freshwater Cleanup Fund. J.C. was also supported by a University of Otago Master's Scholarship, and additional research money from the Brenda Shore Award (University of Otago), New Zealand Coastal Society, the Hutton Fund (Royal Society of New Zealand). M.S. was also supported by a subcontract from the National Institute of Water and Atmospheric Research (Cumulative Effects Programme - C01X1005). We thank Tim Davie and Michael Greer from Environment Canterbury for managing the contract smoothly and also the Whakaora Te Waihora Board for supporting this work in general.

This report has been independently reviewed by Ned Norton (Land Water People).

---

# Section 1

---

## 1 INTRODUCTION

### A FLIPPED LAKE AND THE ROLE OF ECOLOGICAL FEEDBACKS

---

Te Waihora/Lake Ellesmere entered a protracted condition of very poor water quality as a result of the Wahine Storm in 1968, which removed virtually all submerged macrophytes and initiated a period of high turbidity and high phytoplankton biomass which persists into the present (Hughes *et al.* 1974; Gerbeaux 1993; Hamill and Schallenberg 2013). Prior to the Wahine Storm, the lake was known to experience phases of relatively clear water and phases of high turbidity, which were probably driven by the presence or absence of good submerged macrophyte cover, respectively. In 1960, macrophyte cover had been mapped indicating substantial macrophyte beds existed on the margins of the lake, particularly in the Greenpark Sands and Kaituna Lagoon areas (Hughes *et al.* 1974). The macrophytes attracted many water fowl and in 1960, around 80,000 black swan cygnets were estimated to have hatched from nests on the lake margins (Hughes *et al.* 1974). At that time, Te Waihora was the most important brown trout fishery in Canterbury, with large runs of excellent condition spawning fish occurring up the Selwyn River but these runs collapsed between 1970 and 1985 (Jellyman 2012). While there has been much analysis and speculation on the reasons for the collapse of the Selwyn trout fishery since 1970, generally the loss of macrophytes and the shift in ecological regimes are thought to have been a contributing factor (Jellyman 2012). Effects of the regime shift on tuna/eels is not clear because of a lack of published data on tuna in the lake prior to the 1970s and because commercial fishery data collection commenced only in 1973. Kelly and Jellyman (2007) suggested that the benthic invertebrate community shifted from dominance by snails (*Potamopyrgus antipodarum*) to dominance by chironomids as a result of the regime shift. Sediment cores at a number of sites in the lake also revealed the historical presence of freshwater mussels in the lake (*Echyridella* sp.), which indicate historical periods of low salinity and lower turbidity in the lake (M. Schallenberg, unpubl. data). A paleolimnological study by Kitto (2010) indicated

that the Wahine Storm completed the transition of Te Waihora which began in the 1800s with deforestation, increased soil erosion from the catchment and later, artificial openings of the barrier bar. During this transition, the lake shifted from a deeper, lower-nutrient-status lake with a lower salinity and infrequent openings to a shallower lake with higher turbidity, salinity and productivity.

The lack of significant macrophyte re-establishment and the persistence of poor water quality in the 48 years since the Wahine storm indicates that the lake's current poor water quality and lack of substantial macrophyte cover is a new stable state and its ecological resilience to the current and historical pressures that resulted in degraded water quality remains weak. Within the framework of alternate stable states (also known as regime shifts) developed by Marten Scheffer and colleagues (Scheffer *et al.* 1993; Scheffer 2004), the Wahine Storm completed the transition of the lake to an degraded stable state (at least in terms of water quality) and the lake is now in a condition where undesirable ecological feedbacks, such as sediment resuspension and internal nutrient cycling, may resist attempts to restore the water quality of the lake by reducing the external nutrient inputs to the lake (Fig. 1.1).

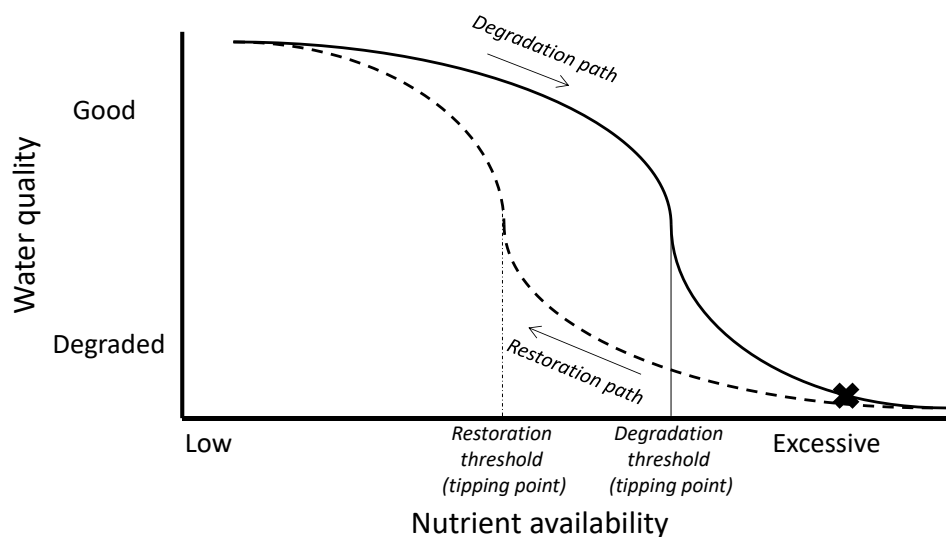


**Figure 1.1.** The theoretical pathways of degradation and restoration in a lake ecosystem dominated by internal ecological feedback mechanisms and by non-linear responses to pressures. X indicates the approximate position of Te Waihora/Lake Ellesmere in this scheme. The difference between the two tipping

points shows the effects of different feedbacks operating to stabilise the lake in either of its two stable states. Adapted from Scheffer (2004).

## INTERNAL NUTRIENT CYCLING

---

Central and regional governments have committed funds to restore the water quality of Te Waihora/Lake Ellesmere. As part of this commitment, research has been funded to fill knowledge gaps concerning the drivers of eutrophication in the lake. Previous studies have pointed out that high nitrate loads are entering the lake from intensifying farming activities in the catchment (Sorrell *et al.* 1998; Larned and Schallenberg 2006; Hamilton 2009; Schallenberg *et al.* 2010; Gibbs & Norton 2013; SW ZIP 2013) and that the mean TN:TP ratio of nutrient loads to the lake (91:1) vastly exceeds the mean ratio of TN:TP of lake water (10:1) (Schallenberg *et al.* 2010). The majority of measured N inputs occur as nitrate whereas the majority P in the lake is in the form of particulate P (Larned and Schallenberg 2006).

Therefore, the skewed N:P ratios suggest that denitrification and/or in-lake P loading could be important processes affecting nutrient cycling and availability, and consequently phytoplankton biomass and production, in the lake. Furthermore, a nutrient balance for the lake indicates that more than one third of the catchment N load could be denitrified or converted to N<sub>2</sub> and N<sub>2</sub>O gas (Hamilton 2009).

Denitrification by microbes proceeds when nitrate and labile carbon (as an energy substrate for denitrifying bacteria) are available and these conditions appear favourable for denitrification in Te Waihora/Lake Ellesmere, particularly near or within the lake bed sediments (Hamilton 2009). If nitrate losses of such high magnitude were to occur in the lake, then denitrification would represent a very important mechanism that contributes to mitigating a negative effect of intensive farming in the catchment (i.e., nitrate losses from farms).

The relatively high mean TP content of the lake water (0.28 µg L<sup>-1</sup>) compared to mean inflow concentration (0.05 µg L<sup>-1</sup>) indicates that large internal sources of P to the water column exist (Schallenberg *et al.* 2010), and one such source is wind-induced sediment resuspension, which is an almost daily occurrence on the large and wind-swept Te Waihora/Lake Ellesmere. Resuspended P bound to sediment particles may not reflect P available to phytoplankton because the sediment-bound P may not desorb in the water column; it may ultimately settle back to the lake bed

again, eventually to be sequestered in the lake bed or flushed out of the lake outlet during a resuspension event. However, a lake P budget suggests that there may be a net internal P load to the lake, potentially from deoxygenated sediment, which can release substantial quantities of P to the water (Hamilton 2009). Such an internal load of bioavailable dissolved phosphorus from the lake sediments could at least partly explain the high in-lake P concentrations and the minor role of P in relation to phytoplankton growth rates that have been measured (Hawes and Ward 1996), estimated (Larned and Schallenberg 2006) and modelled (Hamilton 2009) for the lake.

## ANALYSIS OF PHYTOPLANKTON BLOOMS IN TE WAIHORA

---

To further elucidate the potential relationship between N and P transformations in Te Waihora/Lake Ellesmere and the availability of N and P to phytoplankton, we examined Environment Canterbury's water quality data between 1992 and 2013 to see if discrete phytoplankton blooms were apparent in the record. The record of chlorophyll *a* concentrations in the lake did not show clear seasonal patterns or regular annual or inter-annual blooms (Fig. 1.2). Based on the record, a phytoplankton bloom was defined as a rise in chlorophyll *a* concentration (phytoplankton biomass) to  $> 120 \mu\text{g L}^{-1}$  and using this definition, 14 blooms were identified during the period of record. The blooms were quite variable in maximum chlorophyll *a* concentration and in duration, sometimes lasting just a few months and other times lasting more than 1 year.

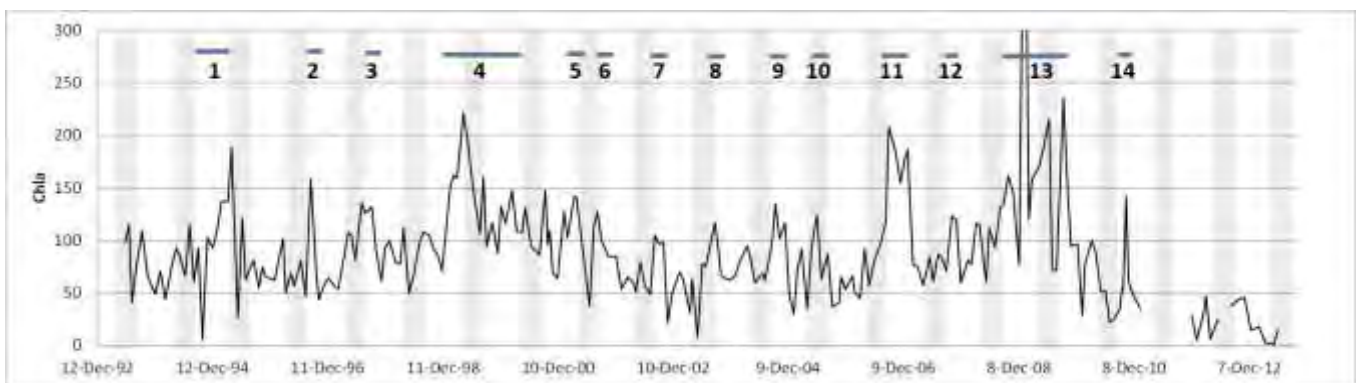


**Figure 1.2.** Environment Canterbury's chlorophyll *a* data from 1992 to 2013, with periods of phytoplankton blooms identified. Vertical shaded bars indicate winter seasons.



In order to identify whether the blooms could have been stimulated by specific prior nutrient conditions (such as a prior pulse of nitrate), nutrient data were scrutinised just prior to the formation of the defined blooms. Similarly, in order to identify whether the blooms exhausted available nutrients, other water quality data recorded during the bloom period were scrutinised. Nutrient conditions prior to the bloom could be interpreted as reflecting conditions stimulatory to blooms, whereas conditions that developed toward the end of the bloom could be interpreted as reflecting conditions relating to bloom collapse. For example, phytoplankton blooms may have been arrested by a nutrient shortage if the available nutrient concentrations declined to below analytical detection limits during the bloom period.

All the blooms, with the exception of blooms 4, 10 and 13 occurred in spring, summer or, autumn. Bloom 10 occurred in winter and blooms 4 and 13 lasted over 1 year (also occurring in winter). Blooms that occurred immediately after peaks in nutrient concentrations were interpreted to have been stimulated by the pulse of nutrients, especially if the nutrient concentrations were drawn down by the bloom.

Table 1.1 shows the water quality factors that were correlated to the formation and collapse of phytoplankton blooms, as determined from the ECAN dataset. Dissolved inorganic nutrients (dissolved reactive P or DRP, nitrate or  $\text{NO}_3$  and ammoniacal nitrogen or  $\text{NH}_4$ ) showed some very large peaks at various times in the record, indicating that the lake is subject to rapid nutrient supply and demand dynamics. It was common for peaks in various water quality parameters to precede phytoplankton blooms and these pre-bloom peaks can be interpreted to have stimulated the blooms, especially when they occurred during times of favourable water temperatures and salinities. It is important to note that this is a correlational analysis from which causation can only be inferred, not proven.

Peaks or spikes in  $\text{NO}_3$ ,  $\text{NH}_4$  and DRP concentrations (together or individually) preceded phytoplankton blooms on most occasions suggesting that sudden increases in nutrient availability often led to phytoplankton blooms in the lake. On three occasions, blooms couldn't be attributed to prior inputs of large amounts of nutrients, however two of these blooms may have been resuspension driven or

facilitated by nitrogen fixation (i.e., nitrogen fixing cyanobacteria) due to simultaneous increases in total nitrogen and turbidity during the phytoplankton blooms. The other bloom that occurred without apparent nutrient stimulation was the unusual winter bloom of 2005.

**Table 1.1.1.** Factors correlated with bloom formation and collapse in Te Waihora/Lake Ellesmere. Data analysed were supplied by ECAN. The pre-bloom period examined was 30 days. NH<sub>4</sub> – ammonium. NO<sub>3</sub> – nitrate, DRP – dissolved reactive phosphorus. Turbidity/Salinity indicates whether these factors appeared to be related to the bloom. A question mark indicates that uncertainty exists about the connection to the blooms.

Bloom	Pre-bloom peak		Depleted during bloom
	Nutrients	Turbidity/Salinity	Nutrients
1. Summer/Autumn 94/95	NO <sub>3</sub>	Salinity decline from 15 ppt to 5 ppt	
2. Spring 1996	NO <sub>3</sub>	Turbidity low	
3. Spring 1997	DRP		DRP, NO <sub>3</sub> , NH <sub>4</sub>
4. Late Summer 1998 – Autumn 2000		Resuspension driven?	
5. Autumn 2001		Resuspension driven?	
6. Spring 2001	NH <sub>4</sub>	Turbidity low	NH <sub>4</sub>
7. Spring 2002		Turbidity low	
8. Spring 2003	NH <sub>4</sub>	Turbidity low	
9. Spring 2004	DRP		DRP
10. Winter 2005			
11. Spring/Summer 06/07	NO <sub>3</sub>		
12. Spring 2006	DRP		
13. Spring 2008 – Summer 09/10	DRP, NH <sub>4</sub>		
14. Spring 2010	DRP, NO <sub>3</sub>		

Based on this analysis of blooms, episodic nutrient availability appears to play an important role in stimulating phytoplankton blooms and the depletion of nutrient appears to play a somewhat lesser role in limiting the duration (and possibly the magnitude of) blooms. Observed prior peaks in nitrogen appeared to stimulate blooms six times while peaks in DRP appeared to stimulate blooms five times (Table 1.2). This suggests that regulation of the availability of both N and P plays a role in

the phytoplankton dynamics in this lake, as has been shown in other studies (Hawes & Ward 1996; Larned & Schallenberg 2006; Hamilton 2009; MacKenzie 2016).

**Table 1.1.2.** Times that available nutrients were correlated with phytoplankton blooms in Te Waihora out of 14 identified blooms (see Table 1.1).

Nutrient	Times peaked prior to bloom formation (as sole nutrient)	Times apparently depleted during blooms (as sole nutrient)
DRP (PO <sub>4</sub> )	5 (3)	2 (1)
Nitrate (NO <sub>3</sub> )	4 (3)	1 (0)
Ammonium (NH <sub>4</sub> )	2 (1)	2 (1)

The importance of both nitrogen and phosphorus to phytoplankton production and blooms raises two key questions with respect to the research undertaken in this report: 1. Does denitrification substantially compete with phytoplankton for available N episodically entering the lake from the catchment, resulting in the common occurrence of N-limitation? 2. Could peaks in DRP that stimulate phytoplankton blooms emanate from the lake bed sediments through anoxic release of sediment-bound P? To answer these questions, we undertook the research that will be presented in the subsequent chapters which shows that, indeed, internal N and P transformations appear to play a moderate role in regulating nutrient availability to phytoplankton in Te Waihora/Lake Ellesmere.



Sub-fossil shells probably from freshwater mussels (*Echyridella menziesii*) found buried in sediment cores from site E6.

---

## Section 2

---

### 2 SPATIAL VARIATION IN SEDIMENT CHARACTERISTICS IN TE WAIHORA/LAKE ELLESMERE

---



Collecting a sediment core using a gravity corer.

## INTRODUCTION

---

### **Sediment variation in lakes**

Lake sediments can contribute to nutrient transformations in the water column. For example, it has been suggested that Te Waihora/Lake Ellesmere may sustain significant rates of denitrification and it may have high rates of P cycling and transfer from the sediment to the water column (Hamilton 2009). The ability of sediments to retain or release P and N to the water column can depend on a range of different factors such as sediment composition, redox potential, bioturbation and temperature (Holdren and Armstrong 1980). As sediment characteristics can vary spatially within a lake, the mechanisms regulating nutrient transformations are also likely to vary (Downing and McCauley 1992). To help understand the potential benthic-pelagic coupling of nutrient transformations in Te Waihora/Lake Ellesmere, we assessed the spatial characteristics of the sediments in the lake.

### **Aims**

In this section of our report, we aimed to investigate the spatial variability of the sediment characteristics likely to influence denitrification and anoxic P release from the sediments into the water column. We also aimed to understand the dominant gradients of sediment variability and the correlations amongst the different sediment variables that are likely to be important to in-lake nutrient cycling.

## METHODS

### Sampling dates and location

Sediment was collected from 18 sites around the lake (Fig. 2.1), in April 2013 and 9<sup>th</sup> – 11<sup>th</sup> April 2014. GPS co-ordinates of the sites are included in Appendix A.

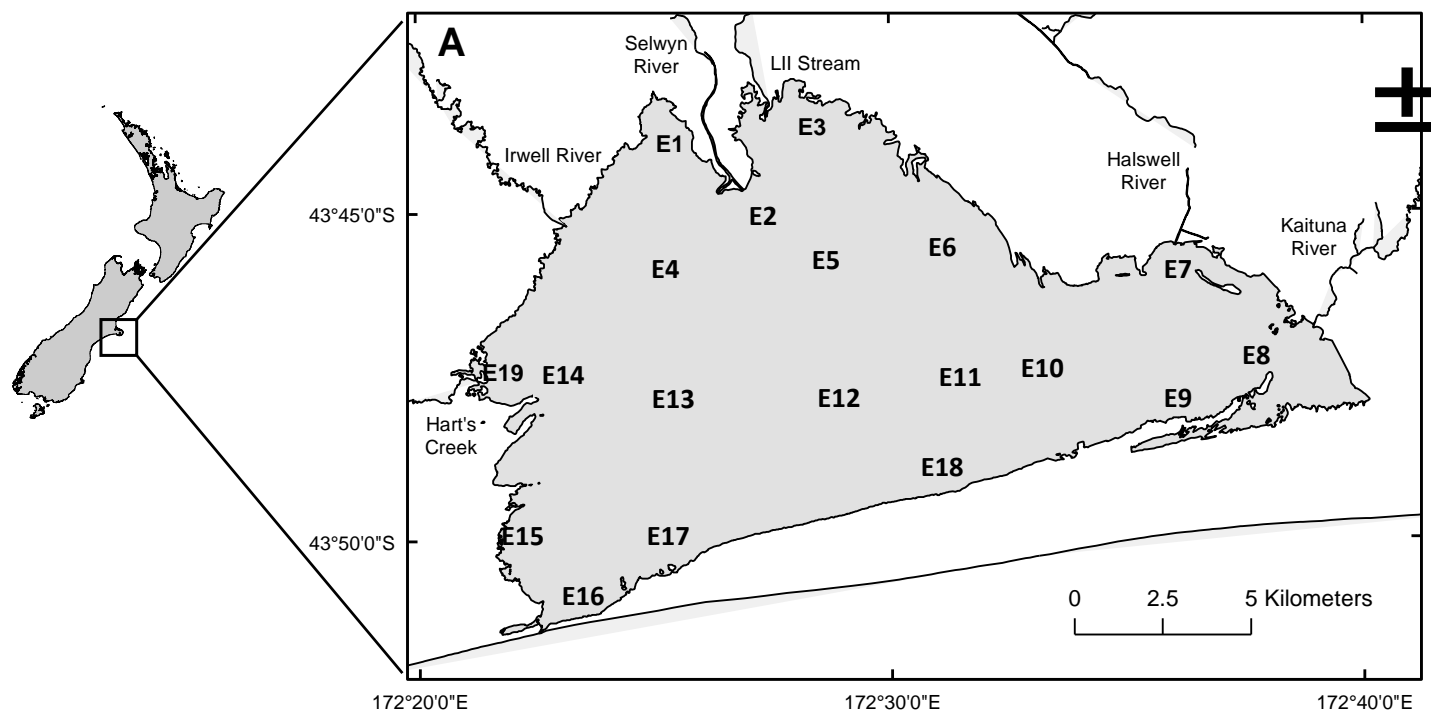


**Figure 2.1.** Location of the 18 sampling sites and the main inflow tributaries.

### Sediment measurements

Three core samples of the top 4 cm of sediment were collected at each site and pooled into one representative sample for sediment characteristics (redox potential, porosity, particle size and loss on ignition/organic matter). Sediment redox potential was measured in this pooled sample with a Schott millivolt meter and redox probe.

Porosity ( $\text{kg m}^{-2}$ ) of the sediment was determined as:

$$\text{Porosity} = \frac{\text{wet weight} - \text{dry weight}}{\text{sample volume}}$$

Dry weight of the sample was determined by drying 5 g of wet sediment at 50°C for 24 hours. Sediment was then transferred to a desiccator to stabilize for 4 hours before weighing.

The sediment organic matter content was determined as:

$$\text{Organic Matter} = \frac{\text{dry weight} - \text{combusted weight}}{\text{dry weight}} \times 100$$

Sediment was combusted at 450°C for 24 hours, and allowed to stabilize in a desiccator for four hours. Organic matter concentrations were also calculated as the dry mass of organic matter per mL of sediment, which could then be converted to areal organic matter concentrations (per m<sup>2</sup>).

The sediment grain size was determined using a laser-diffraction Malvern Mastersizer 2000 in the Otago University Geography Department. Five g of sediment was dried for 24 hours at 50°C. One g of sediment was placed into a 50 mL falcon tube, and treated with 5 mL of hydrogen peroxide (H<sub>2</sub>O<sub>2</sub>) to remove organic matter, and watched over for 4 hours (to ensure no bubbling over). It was then placed in a water-bath at 50°C overnight. It was shaken well in the morning, and another 5 mL of H<sub>2</sub>O<sub>2</sub> was added, and left in the water-bath for another 24 hours. This process was continued until the reaction was complete (noted by no further reaction in the sediment). Samples were centrifuged at 3000 rpm for 12 minutes, then the H<sub>2</sub>O<sub>2</sub> was tipped off, and milli-Q water was added in equal weights, and the process repeated twice, mixing well before each centrifuge. 5 mL of 5% Calgon solution (sodium hexametaphosphate) were added to help with particle dispersion, the day before measuring. It was then gently agitated on a shaker for 2 hours, and kept refrigerated until measurement. Particle sizes were separated into percentages using the following grain size classes: clay (0-2 µm), silt (2-63 µm) and sand (63-2000 µm).

### **Benthic infauna collection & identification**

Five core samples (outer diameter 7 cm, inner diameter 6.4 cm, length 20 cm) were taken at each of the 18 sites (Fig. 2.1). Sediments were passed through a 500 µm sieve. Infauna retained on the sieve were stored in ethanol until processed in the lab. Infauna were identified to species level where possible, using identification



guides by Moore (1997), Gooderham and Tsyrlin (2002), Jones and Marsden (2005) and Landcare Research Website (accessed June - July 2014).

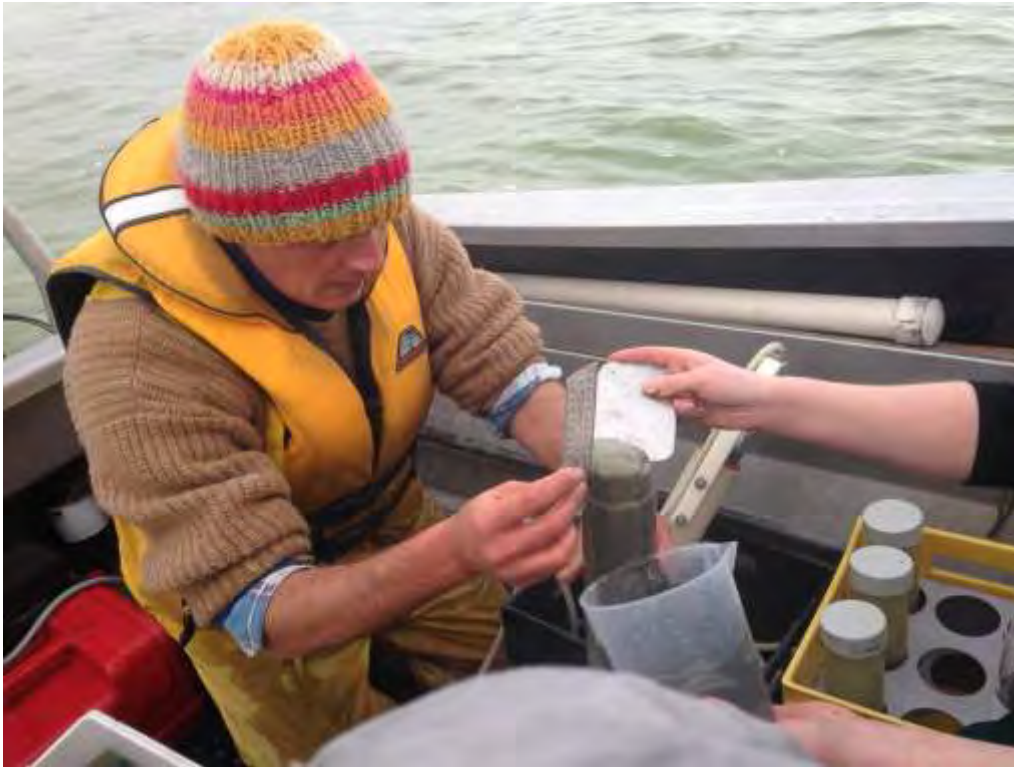
### Statistical Analysis

All statistical analyses were run using R Studio v. 0.98.1049. Graphs were produced in Excel 2013. Linear regression and Pearson's correlations were used to establish the statistical significance of linear trends between sedimentary variables ( $\alpha = 0.05$ ). Spatial contour plots were created in Surfer 11. Ordination plots were made in CANOCO software v. 4.5. Principal components analysis (PCA) was used to investigate relationships between environmental variables. Canonical correspondence analysis was used to then investigate correlations between benthic invertebrate species and the environmental variables.

Species diversity was calculated using the Shannon species diversity index:

$$H = - \sum_{i=1}^S p_i \log_b p_i$$

Where  $p_i$  = proportion of species,  $S$  = total number of species,  $p_i = 1$ , and  $b$  = base of the logarithm.



Collecting the top 4 cm of sediment for analysis of sediment characteristics.

## FINDINGS

### Spatial and temporal variability in sediment characteristics

The average depth of sites sampled was 1.38m in 2014, with a range of 0.53–2.37m (Fig. 2.2A), and an average depth of 1.10m in 2013, ranging from 0.48-2.1m (Fig. 2.2B). Changes in average water depth occur in relation hydrological variability caused by rainfall, evaporation and opening and closure of the lake's barrier bar (Schallenberg *et al.* 2010).

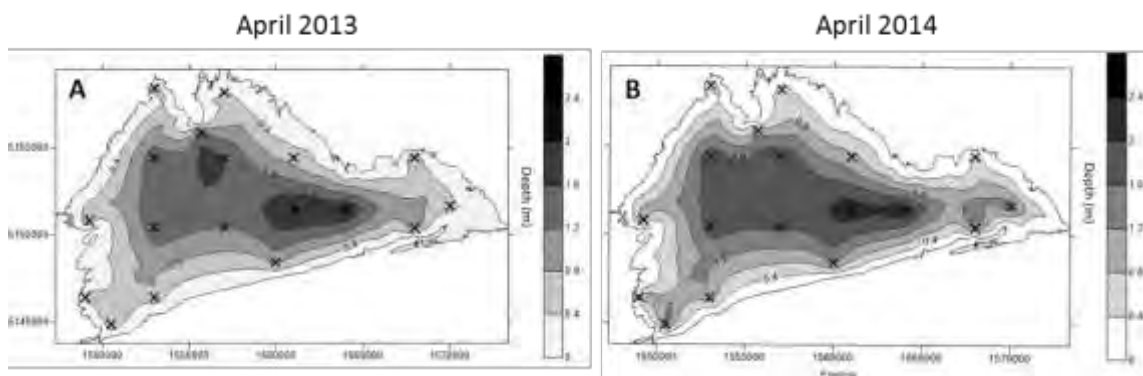


**Figure 2.2.** Water depths (m) at the 18 sites in April 2013 (A) and April 2014 (B).

Sediment grain size fractions were found to vary spatially within the lake, following the depth gradient (Fig. 2.3). The deeper sites were dominated by a silt/clay mix, while the shallow margins contained higher proportions of sand (Fig. 2.3). There was no large change between years in the sediment grain size (Table 2.1), although there was slightly greater clay content across all sites in 2013 compared to 2014. As there were no significant differences between sites over years sampled, we focused on the 2014 data (for which we had measured more variables), however correlations for both years are displayed in Tables 2.2 and 2.3. There was a significant positive relationship between both clay and silt vs depth ( $r=0.91$ ,  $r=0.81$ ), and a significant negative relationship between sand vs depth ( $r=-0.83$ ) (Table 2.3). Sediment porosity (a measure of the amount of water in the sediment) was strongly influenced by the sediment grain size (Fig. 2.4). Porosity ranged from 0.49 to 0.88 g mL<sup>-1</sup> (equivalent to 4.8 to 8.8 kg m<sup>-2</sup>, to a depth of 1 cm). Sediment porosity was also correlated to water depth ( $r=0.78$ ), with a higher sediment porosity (greater water content) associated with deeper, finer sediments (Fig. 2.5A, 2.5B).

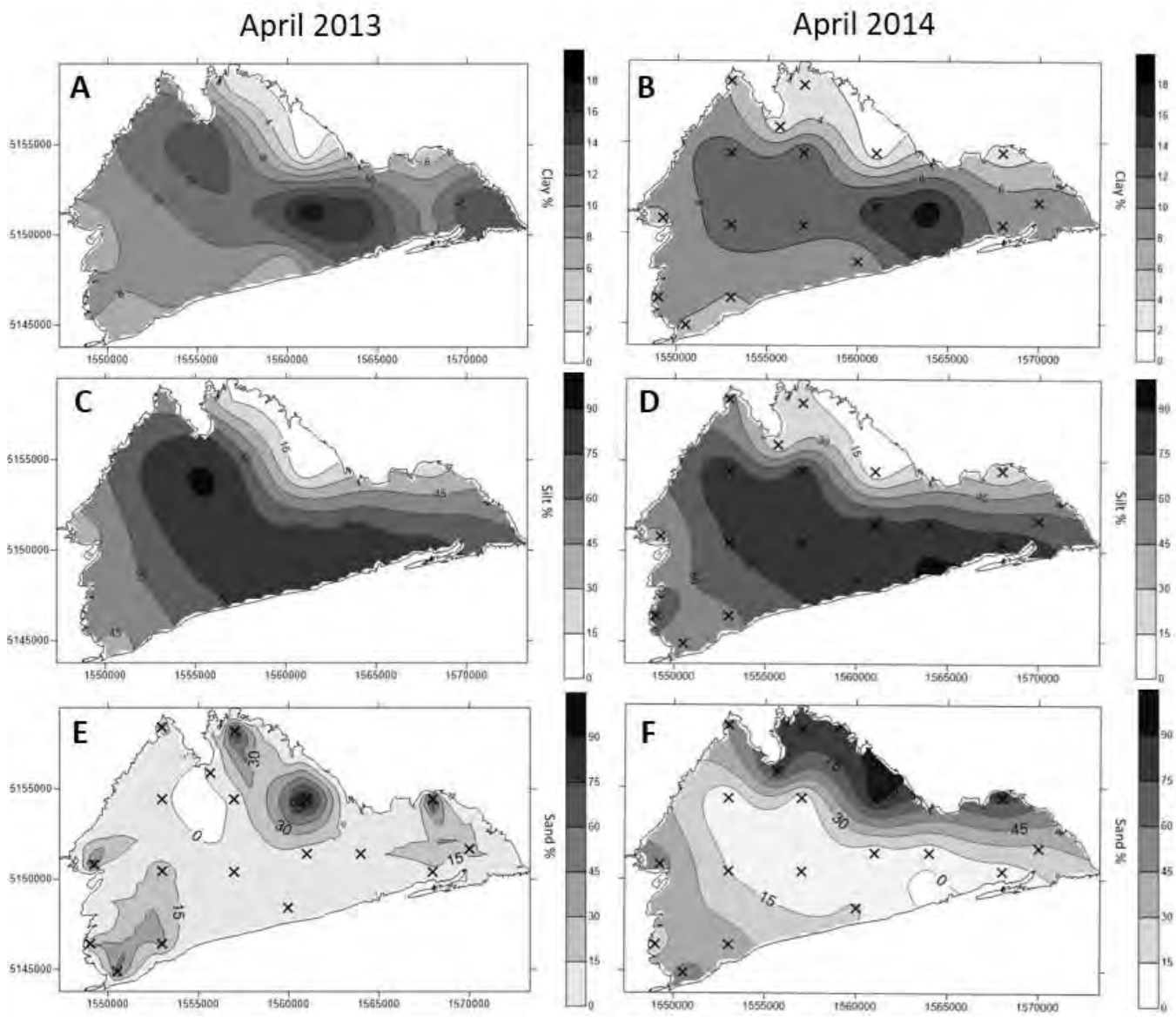


**Figure 2.3.** Maps of sediment grain size at the 18 sites, in April 2013 (A = clay %, C = silt %, E = sand %) and April 2014 (B = clay %, D = silt %, F = sand %).

**Table 2.1.** Pearson correlation analysis of variation in the sediment variables between the two years (2013 and 2014). \*\*\* =  $p < 0.001$ , \*\* =  $p < 0.01$ , \* =  $p < 0.05$ .

Factor	P-value	F-Statistic (1,16 DF)
Depth	$1.532e^{-5}$ ***	37.22
Clay	0.0002323 ***	22.26
Silt	$6.432e^{-5}$ ***	28.35
Sand	$6.845e^{-5}$ ***	28.35
OM	0.008 **	9.058
Porosity	0.009653 **	8.631
Redox	0.1398	2.414

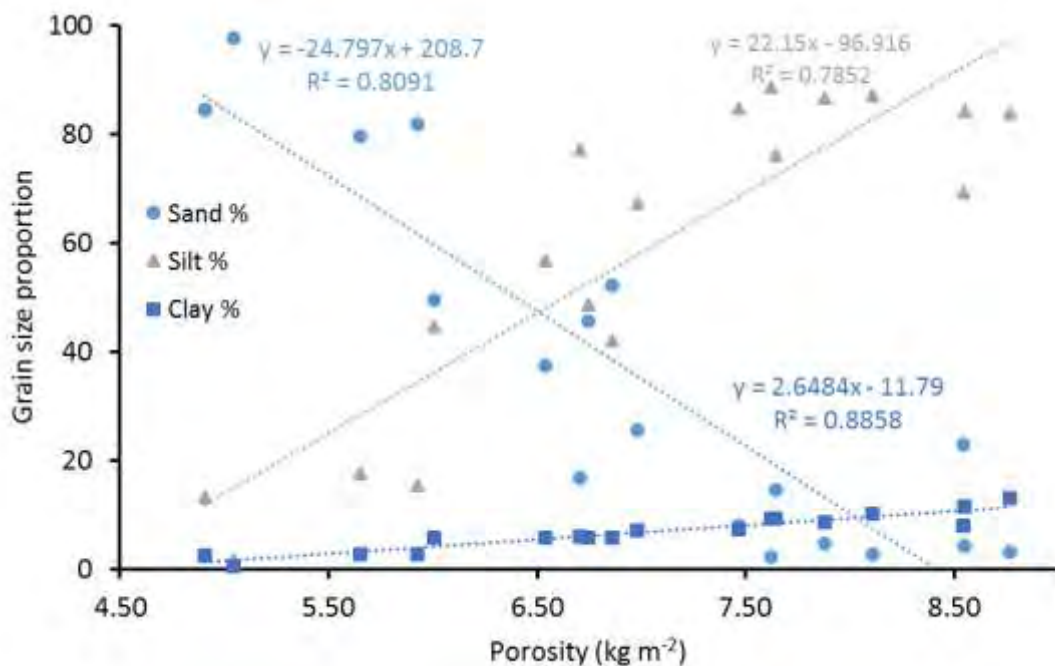


**Figure 2.4.** The relationship between sediment grain size fractions (sand, silt, clay %) and sediment porosity. 2014 survey data.

The redox potential measures how chemically reducing or oxidising the sediments are. The redox potential of the homogenised top four cm of lake bed sediments ranged from +140 to -400 mV across both years (Fig. 2.5 C, D). There was a

significant difference in redox potential between the two sampling years (Table 2.1). In 2013 the most reducing regions were located near the mouth of L2 Stream, and in the deeper basins of the lake, and redox potential was negatively correlated with depth ( $r=-0.48$ ) (Table 2.2). In 2014 the redox potential was most highly reducing in the deep regions of the lake and least reducing at the Greenpark Sands. In 2014 redox potential was negatively related to the sediment grain size characteristics, clay and silt content and porosity ( $r=-0.51$ ,  $r=-0.55$ ,  $r=-0.47$ ), and positively related to sand content ( $r=0.55$ ) (Table 2.3). The smaller particle sizes in fine textured sediments hold more water and encourage anaerobic zones to develop more readily than the larger pores of coarser sediments (Groffman and Tiedje 1989).

Organic content decreased with average particle size across both years (Fig. 2.5E, F) and the clay fraction was most strongly correlated with organic matter content ( $r=0.72$ ,  $r=0.79$ ) (Tables 2.2, 2.3). There was a slightly greater organic content in the deeper basin of the lake in 2013 compared to 2014. Smaller sediment grain sizes can contain a greater percent of organic matter (Vance-Harris and Ingall 2005), potentially harbouring more microorganisms, containing higher nutrient concentrations and driving higher rates of denitrification (García *et al.* 1998; Livingstone *et al.* 2000; Teixeira *et al.* 2010).

Principal component analysis was used to visually display the main gradients of the measured environmental variables. Figure 2.6 shows the strong loadings of the silt, clay, sand, porosity and depth on the first axis, which explained 72% of the variance in the data. The concentration of organic matter and the redox potential were only weakly correlated to the depth-grain size gradient and they constituted the second major independent gradient in the data, explaining 26% of the variation in the data.

**Table 2.2.** Pearson correlation matrix showing pairwise relationships among the 2013 sediment variables. \*\*\* =  $p < 0.001$ , \*\* =  $p < 0.01$ , \* =  $p < 0.05$ .

	Depth	Clay	Silt	Sand	OM	Porosity
Depth						
Clay	0.78***					
Silt	0.69**	0.78***				
Sand	-0.72***	-0.83***	-1.00***			
OM	0.4	0.72***	0.62**	-0.65**		
Porosity	0.86***	0.73***	0.80***	-0.81***	0.42	
Redox	-0.48*	-0.37	-0.26	0.28	-0.37	-0.42

**Table 2.3.** Pearson correlation matrix showing pairwise relationships among the 2014 sediment variables. \*\*\* =  $p < 0.001$ , \*\* =  $p < 0.01$ , \* =  $p < 0.05$ .

	Depth	Clay	Silt	Sand	OM	Porosity
Depth						
Clay	0.91***					
Silt	0.81***	0.90***				
Sand	-0.83***	-0.92***	-1.00***			
OM	0.57*	0.79***	0.74***	-0.75***		
Porosity	0.78***	0.94***	0.89***	-0.90***	0.81***	
Redox	-0.36	-0.51*	-0.55*	0.55*	-0.69**	-0.47*

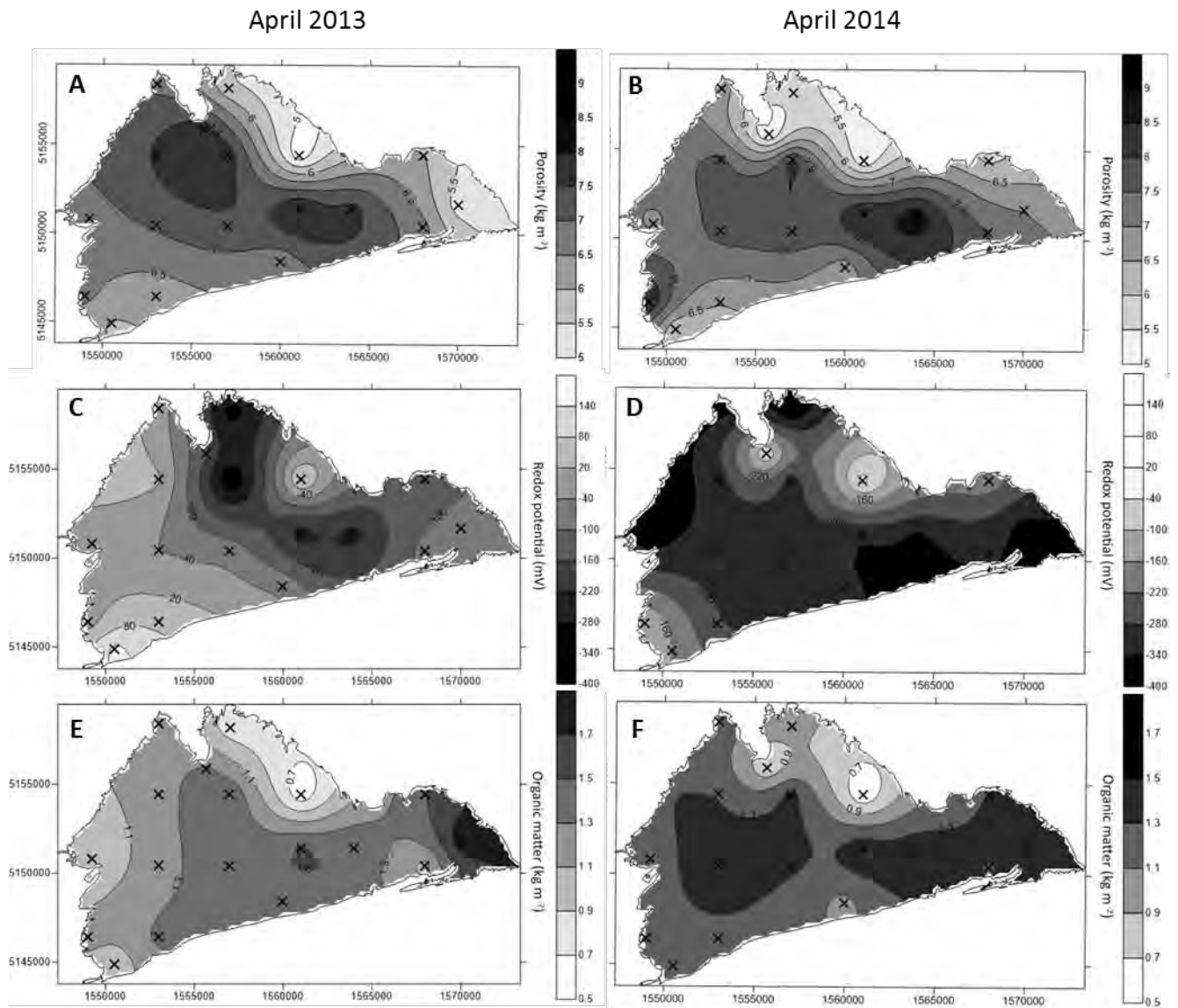


**Figure 2.5.** Maps of sediment characteristics measured in April 2013 (A = porosity ( $\text{kg m}^{-2}$ ), C = redox potential (mV), E = organic matter ( $\text{kg m}^{-2}$ )) and April 2014 (B = Porosity ( $\text{kg m}^{-2}$ ), D = Redox potential (mV), F = organic matter ( $\text{kg m}^{-2}$ )).



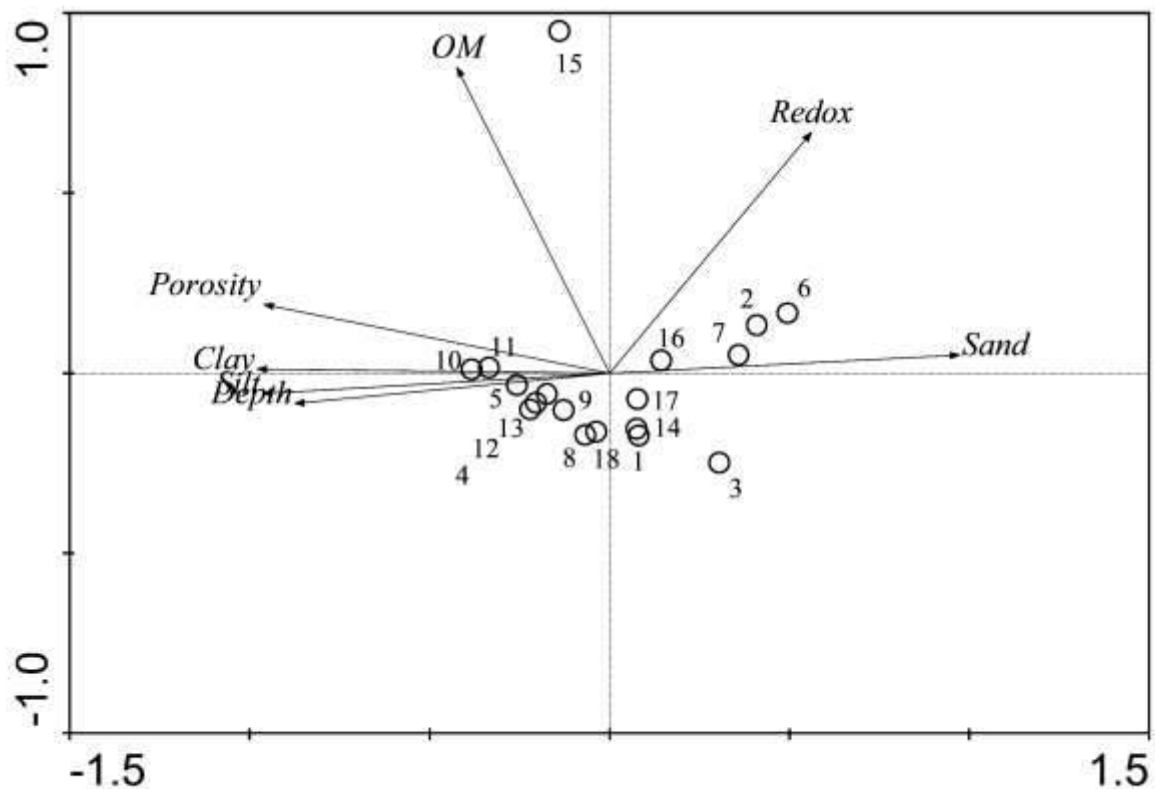


**Figure 2.6.** Principal component analysis showing correlations among variables and the distribution of the sites in relation to the two main gradients in sediment characteristics.

### Spatial patterns in invertebrate communities

Sediment cores retrieved from some of the sites showed that benthic invertebrates, such as chironomids, can have a major impact on sediment structure in Te Waihora/Lake Ellesmere (Fig. 2.7). Thus, they have the potential to greatly affect biogeochemical processes occurring in the sediments.

In 2014, the benthic invertebrate taxonomic diversity was low, with only 11 species recorded (Appendix A). The three most abundant taxa were the amphipod *Paracorophium excavatum*, the mud snail *Potamopyrgus antipodarum* and oligochaetes, respectively. *P. excavatum* and oligochaetes showed the highest density along the Greenpark Sands (Figure 2.8A), with *P. antipodarum* having the

highest density in the Kaituna Lagoon (east end; Figure 2.8B). Total invertebrate density was highest at the Greenpark Sands site (Figure 2.8E).



**Figure 2.7.** Empty chironomid tubes remaining long after inhabitation in a sediment core. No chironomids were found in the core which was collected in April 2014, after a prolonged period of high salinity affected the lake.

Taxonomic richness was negatively correlated to depth ( $r=-0.82$ ), porosity ( $r=-0.71$ ), clay and silt content ( $r=-0.81$ ,  $r=-0.72$ ), while it was positively correlated to sand content ( $r=0.73$ ). The two burrowing species found, oligochaetes and polychaetes, were negatively correlated to grain size (%clay) ( $r=-0.70$ ,  $r=-0.63$ ) and water depth ( $r=-0.65$ ,  $r=-0.75$ ), preferring to inhabit the shallow sandy margins in the lake. This is not surprising because as grain size decreased, so did the oxygen penetration depth into the sediments (Section 3).

Surprisingly, in our sampling in April 2014, we found only two chironomids in the 90 core samples taken from Te Waihora, and the community was instead dominated by amphipods and mud snails. Wilks (2010) and Wood (2008) found densities of 800-12000 individual chironomids per  $m^2$  in Te Waihora/Lake Ellesmere. While we

observed many chironomid tubes (dwellings) in the sediment cores that we collected they were almost all barren (Fig. 2.7).

Salinity can be toxic to invertebrates (James *et al.* 2003), and Wilks (2010) found low invertebrate densities in Te Waihora/Lake Ellesmere at salinities > 8 ppt. At the time of our sampling, the mean salinity of the lake was 9.55 ppt. This level of salinity probably severely impacted the invertebrate community and hence their influence on lake bed biogeochemistry. Lake openings slowly increase the salinity of the lake (Schallenberg *et al.* 2010), and our findings and those of Wilks (2010) indicate that unusually high and prolonged periods saline intrusions could kill off chironomid populations, affecting oxygen dynamics, sediment characteristics and the cycling of nutrients in the lake through the loss of dwellings and the lack of sediment irrigation carried out by these organisms.

Sediment irrigation by high densities of benthic infauna increases oxygen penetration into sediments (Svensson 1997; Nizzoli *et al.* 2007; Shang *et al.* 2013), which is consistent with the higher redox potentials recorded in the Greenpark Sands site. However, we found no significant relationships between either total invertebrate abundance or abundances of individual species vs sediment redox potential, while there was a weak positive relationship between invertebrate taxonomic richness and sediment redox potential ( $p < 0.05$ ). But the lack of relationships was likely due to the virtual absence of chironomids in the lake at the time of sampling in April 2014.

Figure 2.9 shows the correlations among invertebrate taxa across the sites. *P. excavatum*, polychaetes (Neridae) and the oligochaetes form the major gradient in the data, with large numbers of these invertebrates occurring at site 3. *P. antipodarum* forms the second major gradient due to the high density of snails found at site 8.

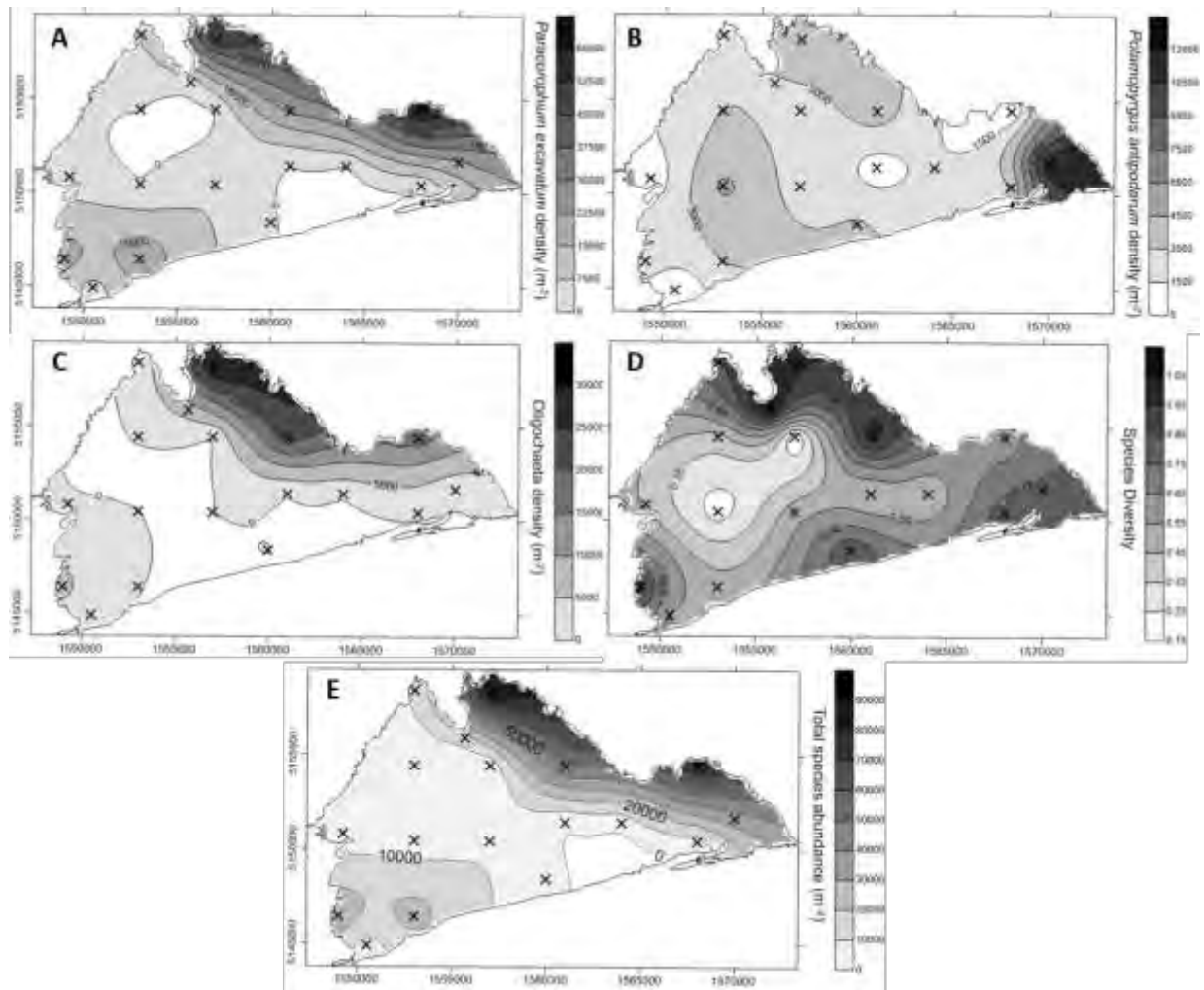


**Figure 2.8.** Maps of invertebrate density in April 2014. A = *Paracorophium excavatum* density ( $m^2$ ), B = *Potamopyrgus antipodarum* density ( $m^2$ ), C = oligochaetes density ( $m^2$ ), D = species diversity ( $m^2$ ), and E = total species abundance ( $m^2$ ).

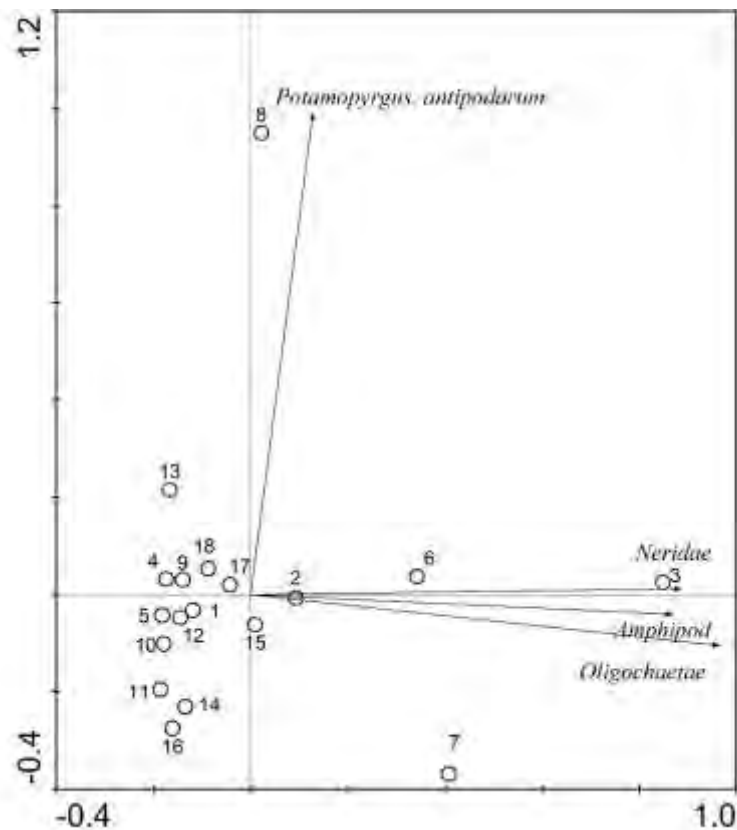


**Figure 2.9.** Principal component analysis showing correlations among invertebrate taxa and the distribution of the sites in relation to the main gradients of community structure.

### Explaining the relationships within sediment variables

We found some strong relationships within the sediment variables in Te Waihora/Lake Ellesmere sediments. Sediment grain size is the dominant factor correlated to many other variables that we measured. Fig. 2.9 depicts conceptually how sediment grain size affects the other variables in this lake. The sediments consist of a range of inorganic sediment particles sizes, from extremely fine sediment to coarse sands, often containing broken shells. Sediment grain size is one factor determining the porosity of the sediment.

In surficial sediment, the presence of very fine particles is associated with greater interstitial spaces where organic matter may be trapped, bound and/or produced by sediment bacteria (Vance-Harris and Ingall 2005). Such sediments become cohesive due to the presence of viscous biogenic polysaccharides which also maintain a high water content in the sediment, suspending the fine sediment in a gelatinous matrix.

By maintaining a high porosity (water content), the polysaccharide-fine sediment matrix may hinder the diffusion of solutes and gases through the sediments, increasing the probability of anoxia developing in these sediments (Groffman and Tiedje 1989; Smith *et al.* 2003; Hamersley and Howes 2005; Solomon *et al.* 2009).

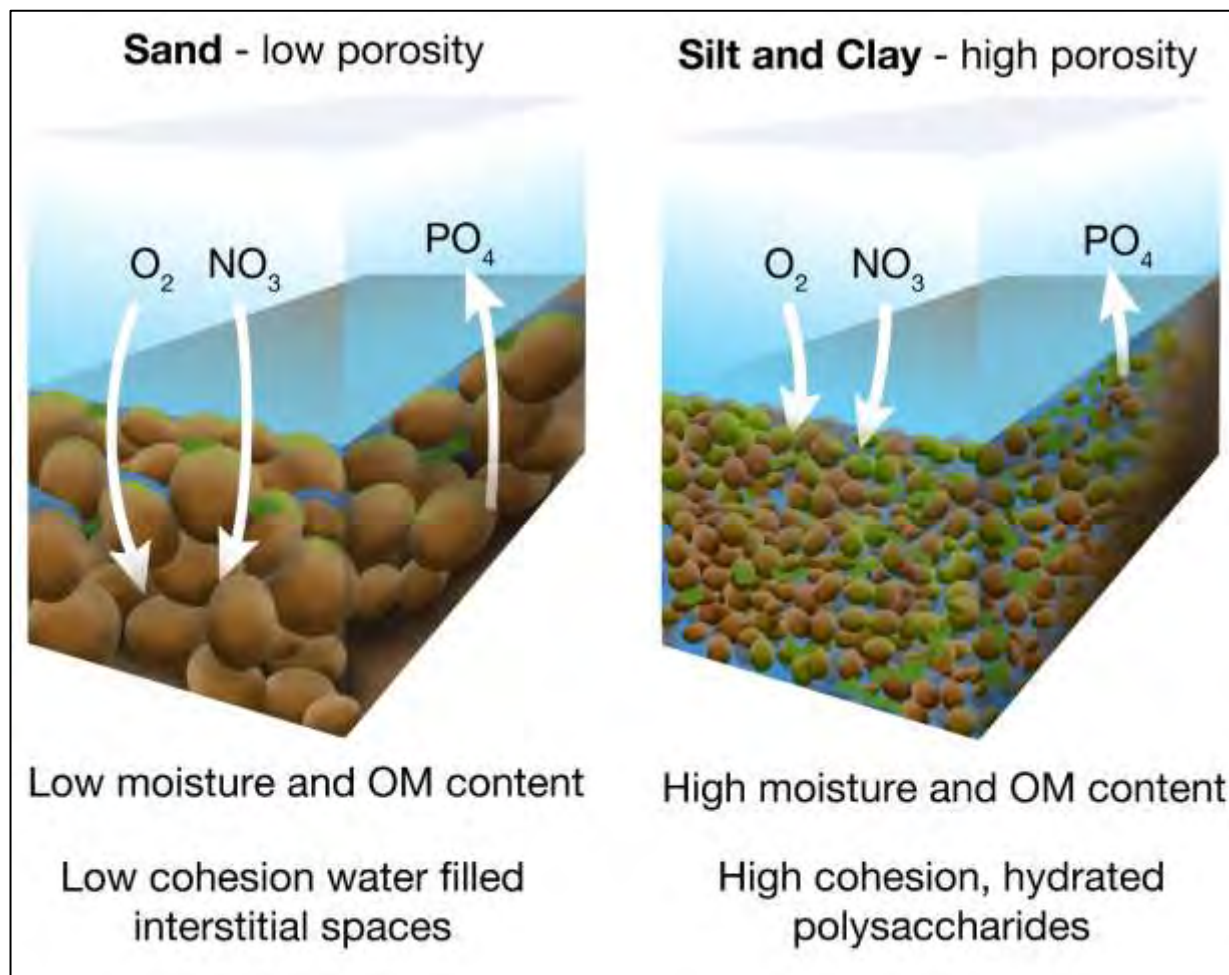


**Figure 2.10.** Conceptual figure describing the relationships between the measured sediment variables. The two dominant sediment types within Te Waihora - A sandy sediment, composing of large particles, low porosity (low water content) and low organic content, and a silt and clay dominated sediment, composed of smaller particles, high porosity (high water content) and high organic content, bound tightly in a gelatinous, polysaccharide matrix (jelly-like).

## CONCLUSIONS

---

Te Waihora/Lake Ellesmere has a strong sediment grain size gradient which is principally related to water depth. The deeper sites are composed of smaller grain sizes (clay and silt), which also correlated with a greater sediment porosity and organic matter concentrations. The interstitial spaces in the fine sediments are probably maintained by organic molecules of biogenic origin, such as microbially-derived and chironomid-derived polysaccharides. Water depth showed a weak negative relationship with the redox potential in 2014. Physio-chemical sediment attributes varied little between years. Our samples were taken at a time when chironomid densities in the lake were unusually low. The recovery of chironomid densities to those reported in previous studies will likely increase the redox potential and organic matter concentrations in the sediment. The invertebrate communities we recorded showed a strong negative relationship with depth, where invertebrates appeared to prefer to inhabit the sandier margins of the lake. The fine, profundal sediments, while having greater water and organic contents, are also more cohesive and may show lower rates of diffusion than the courser-grained sediments.

---

## Section 3

---

### 3 SEDIMENT OXYGEN DYNAMICS IN TE WAIHORA/LAKE ELLESMERE

---



Measuring sediment oxygen micro-profiles using a Unisense oxygen microsensor.



## INTRODUCTION

---

### Importance of sediment oxygenation

Sediment oxygenation is one of the most important indicators of sediment health in coastal lagoons and embayment's (Xu *et al.* 2009). Sediment oxygenation controls the biogeochemical cycling of many elements and compounds in aquatic systems including the conversion of nitrate to N<sub>2</sub> gas via denitrification (Steingruber *et al.* 2001), binding and release of phosphorus to certain minerals (Golterman 2007) and organic matter remineralization (Xu *et al.* 2009; Wang *et al.* 2014). As oxygen is the primary electron acceptor in respiratory processes, shortages in its availability causes shifts to mineralisation processes which use alternate electron acceptors such as nitrate, sulphate, metals and CO<sub>2</sub> (Nielsen *et al.* 1990; Xu *et al.* 2009). Under oxic conditions phosphorus tends to be chemically bound to metal oxyhydroxides in the lakes sediment and if the sediments then become anoxic, the minerals dissolve, releasing phosphate into sediment pore waters, which can diffuse into the overlying water column, eventually stimulating phytoplankton growth.

Denitrification occurs at the boundary of the anoxic/oxic sediment interface where the presence of an oxic sediment layer is known to be important in controlling nitrification and denitrification (Risgaard-Peterson 1999). Generally the oxygen penetration depth in sediments is only tens of micro-meters to a few millimetres, creating strong oxygen gradients within the sediment (Rasmussen and Jorgensen 1992; Wang *et al.* 2014). The shallowness of coastal lagoons allows wave turbulent energy to propagate to the sediment water interface where oxygen and nitrate may be continually supplied to the sediment surface.

Sediment oxygenation can be further enhanced through bioturbation of the sediment by benthic infauna which burrow into the sediment (Aller 1998). The infaunal burrows physically modify the sediment structure, resulting in hotspots of microbial activity due to increased dissolved oxygen and resource supply to deeper sedimentary layers (Svensson 1997; Banks *et al.* 2013; Shang *et al.* 2013; Poulsen *et al.* 2014). The burrowing activity creates oxic zones around the burrows (Fig. 3.1) (Svensson 1997; Aller 1998; Gilbert *et al.* 2003; Nizzoli *et al.* 2007; Stief *et al.* 2009; Shang *et al.* 2013) and the inner walls of such burrows may be fairly permeable to water and cause significant bio-irrigation of the burrow surfaces, thus further

extending sediment oxygenation (Olafsson and Paterson 2004). The continuous renewal of oxygen also stimulates the nitrification of ammonium in the sediment, producing nitrate at deeper sites for denitrification (Stief 2013). Thus, infaunal irrigation of burrows transports nitrate from the overlying waters into the deeper sediment, enhancing denitrification by coupling denitrification with nitrification due to the extension of the oxic layer (Carpenter and Capone 1983; Svensson 1997; Biswas *et al.* 2009; Banks *et al.* 2013).

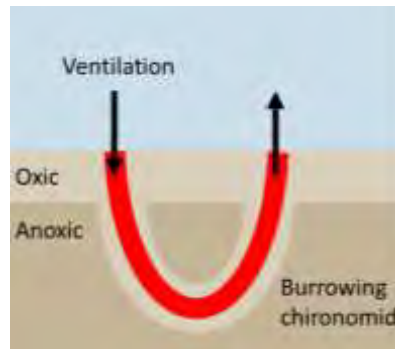


**Figure 3.1.** Ecosystem engineering by sediment infauna, influencing benthic nitrogen cycling in aquatic ecosystems by deepening the zone of oxygen penetration into the sediment (modified from Stief (2013)).

### Research objectives

Because dissolved oxygen is a key driver of important biogeochemical processes relating to N and P cycling in lakes, we undertook studies to understand the seasonal variation in oxygen dynamics within Lake Ellesmere. Detailed studies were undertaken during three sampling campaigns - two in summer and one in winter – to answer the following questions:

1. How do the biological and chemical oxygen demands of the surficial sediments in the lake vary across the lake bed?
2. Do bottom waters become temporarily deoxygenated in the lake?
3. Does sediment oxygen penetration depth vary on a spatial scale?
4. What sedimentary variables influence the sediment oxygen demand and penetration depth?
5. Is there seasonal variability in sediment oxygen penetration depth?

## METHODS

---

### **Biological and chemical oxygen demand**

Sediment oxygen demand of the surficial sediment collected from 18 sites in April 2013 was measured at near *in situ* temperature (12°C). The method was similar to that of Schallenberg & Burns (2004). One mL of sediment taken from a homogenised sample of the top 1 cm of lake bed, and was placed in 300 mL gas-tight bottles filled with milli-Q ultrapure water. Samples were run in triplicate with a series of killed controls (final concentration = 2% formalin) and blanks (only milli-Q water) which enabled the measurement of biological oxygen demand (live samples minus live blanks) and chemical oxygen demand (killed samples minus killed blanks).

Dissolved oxygen (DO) demand was measured using a YSI 158 dissolved oxygen meter and a YSI 5905 BOD probe. The probe was calibrated daily and was thoroughly rinsed in milli-Q water between measurements. The probe was allowed to stabilise (usually 1-2 minutes) prior to reading the stable output of the meter. The experiment was run for 100 hours and 5 readings were taken of each sample during the course of the experiment. DO uptake rates were approximately linear, allowing calculation of the rates using least squares linear regression. Samples which showed no significant rate of DO consumption over the 5 days, compared to the controls, were considered to have shown no DO consumption.

### **In-lake oxygen dynamics**

In-lake DO dynamics were monitored using ECAN's D-Opto optical DO monitoring sensors (Zebra-Tech Ltd). These were placed near the sediment surface and near the water surface on fixed structures at ECAN's central lake and Taumutu sampling sites. Data were downloaded and maintenance/cleaning of the sensors was usually performed every 2 to 4 weeks. Nevertheless, fouling of the optical sensors by algae and sediment accumulation on the optical sensors were often found to result in erroneous readings. Baffles were fitted to the sensors to try to minimise this problem, but they were only partially successful at alleviating it. Consequently, sensor data were carefully screened with the assistance of Alex Ring, ECAN's sensor technician and lake fieldwork officer, who performed sensor maintenance and

downloaded the data. Alex's careful attention to the state of the sensors and documentation of fouling enable the exclusion of anomalous data. Data collection at the mid-lake and Taumutu sites commenced on June 25, 2015 and June 14, 2016, respectively and ended on June 13, 2016, encompassing almost 1 full year of data. Measurements were taken at 15 minute intervals.

### **Oxygen micro-profiling (O<sub>2</sub> diffusive flux/penetration depth)**

Sediment cores for oxygen profiling were collected from a variety of sites over a 2-year period (summer 2015, winter 2015, and summer 2016) (see Section 2 for site map). Clear plexiglass sediment core tubes had an internal diameter of 6.4 cm and a length of 30 cm. Sediment cores were collected from seven sites (1, 2, 3, 5, 6, 14, 19) using a gravity corer. The depth of the sediment cored was around 15 cm, with overlying water of 15 cm. Cores were capped and returned to the lab within five hours. Two 20 L containers of site water were collected for laboratory incubations. Cores were submerged and uncapped in circulating site water maintained at an average *in situ* temperature, circulated by a water pump and aerated using an air stone. The cores were profiled as soon as possible (around two hours after incubation), to get a realistic measurement of *in situ* oxygen conditions. The oxygen sensor was a Unisense 100 µm oxygen microsensor, which was connected to a Unisense microsensor multimeter. The profiles were performed using a motorised micromanipulator. Two oxygen sensors were attached and allowed to polarize for two hours, prior to measurements being made. Once the reading had stabilized, a 2-point calibration curve was done. A 100% oxygen reading was taken from the middle of the oxygenated water column of a sediment core. The probe was then lowered deep into the sediment, until the oxygen reading reached a low stable anoxic reading. During profiling, each core was removed from the tank and placed beside the profiling arm. An air stream gently directed across the water surface to maintain circulation (previously tested for effectiveness by dye-tests) and oxygenation. Each profile began two mm above the sediment-water interface, to ensure starting above the diffusive boundary layer. The microelectrode was introduced stepwise into the sediment using a micromanipulator, run by an automated motor system. The electrode was lowered in 200 µm increments, until constant low DO values were recorded. The manipulator was set to pause three

seconds before measurement, measure two times for three seconds at each depth, and delay for one second between measurements. Three replicate profiles were done in each core, away from the edges of the core tube.

### **Sediment and invertebrate collection**

The sediment from each core was sieved through a 500 µm mesh. All infauna retained were preserved in ethanol. The sediment in the bucket was well mixed, and 200 mL of sediment was collected in a plastic vial, for analysis of particle size, organic matter and porosity. Samples for these analyses were frozen until analysis.

### **Oxygen flux calculations**

Sensortrace profiling software was used to calculate the integrated diffusive flux from the sediments. The boundary conditions were set at “bottom concentration + bottom flux”, with a max zone of 1 (due to only having a pooled measurement of porosity), and a minimum width of 200 µm.

The diffusive flux is calculated according to Fick’s first law of diffusion:

$$J = \Phi \times D \times \left(\frac{\Delta C}{\Delta Z}\right)$$

Where:

J = diffusive flux (nmol cm<sup>-2</sup> s<sup>-1</sup>)

Φ = porosity of the sediment (g/mL)

D = sediment diffusion coefficient (cm<sup>2</sup> s<sup>-1</sup>) – calculated from porosity (see below)

C = oxygen concentration (nmol cm<sup>-3</sup>)

Z = depth (cm)

$\left(\frac{\Delta C}{\Delta Z}\right)$  = concentration gradient (nmol cm<sup>-3</sup> cm<sup>-1</sup>)

The sediment diffusion coefficient ( $D_s$ ) is calculated using the measured sediment porosity ( $\Phi$ ) and the estimated dissolved oxygen coefficient in water ( $D_o$ ) (estimated from tables based on temperature and salinity) (Unisense 2014). The equation used is:

$$D_s = D_o + \Phi$$

### **Sediment Characteristics**

Sediment characteristics (organic content, porosity and particle size) were analysed as described in Section 2.

### **Invertebrate Identification**

Invertebrates were identified using a dissection microscope and identified to the lowest taxonomic level possible using identification guides by (Jones and Marsden 2005), (Moore 1997) and (Winterbourn *et al.* 2006). The wet weight of chironomids was also measured.

### **Data analysis**

All statistical analyses were carried out in R Studio v. 0.98.1049 (R Studio Inc). Linear regression and Pearson correlations were used to examine relationships between sediment characteristics and oxygen diffusive depth, oxygen demand and infaunal density. Multivariate relationships were explored with PCA using CANOCO v. 4.5 software (ter Braak & Šmilauer 2002).

## FINDINGS

### Biological and chemical oxygen demand

In general, oxygen depletion rates in the experiments were linear or near-linear, allowing the simple calculation of sediment oxygen demand by linear regression (Fig. 3.2).

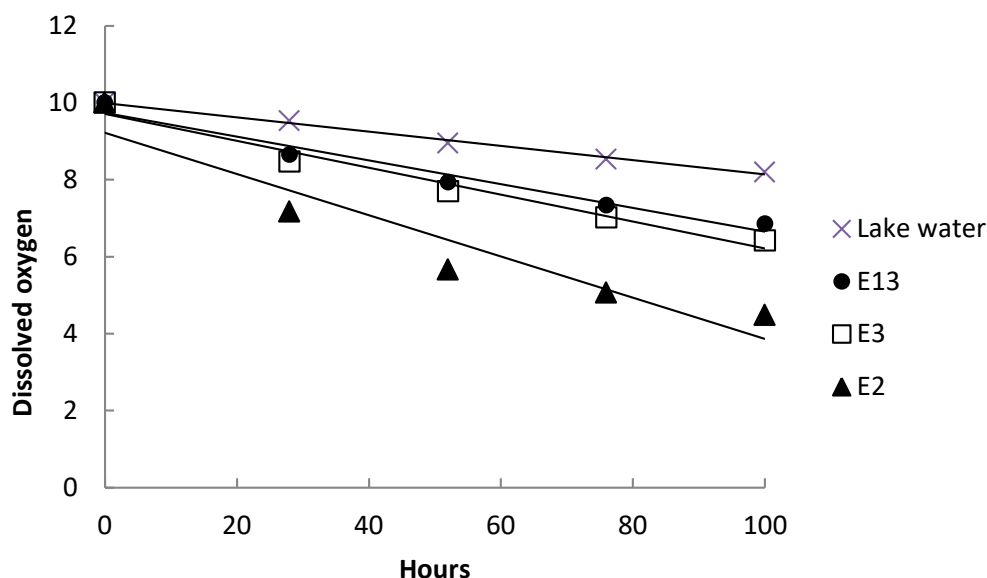


**Figure 3.2.** Range of sediment dissolved oxygen ( $\text{mg L}^{-1}$ ) depletion rates at the sites and oxygen depletion in lake water. Sediment samples were 1 mL of sediment diluted in 300 mL of sterile water. Site E13 had the lowest rate, E3 had the median rate and E2 had the maximum rate of depletion in the lake. The experiment was run near the *in situ* temperature at the time of sampling ( $12^{\circ}\text{C}$ ).

The rates of sediment oxygen demand across all the sites in Te Waihora were remarkably similar considering how different the sediment characteristics were among the 18 sites. The total sediment oxygen demand (TOD) ranged from 0.0088 to 0.0156  $\text{mg O}_2 \text{ mL}^{-1} \text{ h}^{-1}$ , which represents less than a doubling from the lowest to the highest rates (Table 3.1). Biological oxygen demand (BOD) exceeded chemical oxygen demand (COD) of the surficial sediments at all sites, with BOD averaging 75% of total sediment oxygen demand (Fig. 3.3). The depletion rate for whole lake water is shown for comparison.

**Table 3.1.** Total (TOD), chemical (COD) and biological (BOD) oxygen demand at 18 sites and in the water column of Te Waihora/Lake Ellesmere. Rates for sediment are in mg O<sub>2</sub> mL<sup>-1</sup> h<sup>-1</sup>. Rates for the lake water are mg O<sub>2</sub> L<sup>-1</sup> h<sup>-1</sup>. \*rate is for whole lake water.

Site	TOD	COD	BOD
Water	0.0186*		
E1	0.0098	0.0015	0.0083
E2	0.0156	0.0035	0.0121
E3	0.0100	0.0022	0.0078
E4	0.0103	0.0031	0.0072
E5	0.0117	0.0026	0.0090
E6	0.0091	0.0010	0.0081
E7	0.0096	0.0025	0.0071
E8	0.0102	0.0027	0.0074
E9	0.0099	0.0016	0.0082
E10	0.0113	0.0036	0.0077
E11	0.0121	0.0030	0.0091
E12	0.0102	0.0026	0.0076
E13	0.0088	0.0027	0.0061
E14	0.0089	0.0018	0.0071
E15	0.0097	0.0030	0.0067
E16	0.0099	0.0025	0.0073
E17	0.0091	0.0030	0.0061
E18	0.0102	0.0019	0.0082

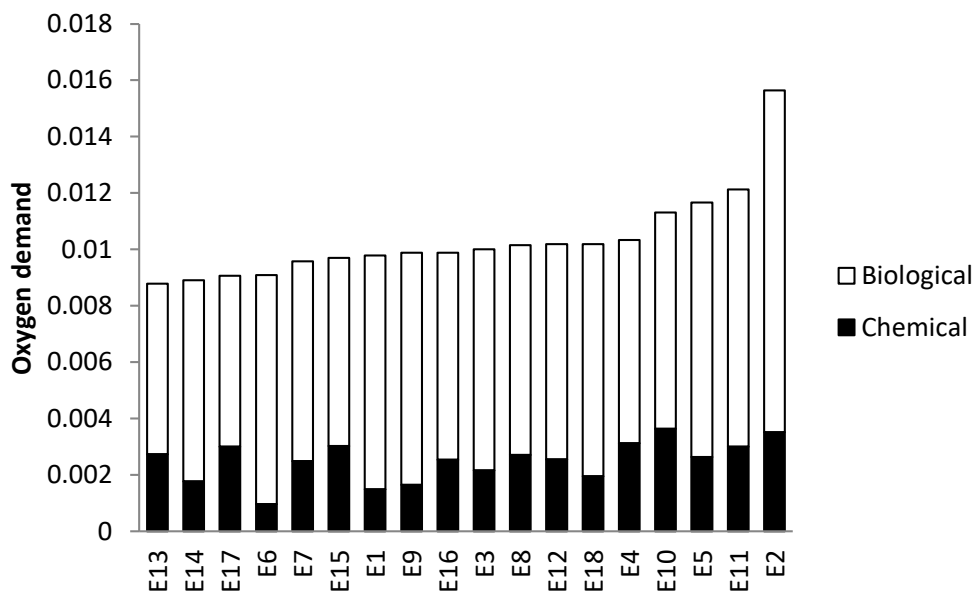


**Figure 3.3.** Sediment biological and chemical oxygen demand (mg O<sub>2</sub> mL<sup>-1</sup> h<sup>-1</sup> at 12°C) at the 18 sites, ranked from lowest to highest total oxygen demand.



Both TOD and COD were correlated to sediment grain size, porosity and redox potential across the sites. BOD did not significantly correlate with any of the sediment characteristics analysed here (Table 3.2).

**Table 3.2.** Pearson correlation matrix focusing on the relationships between total sediment oxygen demand (TOD), biological oxygen demand (BOD) and chemical oxygen demand (COD) and other sediment characteristics. Bolded correlation coefficients are statistically significant ( $P < 0.05$ ).

	TOD	COD	BOD
TOD	1		
COD	0.528	1	
BOD	0.895	0.096	1
Organic content	-0.023	0.277	-0.172
Porosity	0.559	0.555	0.365
%Clay	0.572	0.670	0.320
%Silt	0.469	0.552	0.261
%Sand	-0.498	-0.585	-0.277
Redox potential	-0.493	-0.313	-0.414
Water depth	0.554	0.569	0.351

The correlation structure among the variables is further shown in an ordination diagram generated by a principal components analysis (PCA)(Fig. 3.4). The main axis of variation in the data (axis 1 or the x-axis) represents a gradient defined by depth and sediment grain size and water content. TOD and COD correlated strongly to axis 1, with higher oxygen demand at deeper sites with higher water and clay contents and lower sand contents. TOD was also negatively correlated to sediment redox potential. BOD and organic matter content were not correlated with any variables, except for the correlation of BOD with TOD.

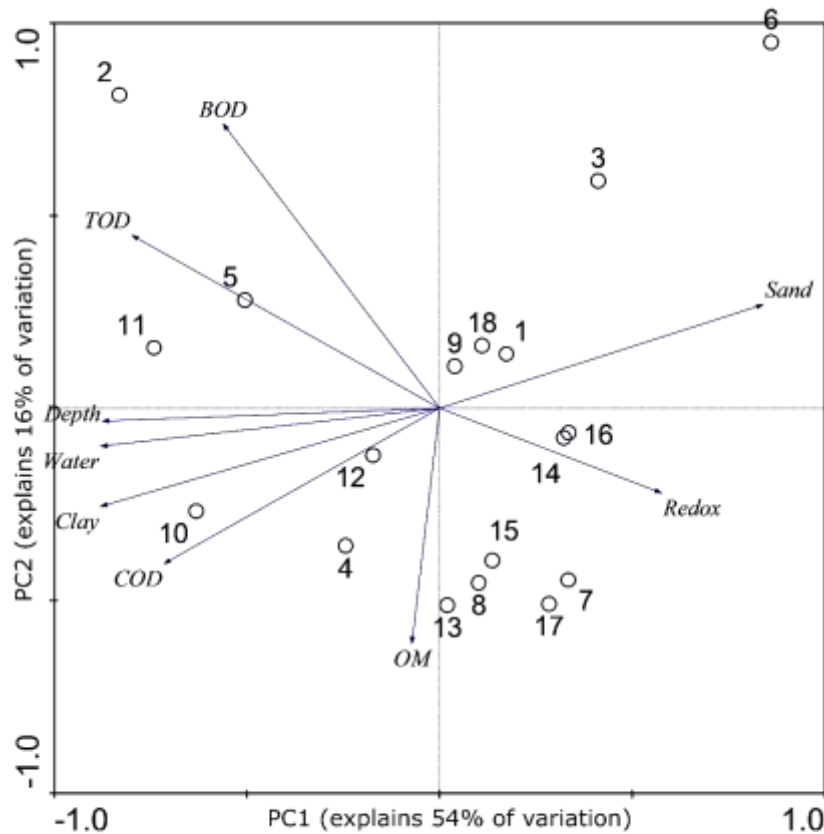


**Figure 3.4.** Ordination diagram of a principal components analysis on the correlation matrix of sediment variables from 18 sites in Te Waihora/Lake Ellesmere. See Table 3.2 for definitions of variable names. Circles and numbers represent sites.

### In-lake oxygen dynamics

Sensor data from the two sites (ECAN’s mid-lake and Taumutu sites) were subject to numerous anomalies due to sensor fouling and the anomalous data were removed from the dataset prior to analysis. At the mid-lake site, DO data were unavailable for the period between February 1 and March 3, 2016, while salinity data were unavailable between Sept 8 and December 18, 2015. Bottom water sensors were located 50 cm above the lake bed and surface water sensors were self-adjusting to maintain a water depth of 30 cm.

The *in situ* DO sensors clearly showed that bottom water DO concentrations did plummet at times at the mid-lake site (Fig. 3.5). Numerous brief dips in DO were recorded in the summer and autumn months only (i.e. December to May).

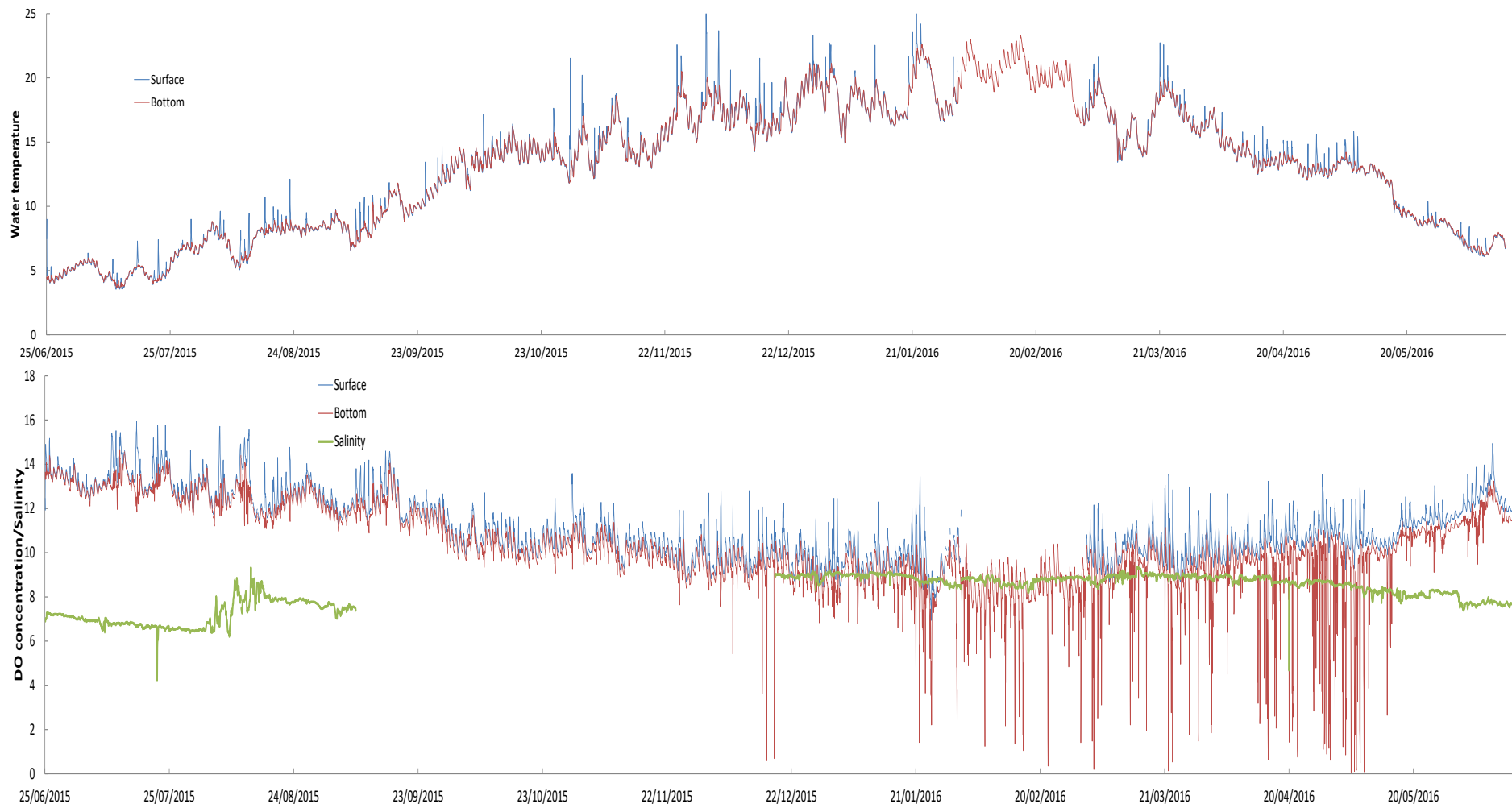


**Figure 3.5.** Temperature, dissolved oxygen ( $\text{mg L}^{-1}$ ) and salinity (ppt) dynamics at the mid-lake site from June 2015 to June 2016. The blue line is data from 30 cm below the lake surface. The red line is data from 50 cm above the lake bed. The green line is salinity (interrupted due to sensor malfunction).

These temporary periods of oxygen depletion were not recorded by the surface DO sensor, indicating that the lake bed was the major driver of oxygen depletion during these periods of hypoxia. As the bottom water data were recorded 50 cm above the lake bed, DO depletion at the sediment-water interface would have been somewhat greater than is indicated in Fig. 3.5.

The number of severe oxygen depletion events recorded at the mid-lake site are shown in Figure 3.6. Only 5 events of complete anoxia occurred at 50 cm above the lake bed, whereas DO decreased to less than 2.0 mg L<sup>-1</sup> on sixty-two occasions, over forty-two days.

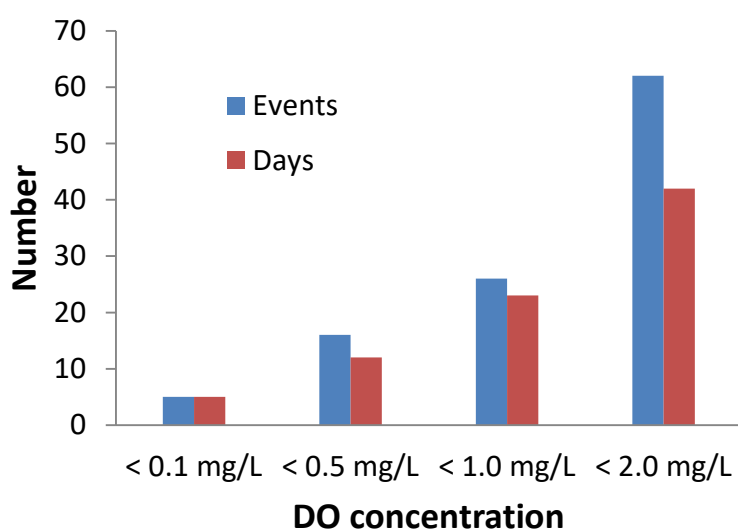


**Figure 3.6.** Number of severe oxygen depletion events over the measurement period at the mid-lake site. Data are shown both as the number of events as well as the number of days during which such events occurred.

In addition to the magnitude of oxygen depletion the severity of hypoxic events is also dependent on their duration. The maximum durations of events of different oxygen depletion magnitudes is shown in Figure 3.7. Hypoxia events where DO declined to below 2.0 mg L<sup>-1</sup> lasted less than 3.5 h and the percentage of time represented by these depletion events was less than 1% of the year (around 2 days in total). Complete deoxygenation (i.e. < 0.1 mg L<sup>-1</sup>) occurred for a total of 1.25 h over the measurement period. In general, oxygen depletion recorded in the deep

waters of the mid-lake site was a transient phenomenon, lasting for minutes to hours and in total comprising a very small proportion of time.

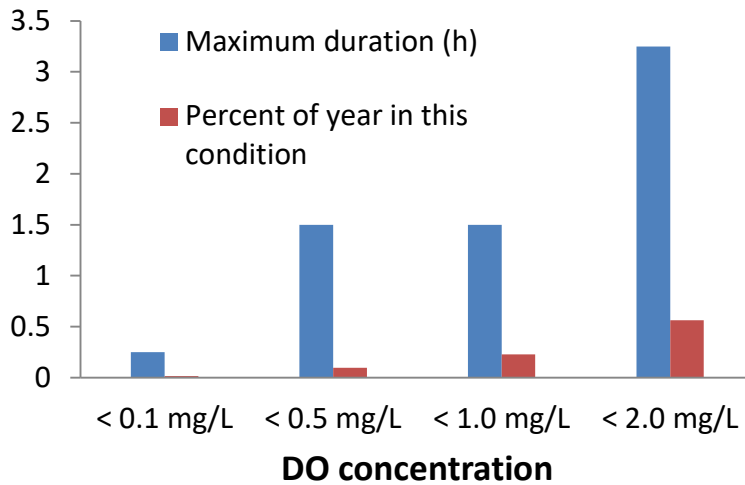


**Figure 3.7.** The maximum durations of deoxygenation events of various severities and the total percentage of time events of various severities were recorded over the study period.

As at the mid-lake site, the transient deoxygenation events that went below  $5 \text{ mg L}^{-1}$  in the bottom waters at the Taumutu site occurred only in the summer and autumn (January to April). However, deoxygenation events at Taumutu were much rarer than at the deeper, mid-lake site and DO in the bottom waters never decreased below  $1.3 \text{ mg L}^{-1}$  (Fig. 3.8); in the most severe case in January 2015, such low levels lasted only 45 minutes before the water was reaerated.

The transient DO depletion events tended to occur during the summer and autumn seasons, when water temperatures were at or above  $15^\circ\text{C}$  at the mid-lake site and  $17^\circ\text{C}$  at the Taumutu site. Respiration by microbes and benthic invertebrates is likely to be a key driver of oxygen depletion and, consequently, depletion events coincided with higher temperatures due to the temperature dependence of respiration in the surficial sediments.

Persistent vertical density stratification could result in the separation of bottom waters from the atmosphere and facilitate deoxygenation. Both temperature stratification and salinity stratification have the potential to cause incomplete water column mixing under certain conditions, potentially resulting in oxygen depletion of

the bottom waters. However, Figure's 3.4 and 3.8 don't show evidence that either temperature- or salinity-driven persistent density stratification occurred at either of the two sites. The temperature dynamics of the surface and bottom waters show little differentiation in temperatures at both sites and when diel surface warming occurred, it wasn't frequently associated with transient oxygen depletion events (see Fig. 3.5). So while seasonal temperature effects are important, diel thermal stratification isn't strongly associated with transient DO depletion in the bottom waters.

Salt wedges, if they form in the lake could also potentially cause DO depletion events. In Figure 3.8, the salinity dynamics at Taumutu clearly show periods when the lake was open to the sea and also show episodic marine spill-over events which caused transient salinity spikes. The salt water entering the lake during barrier bar openings and spill-over events has the potential to cause density stratification due to the higher density of salt water than fresh or brackish water. However, scrutiny of the DO data at Taumutu shows that these saline intrusions didn't result in deoxygenation at the time. However, so far the record of DO dynamics in relation to lake openings is sparse and the potential for salt wedges to form as a result of saline intrusions requires further study.

The salinity time series at the mid-lake site is much less dynamic (Fig. 3.5) because of the farther distances from the barrier bar and opening site and because of the poor tidal flushing of Te Waihora/Lake Ellesmere (Schallenberg et al. 2010). Nevertheless, some minor changes in salinity occurred in response to the lake opening of August 2015. The increase in salinity of around 3 ppt associated with the opening didn't cause deoxygenation. The lack of a deoxygenation event in relation to saline intrusion may have been due to the fact that the event happened in winter instead of summer. While our data show that winter saline intrusions do not cause deoxygenation events in the bottom waters, it is possible that summer intrusions could vertically stratify the lake waters and exacerbate deoxygenation. Continued monitoring of DO concentrations at ECAN's monitoring stations should indicate whether or not salinity stratification in summer intensifies periods of anoxia in the bottom waters of Te Waihora/Lake Ellesmere.

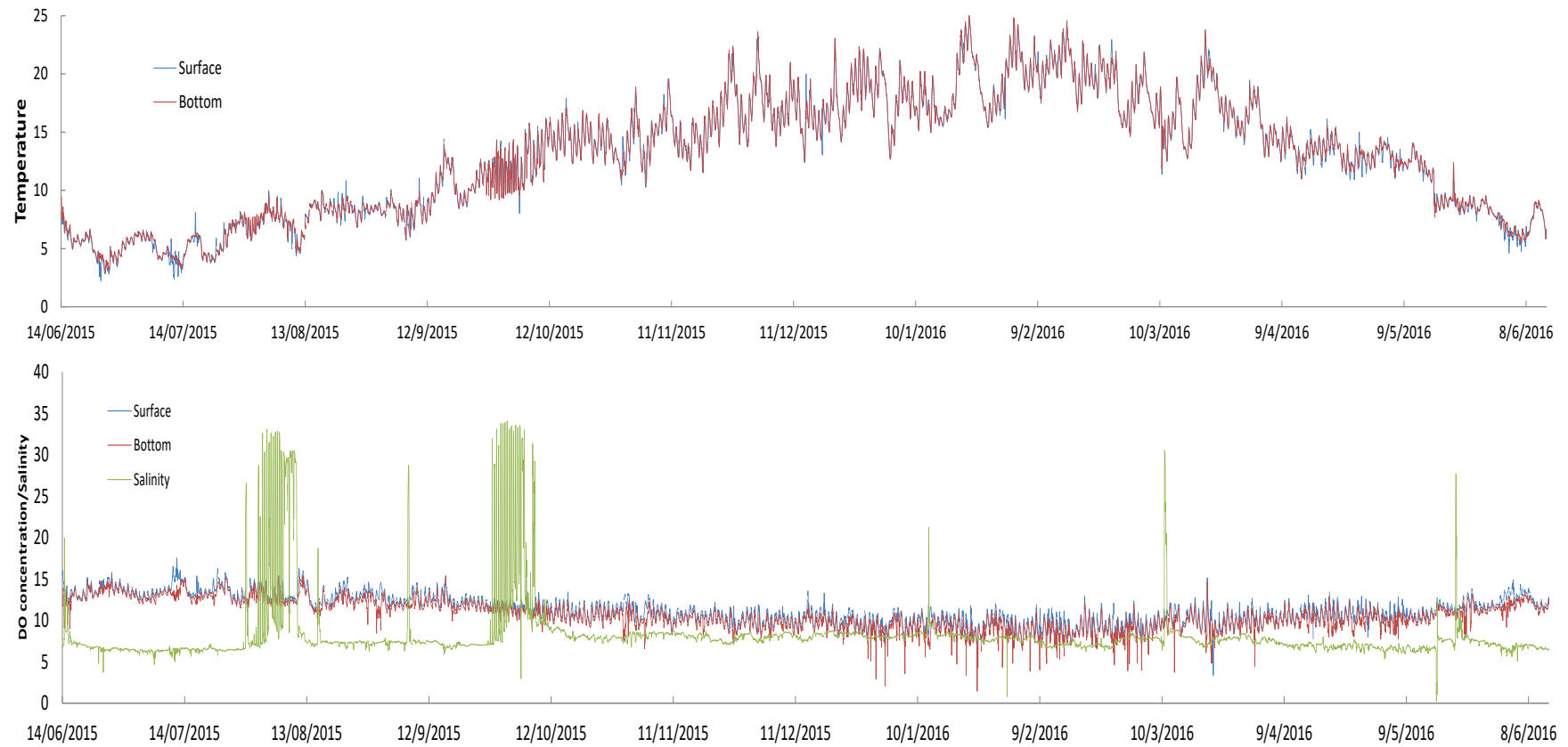


**Figure 3.8.** Temperature, dissolved oxygen ( $\text{mg L}^{-1}$ ) and salinity (ppt) dynamics at the Taumutu site measured from June 2015 to June 2016. The blue line is data from 30 cm below the lake surface. The red line is data from 50 cm above the lake bed. The green line is salinity.

So it appears that density stratification played little, if any, role in stimulating the transient deoxygenation events recorded in the lake. Analysis of wind data collected from the mid-lake monitoring station showed clearly that anoxia events at the mid-lake site only occurred when the wind speed was below 4 m s<sup>-1</sup> (Fig. 3.9). Closer scrutiny of the data showed that wind velocities just prior to the onset of most of the deoxygenation events were less than 2.5 m s<sup>-1</sup> (data not shown). Thus, while density stratification wasn't a key driver of transient oxygen depletion events, calm conditions in summer and autumn did very often encourage such events. In fact, during calm conditions in summer, oxygen depletion in the bottom waters proceeded so quickly that as little as 1.5 or 2 hours of calm conditions (< 2.5 m s<sup>-1</sup>) often produced a decline of DO concentrations from saturation to < 2.0 mg L<sup>-1</sup> in the bottom waters of the lake. An increase in wind velocity to above 2.5 m s<sup>-1</sup> seems to reaerate the bottom waters within 15 minutes.

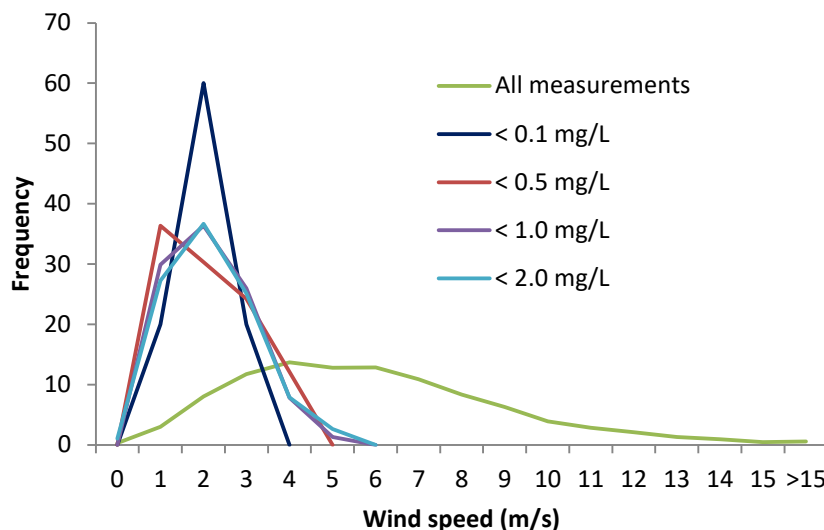


**Figure 3.9.** Frequency plot showing the % frequency distributions of all the wind data (15 minute intervals) from the mid lake site as well as the frequency distributions for winds recorded at the times of oxygen depletion events of various severities. Data cover the study period (see Fig. 3.5 and Fig. 3.8).

These extremely rapid and large magnitude DO dynamics indicate that the bottom waters and sediments of the deeper basin of the lake undergo extremely rapid oxygenation/deoxygenation dynamics and that these are largely driven by wind. However, scrutiny of the time series showed that not all calm periods in summer



resulted in deoxygenation events, but that such events were more likely to occur during calm days than calm nights (although they also occasionally occurred at night too). This suggests an important interaction between the dominant wind driver of deoxygenation and a diel thermal stratification to produce strong bottom water deoxygenation in the deeper waters of Te Waihora/Lake Ellesmere.

### Spatial and seasonal variation in sediment oxygen penetration

To investigate seasonal and spatial variability in sediment oxygen conditions, sediment penetration depth was measured across a number of sites (Fig. 3.10). Figure 3.10 shows the average oxygen penetration depth in the sediments across the sites and sampling dates. A large amount of spatial variation is evident between sites due to variation in sediment grain size.

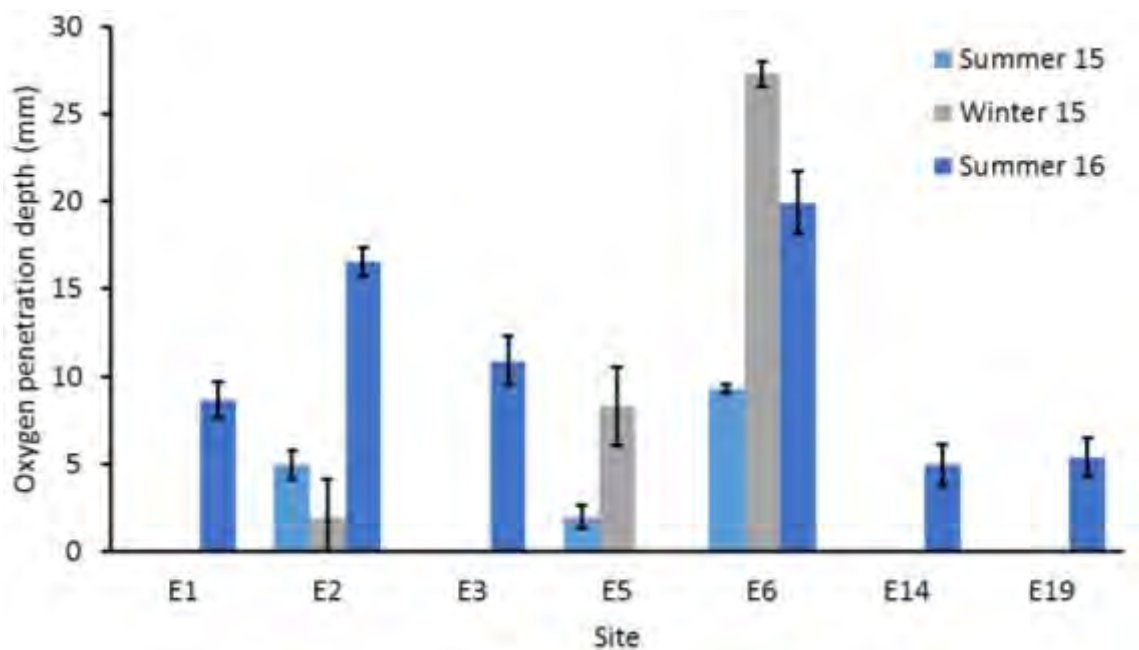


**Figure 3.10.** Sediment oxygen penetration depth measured by oxygen micro-sensors across multiple sites and seasons. Error bars are standard errors. The lack of a bar means DO penetration depth was not measured at that site during that season.

Site 2 showed highly variable sediment characteristics due to the site being located at the mouth of the Selwyn River (Table 3.3). The silt content decreased over our sampling period and consequently, the oxygen penetration depth increased from

summer 2015 to summer 2016. The sediment grain size at sites 5 and 6 did not change significantly over time.

### Sediment controls on oxygen penetration depth

Sediment porosity exerted strong control over oxygen penetration depth (Fig. 3.11); in summer 2016 there were strong negative relationships between oxygen penetration depth and porosity ( $r=-0.87$ ), organic matter concentration ( $r=-0.77$ ), %clay ( $r=-0.62$ ), %silt ( $r=-0.82$ ) and a positive relationship with %sand ( $r=0.82$ ) (Table 3.4). As was shown in Section 2, these sedimentary variables were inter-related throughout the lake. As such, it isn't possible to attribute differences in the oxygen penetration depth to any one variable; rather DO penetration depth related to a gradient of grain size, organic matter and porosity in the lake. These same relationships were quite consistent over the three sampling times (Tables 3.4 to 3.6).

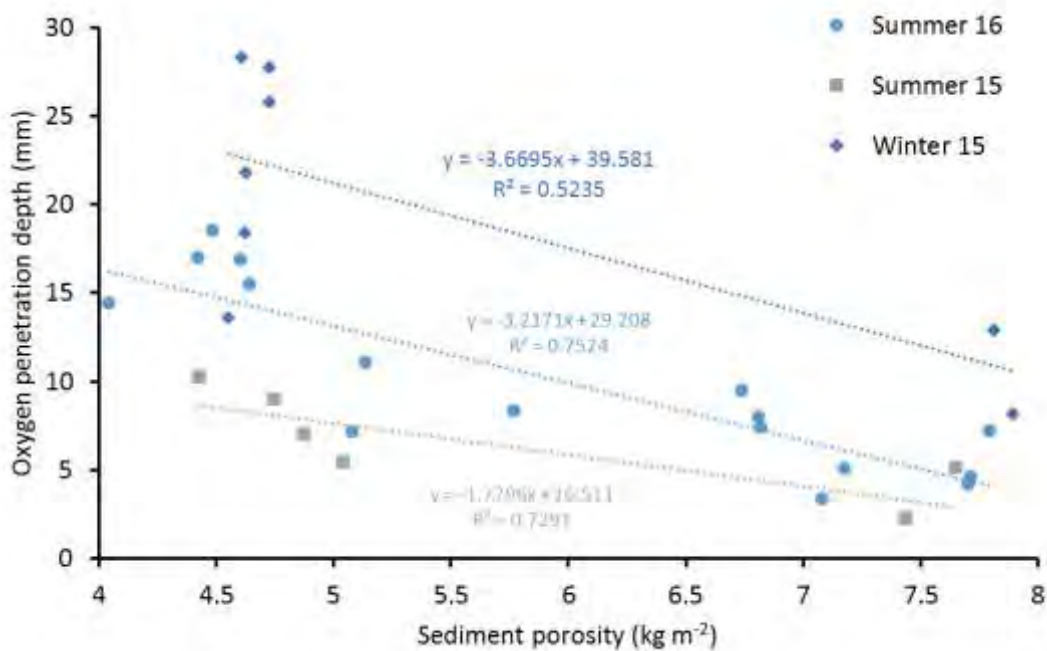


**Figure 3.11.** The effect of sediment porosity on oxygen penetration depth (mm) at the time of the three sampling campaigns.

**Table 3.3.** Sediment characteristics in the cores in which oxygen penetration depth was measured, showing site averages and standard errors across sampling campaigns. NA indicates variables were not recorded.

Variable	E1	E2			E3	E5		E6			E14	Ex
	Sum 16	Sum 15	Win 15	Sum 16	Sum 16	Sum 15	Win 15	Sum 15	Win 15	Sum 16	Sum 16	Sum 16
Temperature (°C)	16.73 ± 0.39	18.06 ± 0.16	8.06 ± 0.14	16.73 ± 0.39	16.73 ± 0.39	18.06 ± 0.16	8.06 ± 0.14	18.06 ± 0.16	8.06 ± 0.14	16.73 ± 0.39	16.73 ± 0.39	16.73 ± 0.39
Porosity (kg m <sup>-2</sup> )	6.44 ± 0.34	5.78 ± 0.83	4.60 ± 0.02	4.56 ± 0.07	4.75 ± 0.35	7.54 ± 0.07	7.85 ± 0.04	4.59 ± 0.16	4.69 ± 0.04	4.49 ± 0	7.02 ± 0.11	7.73 ± 0.03
Organic matter (kg m <sup>-2</sup> ) LOI	0.85 ± 0.06	0.49 ± 0.06	0.41 ± 0.05	0.74 ± 0	0.53 ± 0.02	0.8 ± 0.1	0.77 ± 0	0.43 ± 0.02	0.31 ± 0	0.39 ± 0.01	0.76 ± 0.05	1.22 ± 0.08
Clay %	3.44 ± 1.53	1.61 ± 1.03	0.63 ± 0.42	0	0.29 ± 0.17	3.76 ± 0.12	5.38 ± 0.17	0	0	0.25 ± 0.25	4.66 ± 1.54	3.23 ± 0.15
Silt %	34.21 ± 5.60	39.05 ± 24.81	4.12 ± 2.96	0	2.88 ± 1.50	89.01 ± 0.60	90.71 ± 0.27	0	0	1.42 ± 1.42	48.16 ± 1.17	64.87 ± 2.48
Sand %	62.35 ± 6.58	59.34 ± 25.84	95.26 ± 3.38	100	96.83 ± 1.62	7.23 ± 0.72	3.91 ± 0.21	100	100	98.33 ± 1.67	47.19 ± 1.09	31.90 ± 2.62
Oxygen penetration depth (mm)	8.64 ± 0.46	4.96 ± 1.39	17.93 ± 2.38	16.46 ± 0.48	10.89 ± 2.08	3.53 ± 0.84	8.29 ± 2.66	9.63 ± 0.63	27.29 ± 0.76	19.93 ± 2.14	5.29 ± 1.16	5.38 ± 0.95
Redox potential (mV)	-30.33 ± 25.37	NA	98.67 ± 18.49	80 ± 8.66	116 ± 9	NA	-176 ± 34.43	NA	44 ± 14.47	77 ± 15.70	-65.33 ± 31.25	62.67 ± 42.12

The relationships we observed between sediment porosity and DO penetration depth may seem counterintuitive, but porosity has been shown to decrease oxygen diffusion depth in some cases (Groffman and Tiedje 1991; Smith *et al.* 2003). In Te Waihora/Lake Ellesmere, fine grained sediments have greater porosity which should theoretically enhance the diffusion and advection of gases and solutes. However, in addition to having greater concentrations of organic matter, finer sediments in this lake are also much more cohesive, probably due to the presence of polysaccharides which may inhibit diffusion and advection within the sediments and increase the potential for anoxic microsites formation (Groffman and Tiedje 1991; Solomon *et al.* 2009) and rapid depletion of DO with depth. In fact, sediment oxygen demand was greater in the finer sediments from deeper sites, which is consistent with fine particles provide a greater surface area for microbial organisms to colonize (García *et al.* 1998; Pattinson *et al.* 1998; Inwood *et al.* 2007; Santmire and Leff 2007). In contrast, in the shallower, lower porosity sediments of Te Waihora/Lake Ellesmere, oxygen demand was lower and oxygen penetration depth was deeper, pushing the anoxic sediment boundary further away from the water column.

**Table 3.4.** Pearson correlation matrix for data collected in summer 2016 in cores in which oxygen penetration depth (Diff O2) was measured. \*\*\* =  $p < 0.001$ , \*\* =  $p < 0.01$ , \* =  $p < 0.05$ . *P.ant* – density of *Potamopyrgus antipodarum*; *P.exc* – density of *Paracarophium excavatum*; *Olig* – density of oligochaetes; *Chiro* – density of chironomids; *Neridae* – density of Nereidae.

	Diff O2	OM	Clay	Silt	Sand	Porosity	<i>P.ant</i>	<i>P.exc</i>	<i>Olig</i>	<i>Chiro</i>	<i>Neridae</i>
Diff O2											
OM	-0.77***										
Clay	-0.62**	0.64**									
Silt	-0.82***	0.96***	0.76***								
Sand	0.82***	-0.95***	-0.79***	-1.00***							
Porosity	-0.87***	0.96***	0.74***	0.99***	-0.99***						
<i>P.ant</i>	-0.33	0.16	0.39	0.28	-0.3	0.29					
<i>P.exc</i>	-0.29	0.05	0.46	0.17	-0.19	0.24	0.81***				
<i>Olig</i>	0.38	-0.3	-0.15	-0.25	0.25	-0.26	-0.21	0.01			
<i>Chiro</i>	-0.60**	0.57*	0.71***	0.69**	-0.70**	0.68**	0.85***	0.62**	-0.2		
<i>Neridae</i>	-0.21	-0.03	0.08	-0.1	0.09	0.02	-0.14	0.24	-0.18	-0.2	
Redox	0.43	-0.46	-0.76***	-0.53*	0.55*	-0.52*	-0.55*	-0.51*	0.19	-0.68**	0.02

**Table 3.5.** Pearson correlation matrix for data collected in summer 2015 in cores in which oxygen penetration depth (Diff O2) was measured. \*\*\* =  $p < 0.001$ , \*\* =  $p < 0.01$ , \* =  $p < 0.05$ . *P.ant* – density of *Potamopyrgus antipodarum*; *P.exc* – density of *Paracarophium excavatum*.

	Diff O2	OM	Clay	Silt	Sand	Porosity	<i>P.ant</i>	<i>P.exc</i>
Diff O2								
OM	-0.67							
Clay	-0.90**	0.61						
Silt	-0.90**	0.61	1.00***					
Sand	0.90**	-0.61	-1.00***	-1.00***				
Porosity	-0.85*	0.53	0.99***	0.99***	-0.99***			
<i>P.ant</i>	0.72*	-0.93**	-0.68	-0.69	0.69	-0.66		
<i>P.exc</i>	0.80*	-0.36	-0.5	-0.49	0.49	-0.4	0.5	
<i>Olig</i>	0.85**	-0.23	-0.77*	-0.76*	0.76*	-0.75	0.38	0.81**

**Table 3.6.** Pearson correlation matrix for data collected in winter 2015 in cores in which oxygen penetration depth (Diff O2) was measured. \*\*\* =  $p < 0.001$ , \*\* =  $p < 0.01$ , \* =  $p < 0.05$ . *P.ant* – density of *Potamopyrgus antipodarum*; *P.exc* – density of *Paracarophium excavatum*.

	Diff O2	OM	Clay	Silt	Sand	Porosity	<i>P.ant</i>	<i>P.exc</i>
Diff.O2								
OM	-0.88**							
Clay	-0.88**	0.97***						
Silt	-0.84**	0.96***	0.99***					
Sand	0.84**	-0.96***	-0.99***	-1.00***				
Porosity	-0.72*	0.92**	0.97***	0.99***	-0.99***			
<i>P.ant</i>	-0.77*	0.92**	0.97***	0.97***	-0.97***	0.99***		
<i>P.exc</i>	0.39	-0.39	-0.11	-0.02	0.02	-0.05	-0.01	
<i>Olig</i>	0.91***	-0.81*	-0.76*	-0.70*	0.70*	-0.59	-0.66	0.67*

Oxygen penetration depths in the cores was also strongly positively related to the density of oligochaetes in summer and winter 2015 (Fig. 3.12), which were the only bioturbating infauna present in the cores for which DO penetration depth was measured during these sampling campaigns. Previous research into the bioturbation effect of oligochaetes on nitrogen cycling suggest that in high densities, they can be important in nitrogen cycling, however, they are not as efficient in this as chironomid larvae are (Svensson *et al.* 2001).

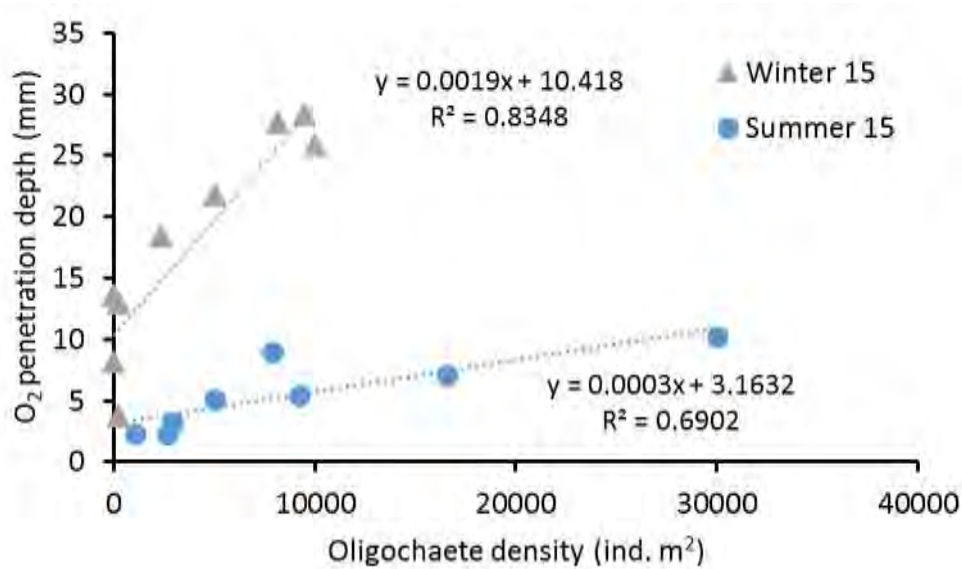


**Figure 3.12.** Relationships between oxygen penetration depth (mm) and the density of oligochaetes in winter and summer 2015.

Chironomid larvae were not present at any of our sites until summer 2016, when their density was positively related to porosity ( $r=0.68$ ), %clay ( $r=0.71$ ), %silt ( $r=0.69$ ) and negatively related to %sand ( $r=-0.70$ ), oxygen penetration depth ( $r=-0.60$ ) and redox potential ( $r=-0.68$ ). As chironomids have visible burrows (tubes) protruding out of the sediment, oxygen penetration measurements were made away from the burrows. Nevertheless, beneath the sediment surface, we sometimes measured DO through burrows and Fig. 3.13 shows how chironomid burrows oxygenate the bulk sediment. Observations of lake sediment containing chironomid burrows showed that the oxygenation effect was limited to sediment in contact with the burrow walls (the polysaccharide tubes). These burrows



increase the oxygenated surface area of the sediment, potentially creating sites of high denitrification activity associated with the burrow walls.

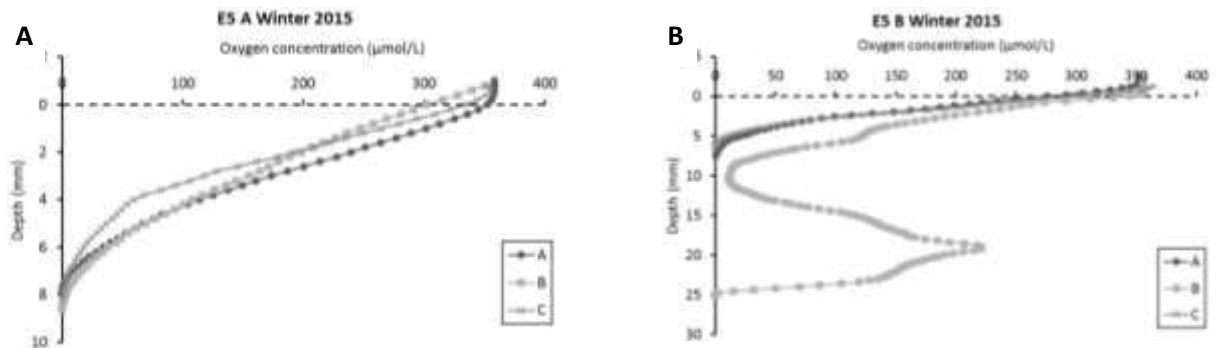


**Figure 3.13.** The effect of benthic infauna burrows on sediment oxygen microprofiles. A = oxygen profiles unaffected by bioturbation, B = two oxygen profiles unaffected by bioturbation, while profile replicate B crossed through an infaunal burrow increasing oxygen penetration in the deeper sediment layers.

By influencing the rate of respiration in the sediments, temperature can influence sediment oxygenation, and hence, biogeochemical processes such as phosphorus binding and denitrification (Fig. 3.14). Summer water temperatures during our sampling campaigns were around 17°C, whereas winter temperatures were around 9°C. At the three sites where oxygen penetration depth was measured in cores, the average penetration depths were shallower in summer than in winter ( $p < 0.01$ ), despite the fact that the effects of winds, turbulence and sediment resuspension are stronger in summer (Hamill & Schallenberg 2013). This suggests that temperature exerts a dominant effect on sediment oxygenation over annual time scales in Te Waihora/Lake Ellesmere.

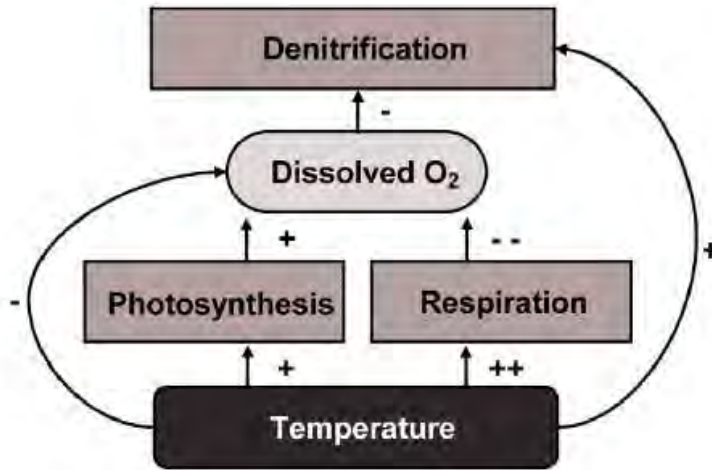


**Figure 3.14.** A schematic diagram of the effects of temperature on dissolved oxygen concentration and denitrification. Taken from (Veraart *et al.* 2011). + and - indicate the direction and strength of relationships.

Principal components analysis was used to help visualize the relationships between sediment variables and oxygen penetration depth. Due to the strong influence of temperature on DO penetration depth, the data collected in the three sampling campaigns were analysed separately. Summer 2015 and winter 2015 showed similar patterns among sediment variables (Figs. 3.15, 3.16), with the dominant gradient being represented by DO diffusion depth and invertebrate densities which were negatively correlated with the finer sediment particle fractions. Sediment porosity and organic matter concentration together represented axis 2 and seemed to be driven by large within-site variation in these variables at site E5 in both winter and summer, 2015 and at site E6 in summer 2015.

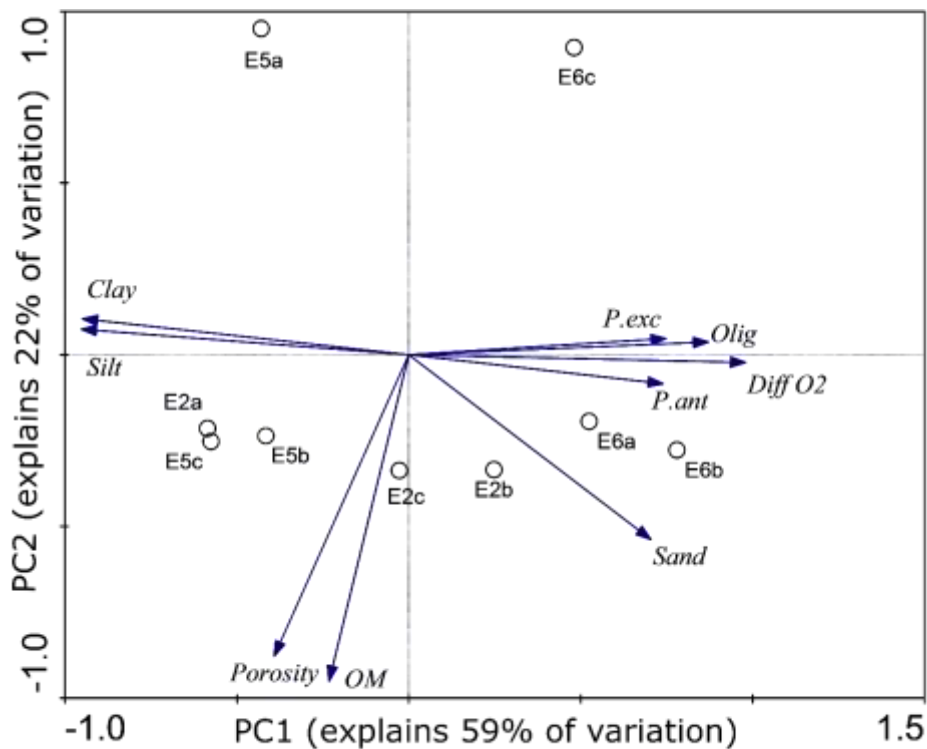


**Figure 3.15.** Principal components analysis showing correlations among variables in summer 2015. *Clay*, *Silt* and *Sand* indicate the percentage composition of sediment particles in the indicated size classes. *OM* indicates sediment organic matter concentration ( $\text{mg m}^{-2}$ ). *P. ant* indicates the density of the snail, *Potamopyrgus antipodarum*. *P. exc* indicates the density of the amphipod, *Paracorophium excavatum*. *Oligo* indicates the density of oligochaetes. *Diff O2* indicates the oxygen penetration depth. Codes and circles refer to sites and replicates (replicate a, b or c).

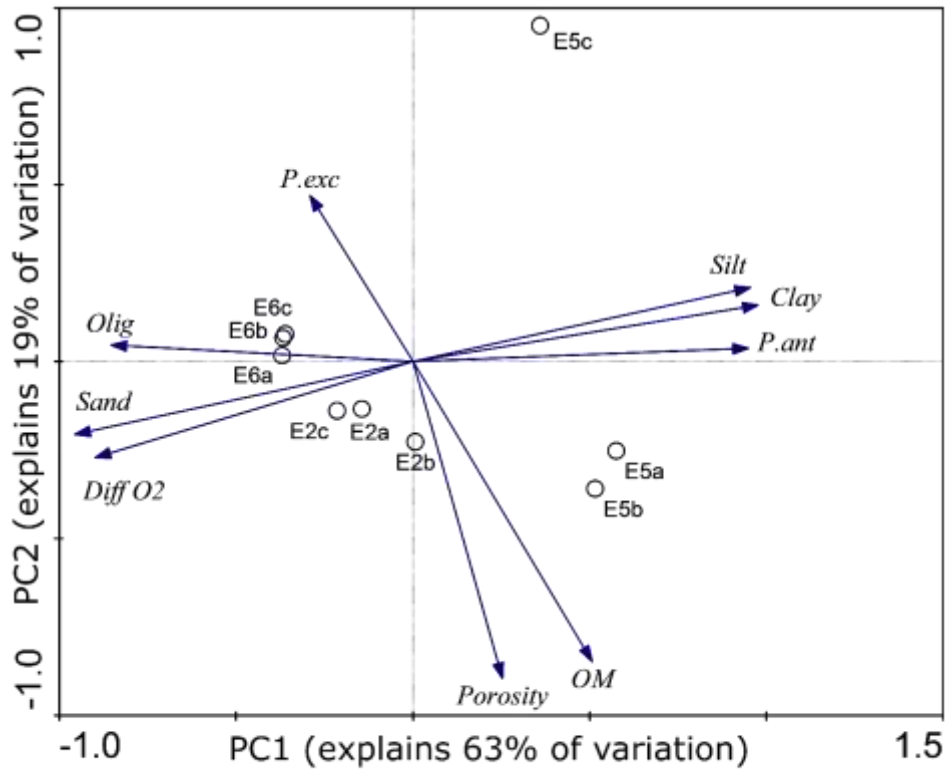


**Figure 3.16.** Principal components analysis showing correlations among variables in winter 2015. See Fig. 3.15 for explanation of symbols and labels. Axes 1 and 2 explained 63% and 19% of the total variation in the data, respectively.

In summer 2016, six sites were studied. Again, the dominant gradient in the data was that of sediment grain size and DO diffusion depth (Fig. 3.15). Sediment redox potential was also measured and it is not surprising that it correlated positively with sand content and DO diffusion depth. Within this larger dataset, porosity and organic content correlated strongly and positively with the silt fraction of the sediment and chironomids correlated positively with the clay fraction of the sediment, whereas, snails and amphipods didn't correlate strongly with the primary sediment and oxygen gradient.

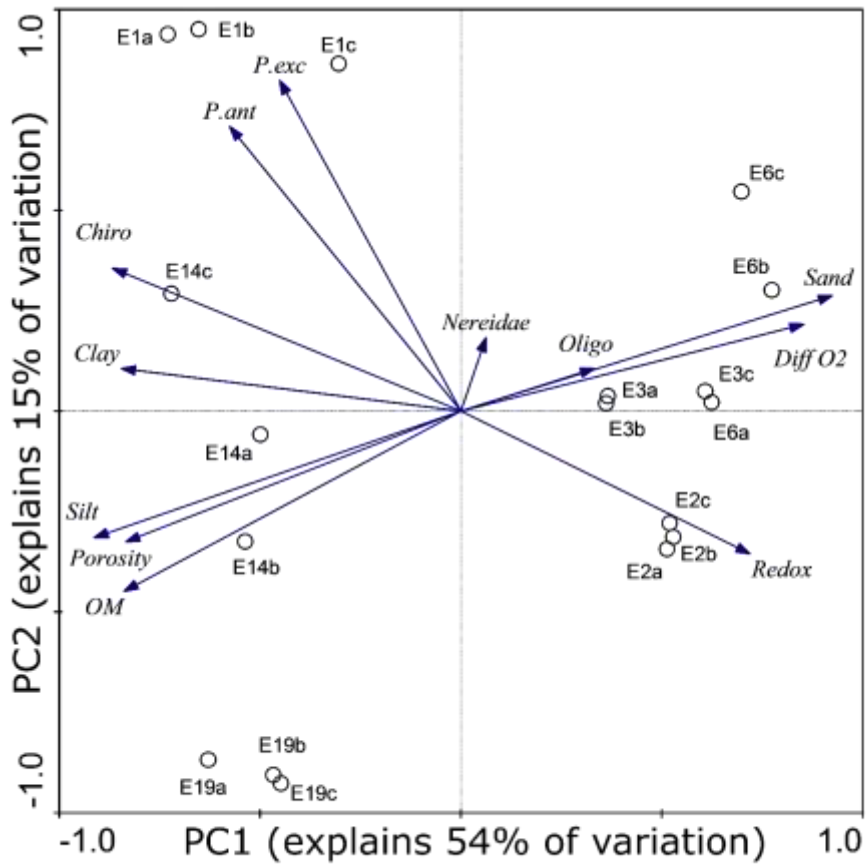


**Figure 3.17.** Principal components analysis showing correlations among variables in summer 2016. *Nereidae* indicates the density of polychaetes. *Chiro* indicates chironomid density. *Oligo* indicates oligochaete density. *Redox* indicates sediment redox potential. See Fig. 3.15 for explanation of other labels and symbols.

## CONCLUSIONS

---

The deployment of in-lake DO sensors provided a highly detailed picture of DO dynamics in the water column at two sites. Episodes of depletion of bottom water dissolved oxygen occurred only during summer and autumn at the sites. Extremely rapid rates of bottom water DO depletion occurred almost exclusively during calm periods, when wind-induced turbulence and reaeration was minimal. While there was a pronounced diel cycle in DO dynamics, the transient DO depletion episodes occurred at any time of day or night when winds were calm, but occurred most often during the day. DO depletion in bottom waters at the mid-lake site almost always occurred as a result of wind velocities falling to below  $2.5 \text{ m s}^{-1}$  and were terminated when wind velocities increased above  $2.5 \text{ m s}^{-1}$ . Density stratification appeared to play only a secondary role in deoxygenation when daytime surface water warming increased water column stability. These result may explain reports of tuna/eels sometimes dying when trapped in fyke nets during warm, calm weather (Gibbs & Norton 2013).

Surficial sediment oxygen demand only varied approximately 2-fold among the 18 sites sampled. Biological DO demand was on average three times greater than chemical oxygen demand. Total sediment oxygen demand was most strongly correlated to a gradient of water depth and grain size, with the highest rates occurring at deeper sites, dominated by fine sediments. Sediment redox potential was also correlated to total and chemical oxygen demand, with more reducing sediments showing greater DO uptake.

Oxygen penetration depths were also controlled by the sediment grain size gradient, with the high water, clay, silt and organic matter contents correlating to shallower DO penetration depths. Oligochaete density in the sediment was positively related to the sediment oxygenation in summer and winter 2015. Higher temperatures in summer reduced oxygen penetration depth, probably due to the stimulation of sediment microbial respiration, but possibly also due to transient thermal stratification events and associated oxygen depletion in the bottom waters.

---

## Section 4

---

### 4 SEDIMENT NUTRIENT POOLS AND FLUXES UNDER CONDITIONS OF ANOXIA

---



Sediment core collected at site E18, containing chironomid tubes.

## INTRODUCTION

---

### Internal P loading

Both nutrient budgets and an analysis of N:P ratios of tributary inflows and lake water suggest that internal P loading could be an important mechanism supplying P to the water column and ultimately to phytoplankton in Te Waihora/Lake Ellesmere (See Section 1).

Wind induced sediment resuspension is a known source of total phosphorus to the water column of the lake (Hamilton and Mitchell 1997), but the extents to which sediment resuspension provides i) phosphorus in forms available to phytoplankton, ii) re-suspends living algae from the surface sediments of the lake bed, or iii) provides a longer term net flux of P to the water column are not known. Schallenberg and Burns (2004) examined these issues in Lake Waiholo, a shallow coastal Otago lake, and found that wind-induced sediment resuspension did entrain algae from the lake bed into the water column (increasing chlorophyll *a* concentrations in the water) but that the amount of available nutrient supplied by these events was not substantial because frequent resuspension events re-equilibrated sediment pore water nutrient concentrations with water column nutrient concentrations. Thus, in lakes that experience frequent wind-induced sediment resuspension, surface sediment pore water nutrient concentrations are not likely to rise much above water column nutrient concentrations.

Te Waihora/Lake Ellesmere is a polymictic lake, meaning that it doesn't undergo vertical density stratification on a seasonal basis. Implicit in the word polymictic is that the lake undergoes mixing frequently and therefore stratifies transiently, if at all. An important question regarding the potential for internal P loading in the lake is, how frequent and persistent are transient vertical stratification events in the lake and could they lead to deoxygenation of bottom waters and a release of redox-exchangeable P from sediments to the pore water and into the water column? Under oxygenated conditions, P binds to a variety of minerals including iron and manganese oxyhydroxides, which are common in many lake sediments. Under anoxia, these minerals dissolve, releasing any P bound to them into sediment pore waters as bioavailable, dissolved phosphate (Golterman 2007). In some seasonally stratified lakes, this anoxic release of previously bound P can represent a major



fraction of the annual P load to the water column and can stimulate phytoplankton blooms (Kalff 2002).

### Research objectives

Our studies aimed to answer the following questions about internal P loading in Te Waihora/Lake Ellesmere:

1. What potentially available fractions of P are found in the sediment of Te Waihora?
2. Does the surface sediment of Te Waihora contain pools of phosphorus that could be released to the water column under periods of anoxia?
3. How does the amount of redox-exchangeable P in the sediment vary across the lake?
4. Do any of the geochemical P fractions in the sediments correlate with the amount of P released from the sediment under anoxic conditions?
5. Does the surface sediment of Te Waihora also release N under anoxic conditions?



The SF Mitchell during the winter 2015 sampling.

## METHODS

---

### Redox-exchangeable P and N

Surficial sediment samples for the measurement of redox-exchangeable P and N were obtained using a gravity corer from 18 sites (E1 – E18) on April 9-10, 2013. A number of sediment cores were immediately extruded and the top 10 mm of the cores were retained for analysis. Samples were pooled into clean falcon tubes until the tubes were filled. They were sealed and placed on ice and subsequently frozen upon returning to the lab.

Sediments were thawed and homogenised in the lab and 1 mL was placed in each of four 15 mL test tubes. Thirteen mL of buffer (2000mM NaHCO<sub>3</sub> made up in Milli-Q water) was added to each tube. Blanks containing only buffer water were also prepared. Two subsamples from each site were placed in an anaerobic glove box (for anaerobic N and P extraction) and two were kept on the lab bench next to the glove box for aerobic N and P extraction. Samples were agitated and then the caps were loosened to allow exchange with the anaerobic and air atmospheres during incubation. At 12 h intervals and at the end of the experiment, samples were sealed, agitated and then the caps were loosened again to facilitate equilibration with their respective atmospheres. Samples were incubated at room temperature for the duration of the experiment (36 h).

At the end of the experiment, samples were sealed and spun in a centrifuge until the pore water was separated from the sediment. Some samples contained very fine sediment which required repeated bouts of centrifugation. Samples were then pipetted into clean test tubes. Samples for N analysis were frozen, while samples for P analysis were preserved with 1% nitric acid.

Tests were carried out to confirm that samples incubated in the glove box were anaerobic and samples incubated on the lab bench were aerobic. The anaerobic indicator, resazurin was placed in some blank test tubes in the glove box and these indicated anoxia was achieved within half an hour of incubation. Dissolved oxygen and pH were measured in surplus aerobic and anaerobic sediment samples at the end of the experiment to confirm that the anaerobic and aerobic dissolved oxygen levels had been properly maintained and that the pH in the samples had been maintained by the buffer in the incubated sediment samples.

Samples for P analysis were analysed by ICP-OES at the University of Otago Geography Department, while samples for N analysis were analysed by standard colorimetric chemistry after wet digestions with potassium persulphate at 121°C (Schallenberg and Burns 2001). ICP-OES was used for P analysis because previous experience had shown that high silica levels in lake sediment extracts could interfere with accurate P measurements done using the standard ascorbic acid-molybdenum blue wet chemistry method (M. Schallenberg, unpubl. data).

Redox-exchangeable P was calculated as the difference between porewater P concentrations under anoxic and oxygenated conditions at the end of the experiment and was expressed as the rate of P dissolution per square meter of lake bed (to 1 cm depth) per day.

### Sequential sediment P fractionation

Sequential P extraction of sediment samples was carried out on dried sediment material collected by gravity cores on April 8 and 9, 2013 (see above for details). A modified Psenner *et al.* (1988) technique was employed to fractionate P in the sediment. This method was used by Sean Waters for his studies of Wairewa/Lake Forsyth (S. Waters, pers. comm.). Briefly, the sequential P fractionation technique extracts P under various chemical solvents as per Table 4.1.

**Table 4.1.** Solvents and inferred P fractions extracted according to the modified (Psenner *et al.* 1988) protocol.

Solvent	Type of P extracted
NH <sub>4</sub> Cl	Dissolved and loosely-bound P
Bicarbonate dithionite	Metal (mainly Fe and Mn) oxyhydroxide-bound P
NaOH	Aluminium-bound P
NaOH after persulphate digestion	Organic P
HCl	Calcium-bound P

After each incubation, samples were centrifuged to separate pore water from sediment and the pore water was removed and preserved in 1% nitric acid. Sediments were washed with milli Q water between extraction steps. Again, samples for P analysis were analysed by ICP-OES at the University of Otago Geography Department because previous study had shown that high silica levels in lake sediment extracts could interfere with accurate P measurements done using the standard ascorbic acid-molybdenum blue wet chemistry method (M. Schallenberg, unpubl. data).

## FINDINGS

---

### Sediment P geochemistry

The measured sediment P fractions and redox exchangeable P release rates at the 18 sites are shown in Table 4.2. The redox-exchangeable fraction of sediment P is considered to be the metal oxyhydroxide-bound fraction and previous studies have shown that the dissolution of this mineral-bound fraction proceeds quickly after anoxic conditions set in. As our experiments lasted 36 h, the redox-exchangeable P measured at the end of the incubations probably constituted the majority, if not all, of the redox exchangeable fraction of P in the lake sediments at that time. However, the experiments were conducted *in vitro*, in a closed test tube, and so ongoing inputs of P to the sediment system and cycling within the sediments were not quantified. So the measurements of redox-exchangeable nutrients by our method represent a pulse conversion of particulate to available dissolved forms when the sediments were made anoxic from an oxygenated state.

In all the samples, the amount of redox-exchangeable P extracted after 36 h was less than the metal-oxyhydroxide-bound fraction measured by sequential extraction and in some cases it was substantially less. For example, at site E12, the metal oxyhydroxide-bound P fraction was 189 mg m<sup>-2</sup>, whereas the P released under anoxic conditions was almost zero.

Figure 4.1 shows that redox-exchangeable P and metal oxyhydroxide-bound P conditions were positively correlated (as expected), albeit weakly, and it also shows that there was an offset of around 100 mg P m<sup>-2</sup> between the two measurement methods. The difference between these may be related to the drying of the sediment samples prior to sequential P extraction because drying the sediments may have facilitated the binding of some or all dissolved and loosely bound P onto Fe and Mn minerals. Of all the sediment sequential P fractions, the metal oxyhydroxide-bound P fraction was the most strongly correlated with redox-exchangeable P (Table 4.3).

When the measurements of the rate of release of redox-exchangeable P are mapped across the lake area, it is apparent that the greatest rates were spatially clustered in sites around the mouth of the Selwyn River and at the north end of Kaituna Lagoon. In contrast, the sediments of the Greenpark Sands and the area

near the lake opening site at Taumutu showed very low rates of redox-exchangeable P release under anoxic conditions (Fig. 4.2).

**Table 4.2.** Sediment P geochemistry at the 18 sites. REP rate is the daily rate of dissolution of redox-exchangeable P and REP is the total extracted redox-exchangeable P, calculated from 36 h incubations. DLB is the dissolved and loosely-bound fraction. MOB is the metal oxyhydroxide-bound fraction. AB is the aluminium-bound fraction. OB is the organic fraction. CB is the calcium-bound fraction.

Site	REP rate	REP	DLB	MOB	AB	OB	CB
	mg P m <sup>-2</sup> d <sup>-1</sup>	mg m <sup>-2</sup>	mg m <sup>-2</sup>	mg m <sup>-2</sup>	mg m <sup>-2</sup>	mg m <sup>-2</sup>	mg m <sup>-2</sup>
E1	38.3	57	84	256	476	1274	1744
E2	118	177	71	292	675	1766	1886
E3	23.7	35	66	130	941	3361	1146
E4	48.7	73	103	182	342	974	2139
E5	45.0	68	104	205	341	918	2111
E6	7.1	11	100	139	122	331	1254
E7	75.1	113	113	157	285	692	1202
E8	N/A	N/A	47	156	488	909	1432
E9	24.5	37	64	156	317	900	1927
E10	48.8	73	90	208	432	1247	1609
E11	38.4	58	165	349	590	1536	1295
E12	2.3	3	100	189	374	1000	2085
E13	61.8	93	94	184	296	1050	1991
E14	28.2	42	68	149	336	854	1956
E15	39.6	59	50	94	235	767	1930
E16	8.0	12	68	73	181	489	1871
E17	2.8	4	N/A	N/A	N/A	N/A	N/A
E18	24.2	36	58	118	295	751	2199

The map of metal oxyhydroxide-bound P also shows clear evidence of the influence of the Selwyn R. inflow, but the Kaituna site that showed high redox-exchangeable P did not show high levels of metal oxyhydroxide-bound P, whereas the deepest site (E11) showed very high levels of metal oxyhydroxide-bound P (Fig. 4.3).

**Table 4.3.** Pearson correlation coefficients between fractions of P (measured by sequential extraction) and redox-exchangeable P (the difference in pore water P concentration between anoxic and oxic sediments). The cumulative P fractions begin with loosely-bound + dissolved P and add each fraction until all fractions have been summed.

P Fraction	Correlation coefficient between the fraction and redox-exchangeable P	Correlation coefficient between the cumulative P fractions and redox-exchangeable P
Loosely-bound + dissolved	0.08	0.08
Metal oxyhydroxide-bound	0.48	0.40
Aluminium-bound	0.30	0.39
Organic-bound	0.19	0.25
Calcium-bound	-0.01	0.27

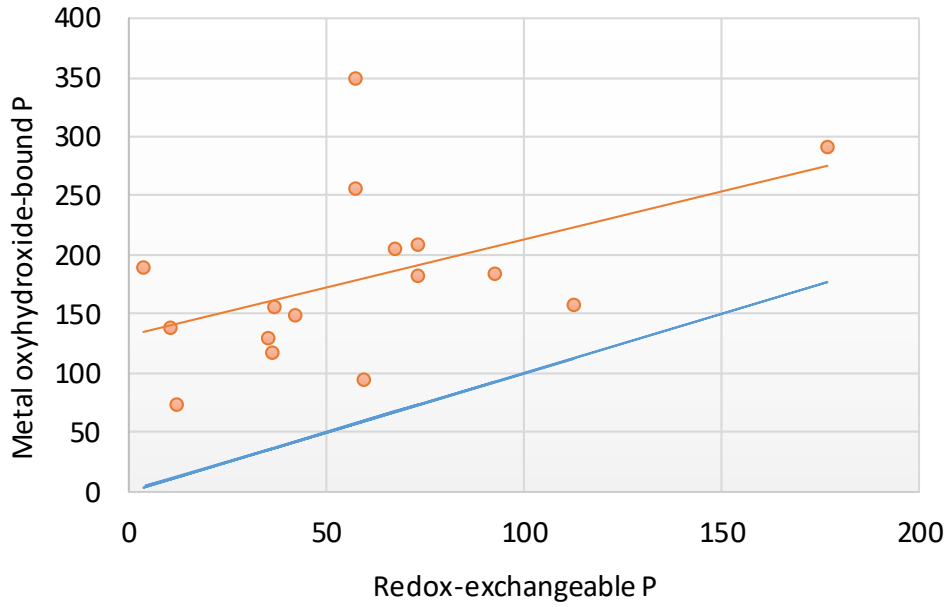


**Figure 4.1.** Correlation between metal oxyhydroxide-bound P ( $\text{mg m}^{-2}$ ) and redox-exchangeable P ( $\text{mg m}^{-2}$ ).  $r = 0.48$ ,  $N = 16$ ,  $P = 0.078$ . The blue line is the 1:1 line.

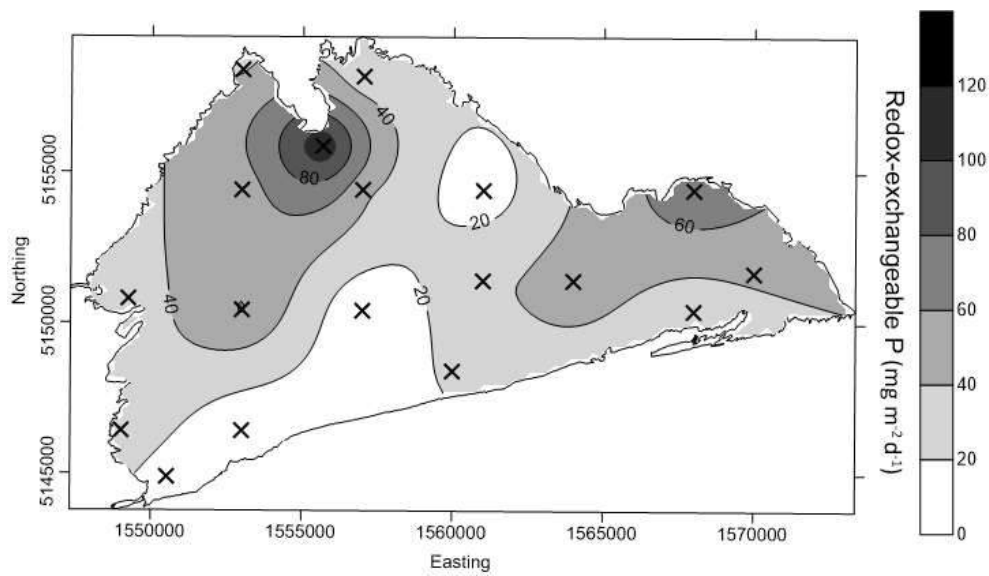


**Figure 4.2.** Map of sediment redox-exchangeable P expressed as a daily rate of release ( $\text{mg m}^{-2} \text{d}^{-1}$ ).



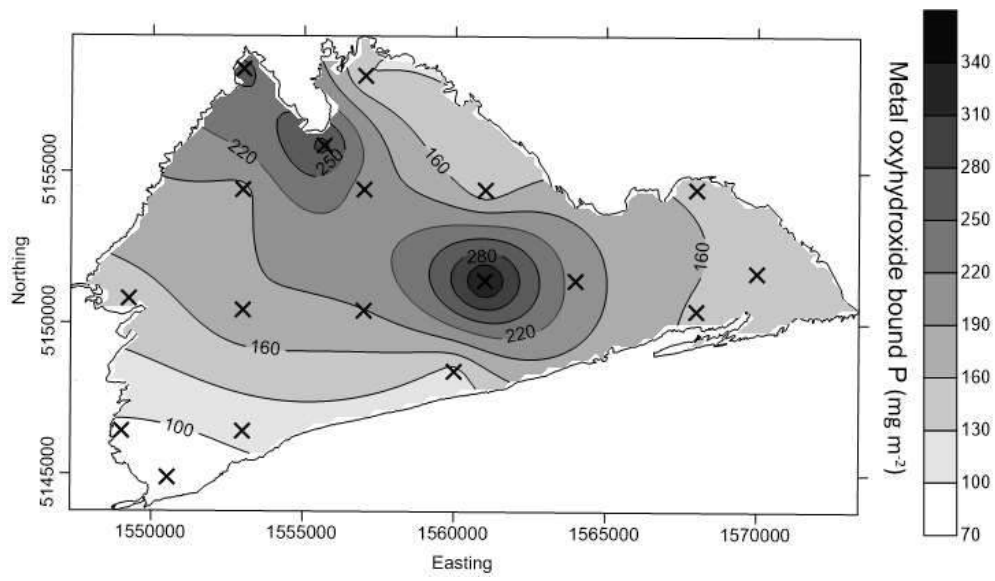


**Figure 4.3.** Map of sediment metal oxyhydroxide-bound P concentration ( $\text{mg m}^{-2}$ ).

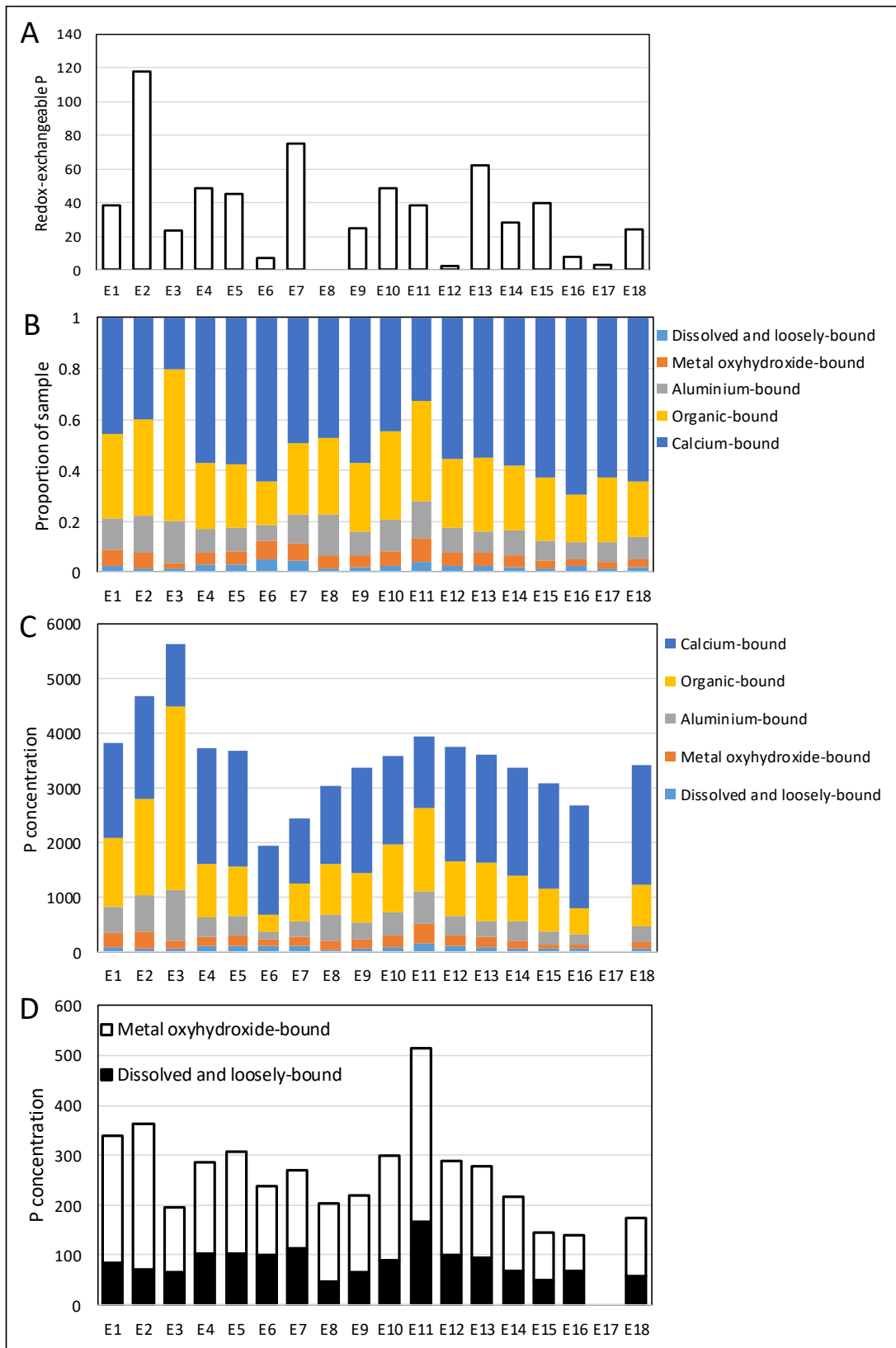


**Figure 4.4.** Sediment P geochemistry by site. Redox-exchangeable P is expressed as a release rate in mg P m<sup>-2</sup> d<sup>-1</sup>. P concentration is in mg m<sup>-2</sup>. In panel A, data for site E8 was unavailable and in panels B to D, data for site E17 were unavailable.

The concentrations of the various P fractions in the sediments were quite variable across the lake (Fig. 4.4). For example, the rate of redox-exchangeable P release ranged from close to zero to almost 120 mg P m<sup>-2</sup> d<sup>-1</sup>. In sites near the Selwyn R. inflow and the northern part of Kaituna Lagoon, anoxic P release rates were high, whereas in sites as different as E6 (Greenpark Sands) E12 (profundal basin) and E16 and E17 (Kaitorete Spit), virtually no P was released under anoxic conditions (Fig. 4.4A). In contrast, the proportions of P bound onto the various sediment fractions was relatively consistent across the sites (Fig. 4.4b). Calcium-bound P generally made up the largest fraction of P at the sites, with organic P making up the next largest fraction. Together these fractions accounted for around 80% of the P at most sites in the lake. The next largest fraction was the Al-bound fraction followed by the metal oxyhydroxide-bound and the loosely bound and dissolved fractions.

Apart from the calcium-bound fraction, the concentrations of the fractions varied much more than their proportions among sites (Fig. 4.4C). The total sediment P concentrations were generally highest in the northern part of the lake and in the profundal zone, whereas the lowest sediment P concentrations were in the Greenpark Sands area and near the Taumutu opening site. Among the sites, the calcium-bound and organic-bound fractions were highly correlated ( $r = 0.95$ ) and the loosely-bound+dissolved fraction and the metal oxyhydroxide fractions were moderately correlated ( $r = 0.64$ ). The latter correlation is also evident from Figure 4.4D.

### **Sediment anoxic N release**

Interestingly, N was also released from sediment into pore water under anoxia at most of the sites, except for site E10, where it was absorbed from the porewater under anoxic conditions (Table 4.4 and Fig. 4.5). From an ecological point of view, these releases of N were not as significant as the P releases because within biota, N concentrations are usually around 10-fold higher than P and this probably reflects the demand stoichiometry to some extent. In comparison, the anoxic N release rates we measured in Te Waihora/Lake Ellesmere were lower than those of P. This indicates that, in terms of anoxic nutrient release from the sediments of the

lake, P release is much more ecologically significant than N release. Nevertheless, these results show that a shift to anoxic conditions at most of the sites also resulted in a release of N to pore water. Mapping the distribution of anoxic N release rates shows that the spatial pattern is not as strongly or clearly defined in the lake (Fig. 4.5) as the distribution of anoxic P release is (Fig. 4.2).

**Table 4.4.** Anoxic N releases and release rates calculated from 36 h incubations.

Site	Sediment anoxic N release rate	Total anoxic N release
	mg N m <sup>-2</sup> d <sup>-1</sup>	mg m <sup>-2</sup>
E1	96	144
E2	24	36
E3	50	75
E4	61	92
E5	8	12
E6	112	168
E7	52	78
E8	-2	-2
E9	60	90
E10	-67	-101
E11	50	75
E12	49	74
E13	66	99
E14	27	40
E15	25	37
E16	73	109
E17	19	29
E18	64	96

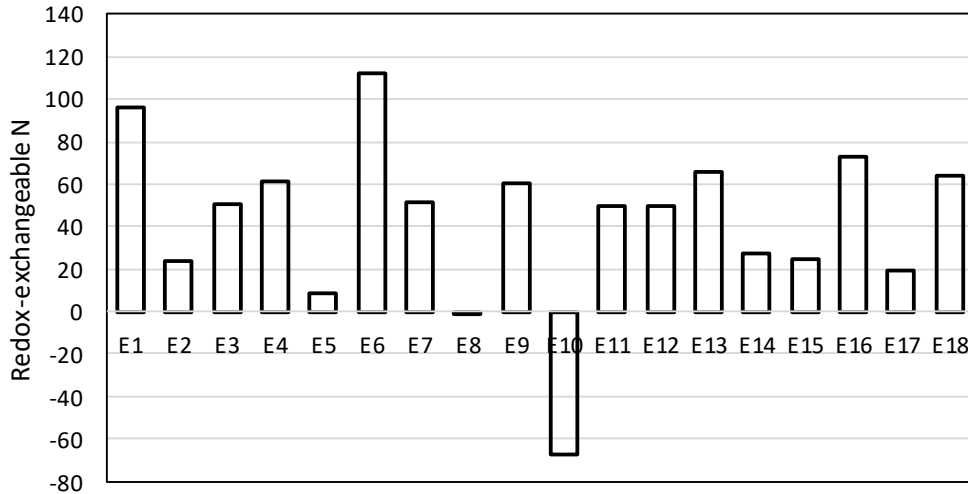


**Figure 4.5.** Daily N release rates from anoxic sediments ( $\text{mg N m}^{-2} \text{d}^{-1}$ ), measured over 36 h incubations.

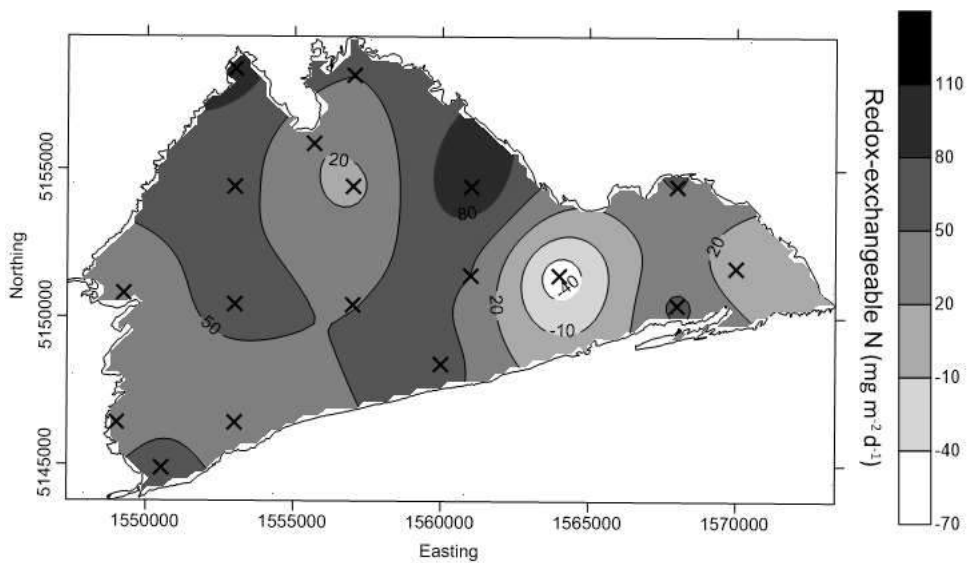


**Figure 4.6.** Map of anoxic N release rates calculated over 36 h incubations ( $\text{mg m}^{-2} \text{d}^{-1}$ ).

## DISCUSSION AND CONCLUSIONS

Our study shows that the sediments of Te Waihora/Lake Ellesmere release both P and N under anoxic conditions. The rates of release of redox exchangeable P into porewater were quite variable across the lake, with the range of rates being similar to that measured in sediments of 11 other New Zealand lakes by the same

method (M. Schallenberg, unpubl. data). The redox-exchangeable pool of P in the sediment correlated weakly with the measurement of metal oxyhydroxide-bound P in the sediment, suggesting that Fe and Mn binding is a mechanism of redox-dependent P binding in the lake sediments. Correlations with various geochemical fractions were generally weak or poor, suggesting that a variety of geochemical mechanisms are probably relevant to sediment P binding in different areas of the diverse lake bed of this lake.

The redox-exchangeable P fraction probably most closely relates to the fraction of P that could be released under transient episodes of sediment anoxia, as were described in Section 3, and this pool of P was generally a small component of the sediment P at all sites. The proportionately small size of this pool could indicate that Fe and Mn minerals are of limited availability in the sediments of this lake, possibly due to the high sulphur/sulphide concentrations in this brackish lake. Under anoxic conditions, sulphur forms stable minerals (e.g., pyrite) with these elements, thereby scavenging them. It is also possible that the small pool size of redox-exchangeable P in the lake sediments is due to the occurrence of transient anoxic episodes at the surface of the lake bed (see Section 3), which may intermittently dissolve metal oxyhydroxide-P minerals, resulting in episodic reductions of this pool of P in the sediment.

The region of the lake influenced by the Selwyn River inflow and the site at the northern end of Kaituna Lagoon had the highest pools of redox-exchangeable P in the sediments. It is not clear whether the relatively large pools of redox-exchangeable P in the sediments at these sites is due to i) higher rates of P loading to the sediments, ii) less frequent periods of anoxia, or iii) lower levels of sulphate/sulphide levels in the sediments resulting in higher Fe and Mn oxyhydroxide binding at these locations.

How important could an anoxic internal P load be to phytoplankton growth in the water column of Te Waihora/Lake Ellesmere? This can be crudely calculated assuming that 1. the redox-exchangeable P measured in the 1 cm deep sediment slice could be released into porewater during transient anoxic events such as those described at the ECAN mid-lake monitoring site in Section 3, and 2. that this additional pore water P is diffused and/or advected into the 2 m deep water

column in the central basin of the lake. The mean redox exchangeable P pool measured in the four sites in the deepest basin of the lake (sites E5, E11, E12 and E13) was 37 mg P m<sup>-2</sup>. Distributing this dissolved P into a 2.0 m deep water column overlying the sediments in the deepest zone of the lake yields a potential augmented P concentration of 17.5 µg P L<sup>-1</sup>, which is much lower than the median lake TP concentration from 1996 to 2013 (220 mg L<sup>-1</sup>), but is significant when compared to the median DRP concentration calculated for that time period (4 µg L<sup>-1</sup>; Fig. 3.13 in Hamill and Schallenberg (2013)). Summer and early autumn are the periods of highest in-lake DRP concentrations and lowest tributary loads of P to the lake and it also corresponds to periods of transient sediment anoxia events recorded at ECAN's mid-lake monitoring site (Section 3). This suggests that transient anoxic periods during this time could augment the water column with DRP at a time when external loads are low, thereby potentially sustaining chlorophyll *a* concentrations in the lake during the summer/autumn period of low inflow loads (Fig. 3.18 in Hamill and Schallenberg (2013).)

We also measured the release of N into sediment pore waters under anoxic conditions and this is most likely to represent a release of ammonium (Zhang *et al.* 2014). The median concentrations of soluble inorganic nitrogen in the lake are much higher (40 µg L<sup>-1</sup>; (Hamill and Schallenberg 2013)) than DRP concentrations and so the lower measured redox-exchangeable N pools in the sediments are not likely to have as strong an effect on nutrient availability to phytoplankton as the anoxic contribution of sediment P.

Our study indicates that the augmentation of P from sediments to the water column due to transient anoxic events during summer and autumn recorded at the mid-lake sites could help sustain summer and autumn phytoplankton productivity and concentrations in the lake. This supports findings in Section 3, showing that the growth of phytoplankton in Te Waihora/Lake Ellesmere is at times likely to be stimulated by DRP availability and that DRP is sometimes depleted during phytoplankton blooms in the lake.

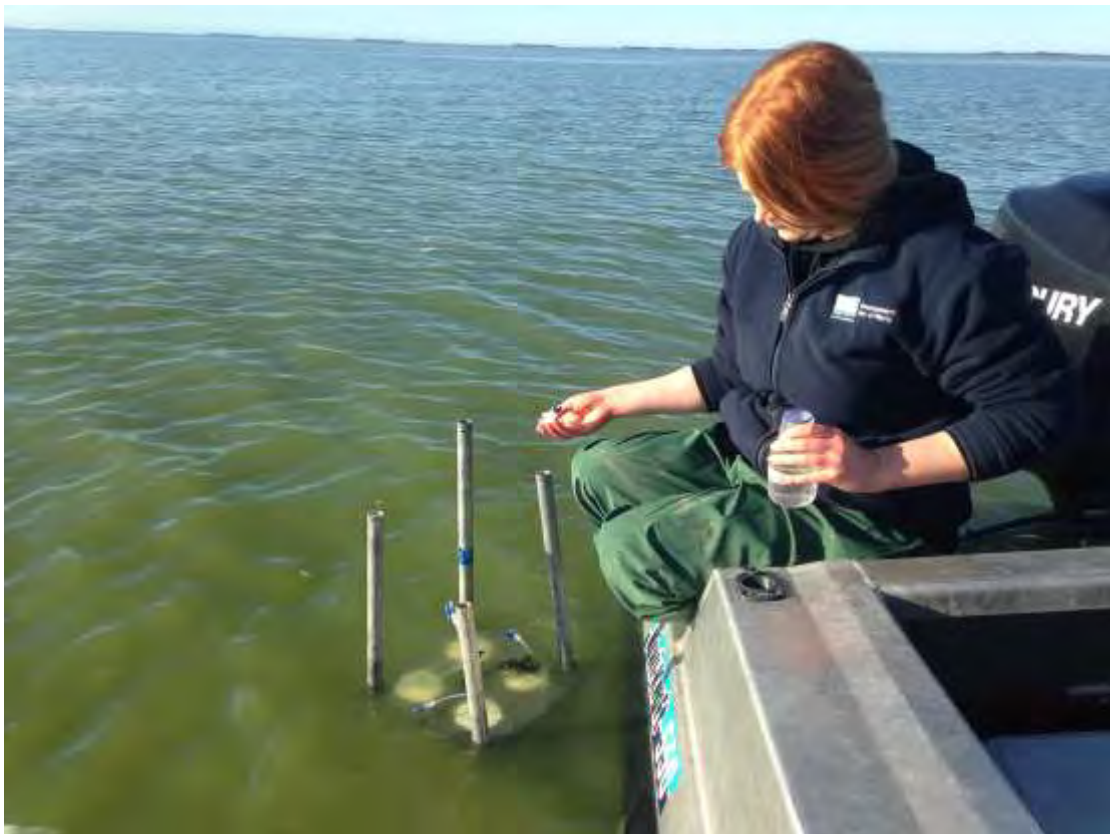
---

## Section 5

---

### 5 DENITRIFICATION IN THE SEDIMENTS OF LAKE ELLESMERE/TE WAIHORA

---



Carrying out measurements of nitrate conversion to  $N_2$  gas in custom-made enclosures.



## INTRODUCTION

---

### Eutrophication of coastal waters

Intensifying agricultural development in catchments around coastal water bodies is leading to increased nutrient loading, causing eutrophication (Piña-Ochoa and Álvarez-Cobelas 2006; Schallenberg *et al.* 2010; Knuth and Kelly 2011). Coastal ecosystems are generally nitrate limited (Howarth 1988), and quickly assimilate available nitrate, usually resulting in increases in phytoplankton biomass. Phytoplankton blooms can have numerous undesirable effects on the receiving ecosystem including the suppression of submerged macrophytes, the enhancement of deoxygenation, and the production of toxins. However, uptake by phytoplankton is not the only sink for nitrate in coastal ecosystems. Denitrification is the microbially mediated process, where nitrate from the water column can be converted to nitrogen gas, usually within the sediments (Nielson *et al.* 2004). This process of removing bio-available nitrate from the system can be important in buffering the potential effects of eutrophication (Laverman *et al.* 2007; McCrackin and Elser 2010) and may thus in this respect be considered an ecosystem service. Other sediment microbial processes, such as anaerobic ammonium oxidation, assimilatory nitrate reduction and other forms of dissimilatory nitrate reduction, can also ultimately remove nitrate from the water column.

### Research rationale

Section 2 of this report showed that the sediment environment within Te Waihora/Lake Ellesmere is spatially heterogeneous, with strong gradients of redox potential, organic matter, sediment particle size, and porosity occurring across the lake. In addition, water quality data from the inflow tributaries to the lake shows that nitrate loads from them to the lake are high and nitrate levels in the lake will be highest near these inflows. Therefore, the spatial distribution of the denitrification capacity of sediments in lake is expected to be highly variable. Nitrate concentrations in Te Waihora/Lake Ellesmere also show strong temporal variability (Hamill & Schallenberg 2013), with episodic pulses of up to 1 mg L<sup>-1</sup> of nitrate recorded even at ECAN's mid-lake monitoring site (Fig. 5.1). Analysis of the mid-lake nitrate data showed that there were 16 episodic pulses of nitrate >

0.3 mg L<sup>-1</sup> within the period of 1993-2013 and that all of these pulses of nitrate occurred in winter and/or spring (for analyses of nitrate pulses from the Selwyn River and at the mid-lake site, see Appendix C). The nitrate time series in Fig. 5.1 shows that nitrate concentrations decline rapidly. While phytoplankton probably take up some of this, denitrification may also contribute to the loss of nitrate, which would remove nitrogen from the lake, making it unavailable to phytoplankton.

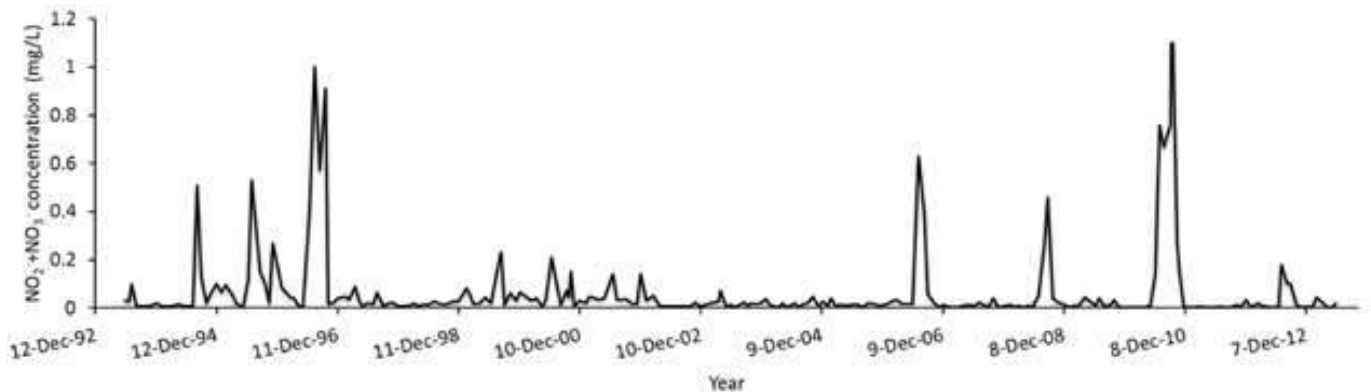


**Figure 5.1.** Mid-lake nitrate concentrations from 1993-2013. ECAN data.

Schallenberg *et al.* (2010) reported a 30-fold reduction in dissolved inorganic nitrogen from the Selwyn River inflow to the middle of the lake. The authors suggest this may be due to phytoplankton uptake and subsequent sedimentation and/or denitrification. As these pulses of nitrate occur in winter and spring, the denitrification potential could be enhanced subsequent to the inputs. On the other hand, low water temperatures in winter and spring may retard or inhibit the microbial conversion of nitrate to N<sub>2</sub> and, consequently conversion rates may increase as the water temperature warms in spring and summer. Therefore, it is important to examine the conversion of nitrate inputs seasonally, across a temperature gradient.

### Research Aims

Mass balance studies show that a reduction in total nitrogen concentration occurs between the inflowing river water and the middle of the lake (Schallenberg *et al.* 2010). We aimed to quantify the extent to which microbial conversion of nitrate to

$N_2$  in the sediments of the lake could contribute to reducing high nitrate and total N loads to the lake. We also quantified the seasonal and spatial variation in nitrate conversion rates and investigated how the variable sediment characteristics in the lake related to the nitrate conversion rate. The specific research questions we addressed were:

1. Do 'hotspots' of denitrification potential exist in certain parts of the lake?
2. Is the microbial denitrification rate limited by nitrate supply, carbon, or both?
3. Are there seasonal differences in nitrate conversion rates?
4. What proportion of a nitrate pulse can be converted to  $N_2$  gas?
5. Are nitrate conversion rates related to sediment variables (e.g. grain size, porosity, organic content)?
6. Do benthic infauna play a role in stimulating nitrate conversion?

## METHODS

### Study sites

We used two different approaches to study denitrification in the lake. We examined the denitrification potential of the sediment using an *in vitro* laboratory technique at 18 sites in the lake. In addition, we measured *in situ* rates of nitrate conversion to N<sub>2</sub> gas at a subset of 7 of the sites (Fig. 5.2). These sites were selected to cover different distances from the mouths of the Selwyn, L2 Rivers and Hart's Creek, which are the main tributary sources of nitrate to the lake (Hamill and Schallenberg 2013). The sites also cover gradients of porosity, organic matter, redox potential and sediment particle size. Below is a brief overview of the methods; for more detail please refer to Appendix C.

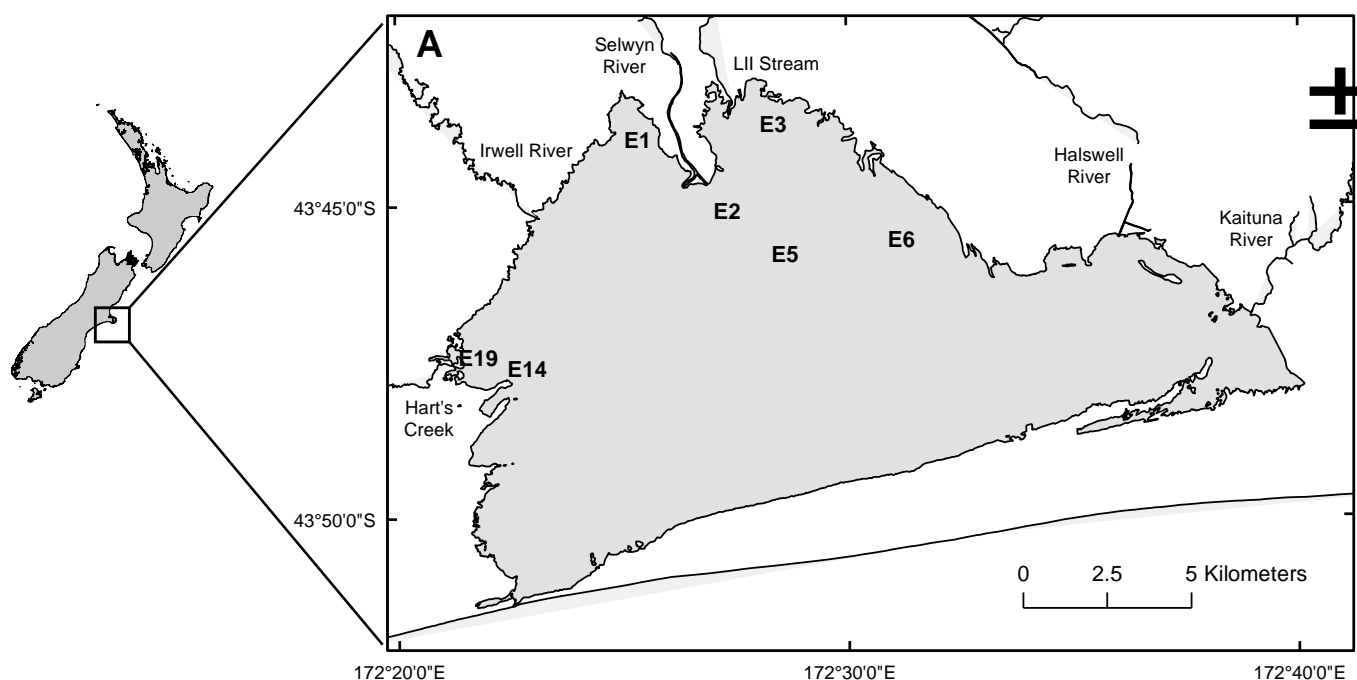


**Figure 5.2.** Study sites. Site numbers indicate the sites of *in situ* denitrification measurements.

### Denitrification enzyme assay (DEA) or denitrification potential

Sediments were sampled with a gravity corer and the top 4 cm of the cores were homogenised and placed into sealable containers. Tubes were filled so as to

minimise exposure of the sediment to air. A water sample from the lake was also collected to use in dilutions. The samples were kept on ice and transported to the University of Waikato. Briefly, samples were diluted in lake water and four treatments were set up: water (lake water only), + nitrate (+N), + glucose (+C), and + glucose+ nitrate (+C+N). The denitrification potential of the sediment was measured as the rate of production of  $N_2O$ , using the acetylene inhibition technique (Bruesewitz *et al.* 2011).

### Isotope pairing technique applied to flexible core structures

Nutrient fluxes and nitrate conversion rates were measured in custom built *in situ* enclosures containing both sediment and overlying water (henceforth called “enclosures”) (Fig. 5.3), which allowed the transfer of turbulent wave energy into the enclosures. Turbulence and advection are potentially a key driver of nitrate supply to the sediment microbial community (Risgaard-Petersen *et al.* 1999). The experiment was designed based on similar studies (Nielsen and Glud 1996; Risgaard-Petersen *et al.* 1999; Hamilton and Ostrom 2007; Gongol 2010). Enclosures were spiked with  $^{14}NO_3^-$  to 1mg/l. A final enrichment of 50% was achieved by additionally spiking the enclosures with unlabelled  $NaNO_3^-$  to a concentration of 1.0 mg  $L^{-1}$ . The incubation was run for 48 hours, with 50 mL samples taken at 0, 4, 24, 30 and 48 hours for dissolved nutrients and labelled  $N_2$  pairs.

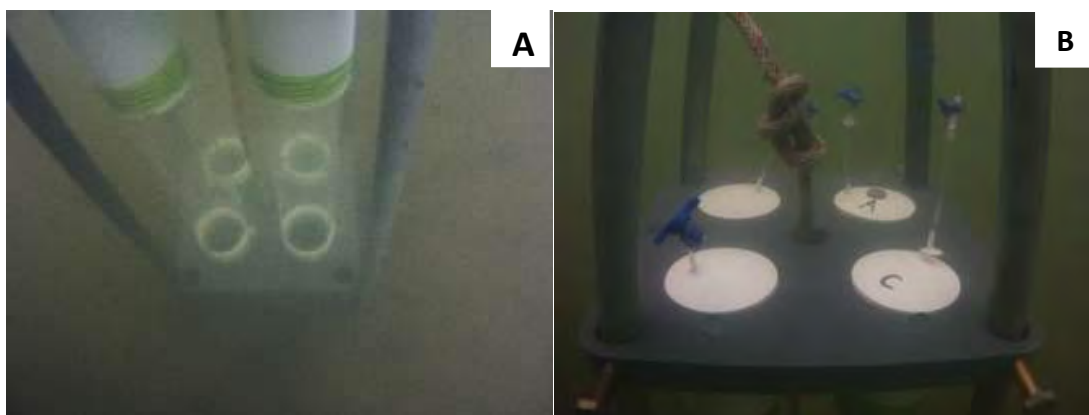


**Figure 5.3.** *In situ* core enclosure deployed in the lake bed. A = bottom section of core structure pushed into the sediment, with flexible polyethylene tubing running

up to rigid cylinders at top, B = lids at the top of the enclosures, showing the sampling ports. \*Note photos are taken from setup in Tomahawk Lagoon (Dunedin), as the underwater visibility was too poor in Te Waihora/Lake Ellesmere to photograph the deployed cores.

### **Statistical Analysis**

All statistical analyses were carried out in R Studio (v.0.98.1049) (R Studio Team 2015). Seasonal variation in denitrification rates was assessed using analysis of variance, with a  $\alpha=0.05$ . Linear regression was used to quantify relationships between sediment characteristics and nitrate conversion rates. Relationships between sediment variables and nitrate conversion were explored with PCA on the untransformed correlation matrix using CANOCO v. 4.5 (ter Braak and Šmilauer 2002).

## FINDINGS

### Hotspots of denitrification potential

Denitrification potential was found to be highly variable across the lake (Fig. 5.4). There was no significant  $\text{N}_2\text{O}$  production recorded in the water alone, in unamended sediment, or in the +C treatments.  $\text{N}_2\text{O}$  production in the +N treatments ranged from 19 to  $407 \mu\text{mol N}_2\text{O m}^{-2} \text{h}^{-1}$  (Fig. 5.4a). In the combined +N+C treatments, the  $\text{N}_2\text{O}$  production increased greatly, and showed a large variation between sites (183 to  $2574 \mu\text{mol N}_2\text{O m}^{-2} \text{h}^{-1}$ ) (Fig. 5.4b). Our spatial profiling shows that hotspots of denitrification potential were located in the littoral sites, particularly those located close to the Selwyn and L2 River inflows

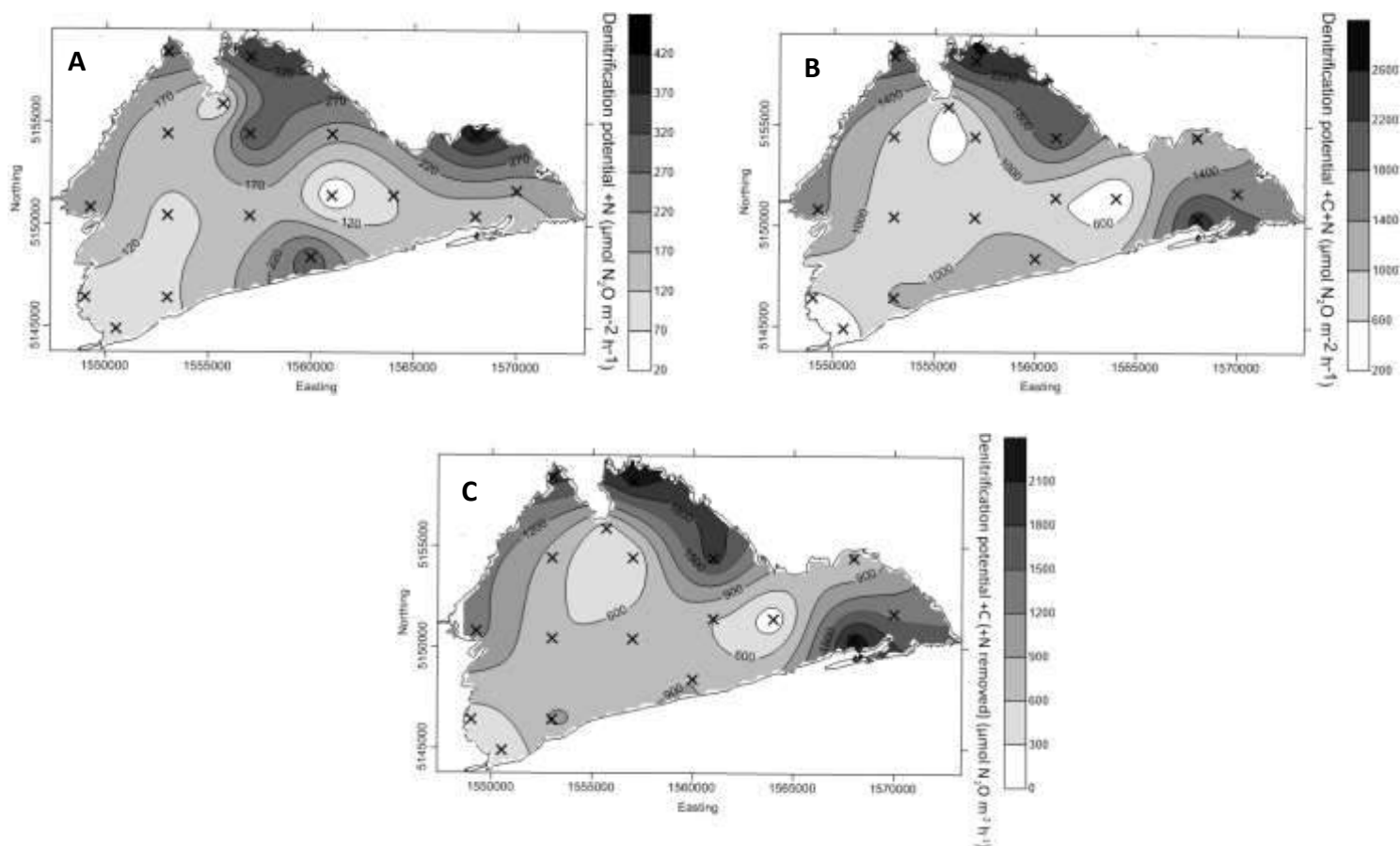


**Figure 5.4.** Spatial contour plots showing the denitrification potential in different treatments. (A) nitrate amended. (B) carbon and nitrate amended and (C) the effect of carbon addition (+C+N response minus +N response). The data were collected in April 2014.

and near Kaituna Lagoon (Fig. 5.4b). In the deeper zone of the lake, the denitrification potential was much lower in both the +N and +N+C treatments.

### **Sediment drivers of denitrification potential**

The rates of N<sub>2</sub>O production increased with the addition of nitrate, indicating that denitrification in the sediments is generally nitrate limited. In addition, further increases in N<sub>2</sub>O production with the addition of carbon suggests that denitrification rates in the sediments were secondarily carbon limited (Zhong *et al.* 2010). A positive correlation between denitrification potential and sediment organic carbon has been found in various studies (Inwood *et al.* 2007; Dodla *et al.* 2008), but was not found in our study (Table 5.1). This may be due to the greater importance of other variables in relation to denitrification potential in Te Waihora/Lake Ellesmere or it may indicate that much of the organic matter present is of low lability or quality. The denitrification potential rates of both the +N and +N+C treatments showed weak negative relationships with water depth ( $r=-0.50$ ,  $r=-0.54$ ) (Table 5.1) and this has been observed in other studies (Ahlgren *et al.* 1994; Saunders and Kalff 2001). Saunders and Kalff (2001) suggested that this relationship may be due to the decreased quality and quantity of organic matter that reaches the profundal zone, although that is unlikely to be applicable to a lake as shallow as Te Waihora/Lake Ellesmere. Denitrification potential was also weakly related to infaunal densities, particularly *Paracorophium excavatum* density ( $r=0.58$ ) polychaete (Neridae) density ( $r=0.49$ ), and oligochaete density ( $r=0.47$ ). Caution must be exercised in inferring causality in these relationships because these infauna also showed negative relationships with water depth.



**Table 5.1.** Pearson’s correlation matrix showing the relationships between the denitrification potential measured in Ellesmere summer 2014, and the associated sedimentary variables. \* =  $p < 0.05$ , \*\* =  $p < 0.01$ , \*\*\* =  $p < 0.001$ .

	+N	+CN	Depth	OM	Clay	Silt	Sand	Porosity	Redox	<i>P.ant</i>	<i>P.exc</i>	<i>Olig</i>
+N												
+CN	0.43											
Depth	-0.50*	-0.54*										
OM	-0.12	-0.35	0.57*									
Clay	-0.39	-0.52*	0.91***	0.79***								
Silt	-0.32	-0.34	0.81***	0.74***	0.90***							
Sand	0.33	0.36	-0.83***	-0.75***	-0.92***	-1.00***						
Porosity	-0.3	-0.41	0.78***	0.82***	0.94***	0.89***	-0.90***					
Redox	-0.22	-0.25	-0.36	-0.69**	-0.51*	-0.55*	0.55*	-0.47				
<i>P.ant</i>	0.00	0.31	0.02	-0.04	-0.04	0.08	-0.07	-0.06	-0.19			
<i>P.exc</i>	0.58*	0.36	-0.71***	-0.22	-0.60**	-0.63**	0.64**	-0.47*	0.15	0.08		
<i>Olig</i>	0.46	0.47*	-0.65**	-0.63**	-0.70**	-0.77***	0.77***	-0.60**	0.33	0.02	0.80***	
<i>Neridae</i>	0.41	0.49*	-0.57*	-0.62**	-0.63**	-0.64**	0.64**	-0.61**	0.07	0.11	0.57*	0.83***

Denitrification potential provides an understanding of the potential capacity for denitrification under conditions where the key substrates, nitrate and carbon, are not limiting. Within Te Waihora/Lake Ellesmere there is large spatial variation in denitrification potential, correlating with a change in water depth and sediment grain size. This variability highlights the importance of measuring denitrification with high spatial resolution rather than relying on few measurements to calculate lake-wide denitrification rates – an important consideration that has also been made by others (Saunders and Kalff 2001; Piña-Ochoa and Álvarez-Cobelas 2006).

### Seasonal *In situ* denitrification rates

To examine the seasonality of nitrate conversion to N<sub>2</sub>, *in situ* conversion rates were measured at three sites during summer (March 2015; 18°C), winter (August 2014; 8°C) and summer (January 2016; 16.7°C) (Table 5.2).

**Table 5.2.** Measured physiochemical variables taken during *in situ* nitrate conversion experiments.

Season	Date	Temp (°C)	Salinity (ppt)	pH	Secchi depth (cm)	Dissolved O <sub>2</sub> (µmol L <sup>-1</sup> )
Summer 2015	11/03/2015	18	9.0	8.5	9.5	638
Winter 2015	05/08/2015	8	6.3	-	14.5	714
Summer 2016	27/01/2016	16.7	8.8	-	13.7	593

Nitrate conversion varied among the seasons (Fig. 5.5), with the highest rates occurring during January 2016. No nitrate conversion was measured during winter, where temperatures reached a low of 7°C. Temperature control on denitrification has been shown in the literature (Veraart *et al.* 2011; Nizzoli *et al.* 2014). For example, Veraart *et al.* (2011) reported a 24 to 28% increase in denitrification rates with a 1 degree rise in temperature, concluding that altered oxygen dynamics were the ultimate driver of this change in denitrification. Another study found denitrification to be entirely suppressed below 6 degrees Celsius (Smith *et al.* 2003).

Te Waihora/Lake Ellesmere receives greater nitrogen loading in winter compared with summer due to increased runoff ((Hamill and Schallenberg 2013); Figs. 3.12, 3.19). If nitrate is not able to be converted to  $N_2$  during winter due to temperature suppression of microbial denitrification, then most, if not all of the nitrate load will be available to the phytoplankton for growth. On average, chlorophyll *a* concentrations in the lake increase during August and September, indicating that phytoplankton net production occurs at this time ((Hamill and Schallenberg 2013), Fig. 3.18). Phytoplankton activity may be slowed down during colder temperatures, thus decreasing nitrate uptake rates, however our nitrate uptake measurements in winter 2015 suggest that, although their activity might have been slowed somewhat, phytoplankton still remove our  $2.0 \text{ mg L}^{-1}$  nitrate spike within 48 hours (Fig. 5.8).

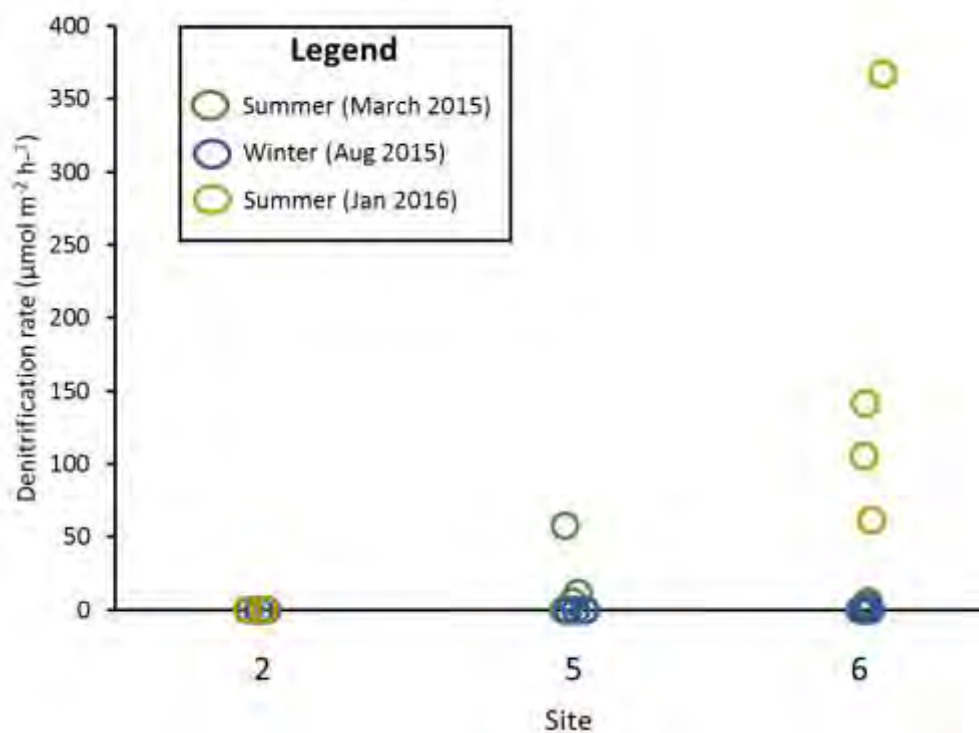


**Figure 5.5.** Seasonal denitrification rates ( $\mu\text{mol N m}^{-2} \text{ h}^{-1}$ ) measured in Lake Ellesmere across three sites in three different seasons. Summer 2016 rates were not measured at site 5 due to rough lake conditions. Each circle indicates a rate measurement for each core.

## Spatial variation in nitrate conversion rates

In Section 2 we examined the variation in the sediments at 18 sites. Based on this data, seven sites were selected, covering a substantial variation in the sedimentary environment, for the measurement of nitrate conversion rates to N<sub>2</sub> gas.

Conversion rates ranged from 0 to 4227  $\mu\text{mol m}^{-2} \text{h}^{-1}$  during the autumn and summer sampling seasons (Fig. 5.6). Recorded rates were extremely variable, both within the sites and between sites. As such, the data we present is not averaged, but each point on Fig. 5.6 shows an individual replicate core for each site.

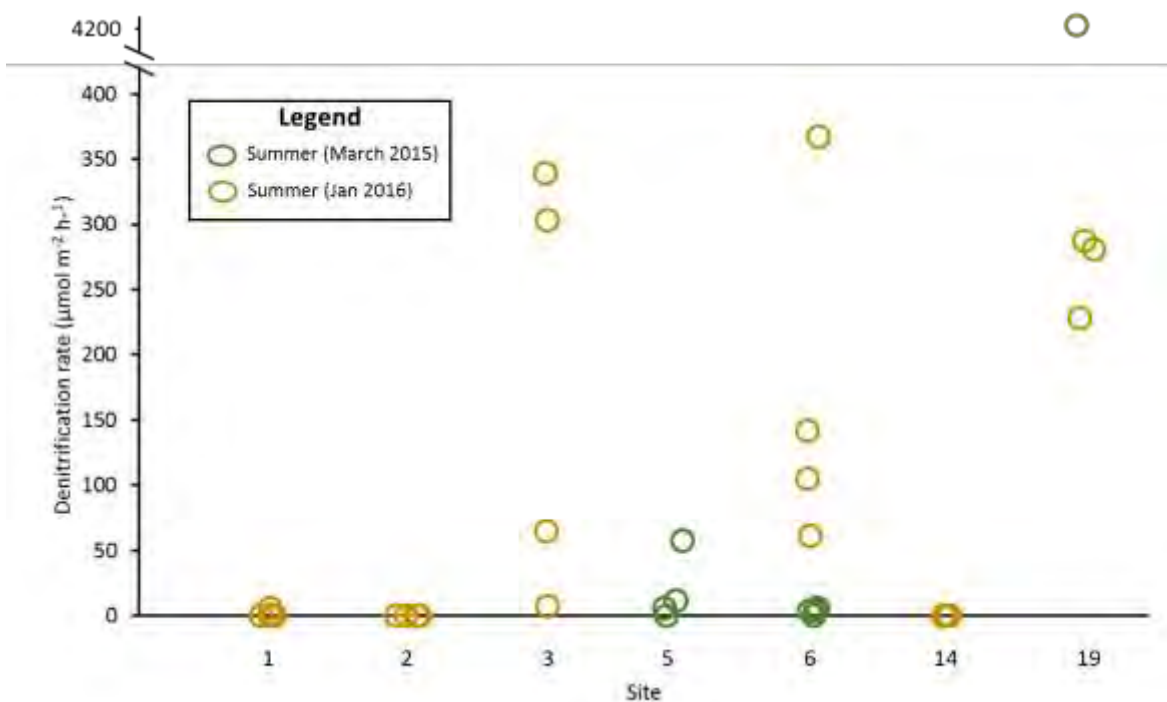


**Figure 5.6.** Nitrate conversion rates ( $\mu\text{mol N m}^{-2} \text{h}^{-1}$ ) across seven sites in the summer seasons (March 2015 and January 2016). Each circle indicates the rate for a core. Note the break in the y-axis.

The highest rates of nitrate conversion recorded were at site 19, located at the inflow of Hart's Creek. This site was added to our study after we had difficulties deploying our enclosures at site E5 due to rough lake conditions. Salinity at site 19 was relatively low (3 ppt compared to 8 ppt across the rest of the lake), and the ambient nitrate concentration was relatively high ( $16.37 \mu\text{mol L}^{-1}$  compared to a

range of 0.61-2.56  $\mu\text{mol L}^{-1}$  at other sites) (Appendix C, Table 9.2). Being so near a nitrate source, this site is likely to experience sustained inflows of nitrate. The maximum nitrogen conversion rate recorded in Lake Ellesmere was recorded at this site ( $4227 \mu\text{mol m}^{-2} \text{h}^{-1}$ ), which also had a high sediment organic matter concentration ( $\text{kg m}^{-2}$ ) ( $1.22 \pm 0.08$ , excluding coarse particulate matter)(Table 5.3). At the end of the incubation, this core was the only core in all our experiments to reach hypoxic levels ( $<2 \text{ mg L}^{-1}$ ). We maintained DO levels in all our cores to within 20% of saturation during the experiments, so as not to artificially influence nitrate conversion rates by enclosure. The high organic matter concentration at this site may have fuelled high rates of microbial activity, including denitrification. In terms of site average conversion rates, similar rates were recorded at sites 3 and 6, again with large within site variability (range =  $0.27 - 368 \mu\text{mol m}^{-2} \text{h}^{-1}$ ). Due to this large within site variability, no significant differences were found between average nitrate conversion rates at the sites (ANOVA,  $p=0.232$ ). Very low nitrate conversion rates were recorded at sites 1, 2 and 14.



Setting up the *in situ* denitrification enclosure.

**Table 5.3.** Mean (+/- standard errors) sediment characteristics from cores enclosed in the *in situ* denitrification experiments (measurements taken from 2016 sampling with exception of site 5, which was from summer 2015).

Site	Grain size %			Organic matter (kg m <sup>-2</sup> )	Porosity (kg m <sup>-2</sup> )	Redox potential (mV)
	Clay	Silt	Sand			
1	3.52 ± 1.1	24 ± 4.07	72 ± 5.17	0.85 ± 0.06	6.35 ± 0.25	11 ± 29
2	0.75 ± 0.31	6.50 ± 1.0	93 ± 1.31	0.74 ± 0.00	4.82 ± 0.08	81 ± 14
3	0.61 ± 0.07	3.16 ± 0.62	96 ± 0.69	0.53 ± 0.02	5.35 ± 0.05	109 ± 12
5	3.11 ± 0.26	84 ± 4.76	13 ± 4.5	0.80 ± 0.10	7.57 ± 0	-106 ± 20
6	0 ± 0	0 ± 0	100 ± 0	0.39 ± 0.01	4.81 ± 0.14	71 ± 8
14	3.09 ± 0.05	53 ± 2.11	44 ± 2.16	0.76 ± 0.05	7.18 ± 0.10	-49 ± 16
19	3.2 ± 0.03	62 ± 0.42	35 ± 0.45	1.22 ± 0.08	7.55 ± 0.06	85 ± 22

In summer 2015, nitrate conversion rates showed diverse temporal trends among the sites, with denitrification exhibiting lag periods between nitrate spiking and N<sub>2</sub> gas production (Fig. 5.7). At site 5, gas production was not recorded until 48 hours into the incubation, whereas at site 6 gas production began at 8 hours and at site 2, no nitrate conversion was recorded.

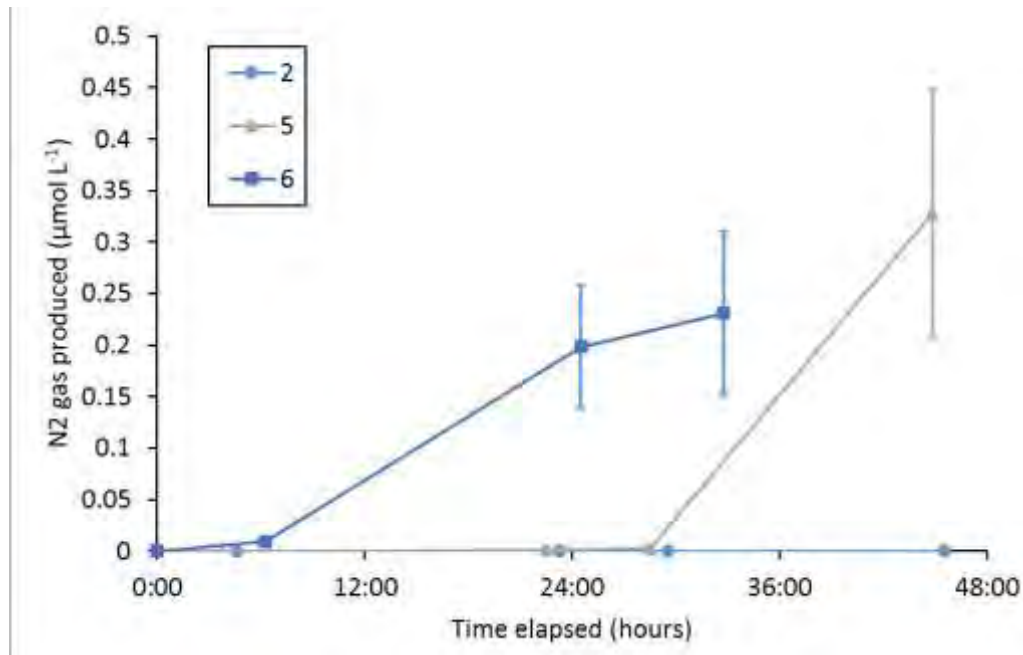


**Figure 5.7.** Time series of N<sub>2</sub> produced (µmol N L<sup>-1</sup>) in three sets of enclosures in summer 2015 (March). Error bars show the standard error for each of the 4 replicates at each site.

### Nutrient removal rates in enclosures

Nitrate depletion within the cores was rapid in both summers across all sites. Enclosures at the majority of sites showed nitrate dropping to low levels within 24 hours (Fig. 5.8A, C), with a maximum loss rate of 125 mmol m<sup>-2</sup> h<sup>-1</sup> occurring at site 5 in summer 2015 (Table 5.4). In summer 2015, nitrate concentrations at site E6 remained stable at around 40 µmol L<sup>-1</sup> (Fig. 5.8A). Sustained nitrate concentrations at this level could indicate nitrate replenishment in the enclosures either by seepage of groundwater into the enclosures, by the conversion of mineralised N (ammonium) to nitrate (nitrification), or by the release of ammonium from anoxic sediment. Groundwater sources such as this may be

common in the shallow, sandy sediments such as the Greenpark Sands where site 6 is located.

In winter, nitrate removal from the water column was slower ( $46 \text{ mmol m}^{-2} \text{ h}^{-1}$ , Table 5.4; Fig. 5.8B), probably due to decreased biological activity in colder temperatures. The nitrate within the cores was entirely consumed at two of three sites in winter, but at a slower rate than in summer 2016 (ANOVA,  $p=0.001$ ). Nitrate depletion rates in summer 2016 were generally greater than in summer 2015 (ANOVA,  $p=0.001$ ).

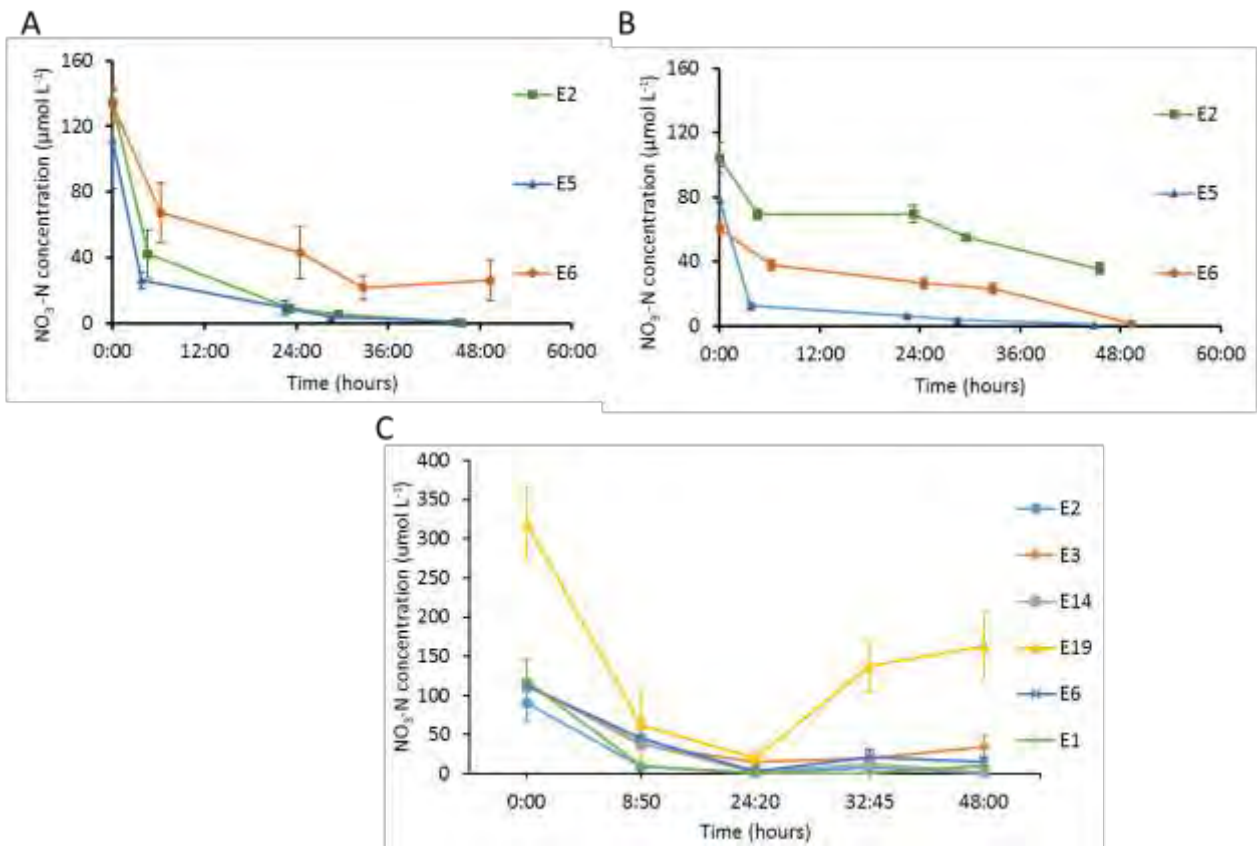


**Figure 5.8.** Nitrate concentrations measured in enclosures over time in summer 2015 (March) (A), winter 2015 (Aug) (B), and summer 2016 (Jan) (C). Standard errors are shown.



**Table 5.4.** Nitrate uptake rates in the first 24 h (due to depletion of nitrate around 24 hours) during the *in situ* nitrate conversion experiments in summer 2015, winter 2015 and summer 2016.

Site	Nitrate uptake rates (mmol m <sup>-2</sup> h <sup>-1</sup> )		
	Summer 2015	Winter 2015	Summer 2016
1	-	-	-94 ± 8
2	-67 ± 4	-19 ± 2	-73 ± 4
3	-	-	-41 ± 6
5	-125 ± 34	-94 ± 26	-
6	-42 ± 5	-24 ± 3	-66 ± 4
14	-	-	-96 ± 19
19	-	-	-108 ± 15
<b>Average</b>	<b>-78 ± 15</b>	<b>-46 ± 13</b>	<b>-80 ± 6</b>

Although episodic spikes of nitrate are sometimes recorded in Te Waihora/Lake Ellesmere (Appendix C, Fig. 9.2), nitrate levels were consistently relatively low during our samplings, averaging between 0.60 – 16.37 µmol L<sup>-1</sup>. A 2-fold deficit in nitrogen has been shown by Hamill and Schallenberg (2013) from the Selwyn River mouth to a mid-lake site, suggesting that substantial nitrogen transformations occur once nitrate enters the lake. Results from our enclosure work show that nitrate added to lake water is rapidly taken up and transformed in winter as well as in summer, but in winter no N<sub>2</sub> production was observed, indicating the nitrate is probably taken up by phytoplankton.

### Nitrogen fixation

Nitrogen fixation was not directly measured in our experiments, however our experiments in the summer of 2016 showed reuptake of N<sub>2</sub> gas (Fig. 5.9A). For example, at site 19, nitrate was depleted after 24 h (Fig 5.9B), and subsequently N<sub>2</sub> gas concentrations decreased in the enclosures. Furthermore, ammonium levels subsequently increased in the enclosures after having been depleted (Fig. 5.9C). Such decreases in N<sub>2</sub> gas and increases in ammonium concentrations (suggesting nitrogen fixation) were evident at all sites except site 3, in summer 2016.

Various N-fixing cyanobacteria taxa (e.g., *Anabaena* sp., *Nodularia spumigena*) have been reported in the lake (Larned and Schallenberg 2006), and they probably fix nitrogen gas from the water column in times of nitrogen limitation. Planktonic nitrogen fixation can be substantial in eutrophic lakes (0.2-9.2 g N m<sup>-2</sup> y<sup>-1</sup>), generally occurring when the water column N:P ratio is low (Howarth *et al.* 1988). A study on nitrogen fixation in marine sediments has shown that sulphate reducing bacteria can potentially fix nitrogen produced by denitrification (Bertics *et al.* 2010), especially under conditions of organic carbon limitation (Fulweiler *et al.* 2013), impacting on gross and net nitrogen flows. Further research into the responses of N<sub>2</sub> fixation and denitrification under varying carbon supply conditions would be valuable to help understand the nitrogen budget for Te Waihora/Lake Ellesmere.

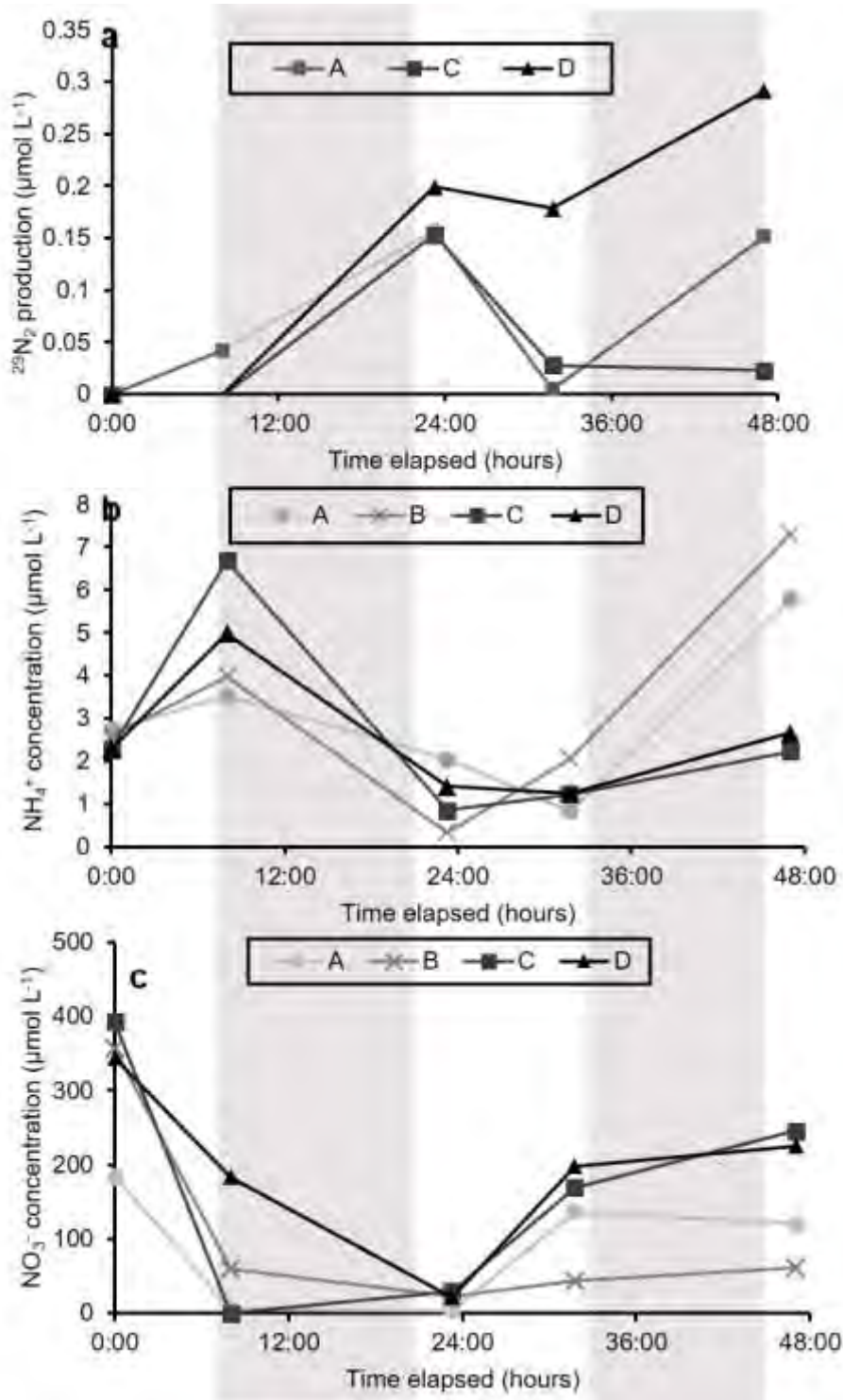


**Figure 5.9.** Nitrogen dynamics during the enclosure experiments at site 19 in summer 2016. A -  $^{29}\text{N}_2$  gas production ( $\mu\text{mol L}^{-1}$ ). B - Ammonium concentrations. C - Nitrate concentrations. Dark shading indicates night; no shading indicates daylight hours.

### Factors related to nitrate conversion rates

Our third aim was to find out if nitrate conversion varied spatially within the lake, and we hypothesized that rates would vary depending on the sediment variables such as sediment particle size, redox potential, porosity and organic matter concentration. Table 5.3 shows the sediment characteristics at the sites at the time of each sampling. For the *in situ* enclosure studies, we specifically chose sites covering a large range in grain size (Fig. 5.10).

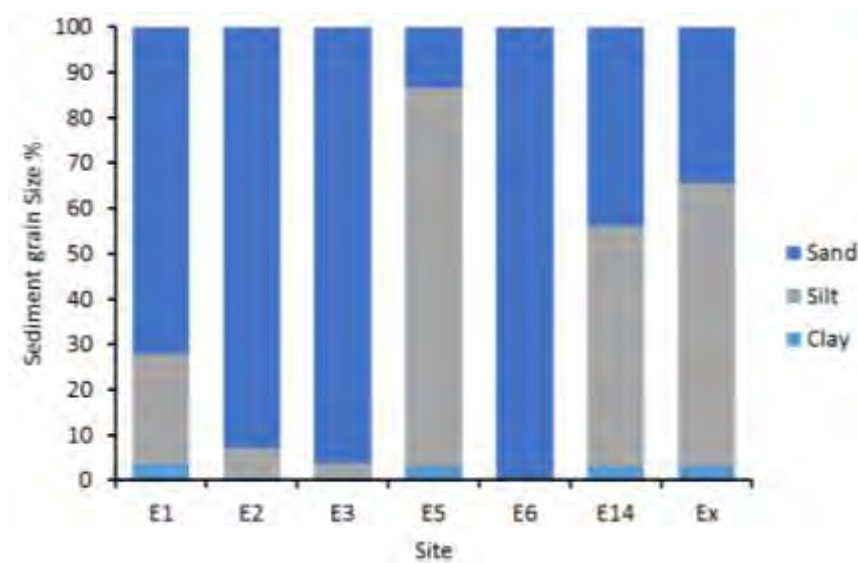


**Figure 5.10.** The sediment grain size fractions - sand (63-2000  $\mu\text{m}$ ), silt (2-63  $\mu\text{m}$ ) and clay (0-2  $\mu\text{m}$ ). Data is from the enclosure cores in summer 2016, with the exception of site 5 which was measured in summer 2015.

Pearson's correlations were used to investigate possible relationships between sediment variables and nitrate conversion rates in summer 2016 (Table 5.5). Conversion rates were positively related to the % organic content of the sediment ( $r=0.58$ ). No other sediment variables showed significant relationships with the conversion rates. As shown in Section 2, there are strong relationships present between the sediment variables including organic matter, porosity, clay, silt and sand ( $p<0.001$ ) (Table 5.5). We can conclude from this that the organic matter content was the sediment variable most strongly related to nitrate conversion rate at the sites.

It has been well documented that siltier, organic rich sediments have greater denitrification rates compared to larger grained sediments (Vance-Harris and Ingall 2005; Inwood *et al.* 2007). An *in situ* stream study across sediment types by Smith *et al.* (2009) found greater denitrification rates at sites with finer sediments compared to those with coarse sediments, with silt producing 1000  $\mu\text{mol m}^{-2} \text{h}^{-1}$  and in coarser sandy sediments only 200  $\mu\text{mol m}^{-2} \text{h}^{-1}$ . Other studies that have reported the same relationship include (Hamersley and Howes 2005; Solomon *et al.* 2009; Jia *et al.* 2016).

Many studies quantifying denitrification have not taken into consideration spatial variability in the sediments (Saunders and Kalff 2001), only sampling one area within a system and assuming the denitrification rate measured at one site is representative of the whole system (e.g., Piña-Ochoa and Álvarez-Cobelas 2006). Our study highlights the importance of investigating a variety of sediment types and spatial and temporal scales to understand the dynamic nature of nitrogen cycling within coastal lakes/lagoons.

**Table 5.5.** Pearson correlation matrix showing the relationships between the denitrification rates recorded in summer 2016 and sediment variables. \* =  $p < 0.05$ , \*\* =  $p < 0.01$ , \*\*\* =  $p < 0.001$ .

	D15	Redox	OM	Porosity	Clay	Silt
D15						
Redox	0.28					
OM	0.58*	0.11				
Porosity	0.35	-0.16	0.83***			
Clay	0.25	-0.23	0.82***	0.90***		
Silt	0.41	-0.21	0.87***	0.97***	0.86***	
Sand	-0.4	0.22	-0.87***	-0.97***	-0.87***	-1.00***

### Invertebrates and denitrification

The biodiversity of species present within Te Waihora is low, consisting of only seven identifiable taxa. The most abundant taxa within the enclosures were the mud snail *Potamopyrgus antipodarum*, the amphipod *Paracorophium excavatum* and oligochaetes. A couple of sites had high densities of chironomid larvae. The

other three taxa found were the mysid shrimp *Tenagomysis chiltoni*, and the polychaete worms of the families Nereidae and Spionidae.

Fig. 5.11 shows the densities of the three most abundant species in the enclosures during the three enclosure experiments. *P. antipodarum* was present in high densities at sites 1, 5 and 14 (Fig. 5.11A) and this snail bioturbates sediment and directly and/or indirectly enhances microbial processes and sediment oxygenation (Jones *et al.* 1994; Pelegrí and Blackburn 1994; Kristensen 2008; Dunn *et al.* 2009). *P. excavatum* also burrows into the sediment and this amphipod was also present in high densities around the lake (up to 50,000 ind. m<sup>-2</sup>) (Fig. 5.11B). Previous research has shown that amphipods can influence benthic metabolism (Dunn *et al.* 2009), and increase overall mineralization processes and denitrification due to burrow creation and sediment irrigation (Pelegrí and Blackburn 1994). Oligochaete were the most abundant infaunal species recorded in Te Waihora/Lake Ellesmere, with densities recorded up to 16,000 individuals per m<sup>-2</sup> (Fig. 5.11C) and these worms have also been shown to stimulate denitrification (Nogaro and Burgin 2014) (Chatarpaul *et al.* 1979; Pelegri and Blackburn 1995). An experiment using oligochaete densities of 27,000 individuals m<sup>-2</sup> found that they stimulated water column nitrate supported denitrification by 64% (Svensson *et al.* 2001). While they can stimulate denitrification, they are less efficient at mobilizing the nitrate to deeper sedimentary layers than chironomids are (Svensson *et al.* 2001), due to differences in their bioturbation activities.

Chironomid larvae would have the most pronounced effect on stimulating denitrification, due to their creation and maintenance of stable sediment burrows (Olafsson and Paterson 2004). Sectioned cores from Te Waihora/Lake Ellesmere showed the large influence that chironomid burrows can have on the surrounding sediment (Fig. 5.12), where their burrow tubes oxidised sediment that contacted the walls of the tubes. In summer 2016, chironomids showed a strong positive relationship with sediment organic matter ( $r=0.84$ ; Appendix C, Table 9.3), but their densities were not related to nitrate conversion rates in our enclosures, which was likely due to their unusually sparse densities in our enclosures and in the lake at the time of sampling.

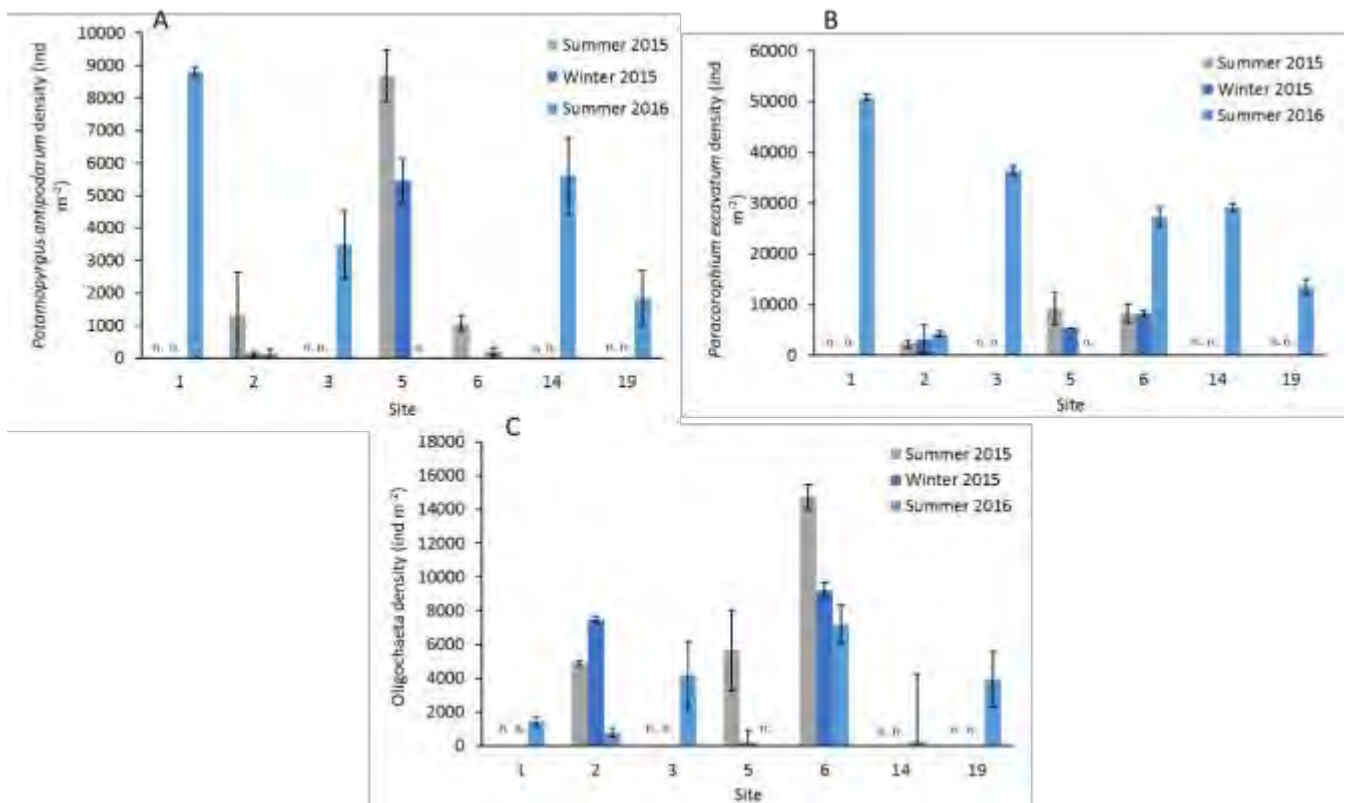


**Figure 5.11.** Densities of the three most abundant infauna species (individuals  $m^{-2}$ ) collected from the enclosure cores. A = the mud snail *Potamopyrgus antipodarum*, B = the amphipod *Paracorophium excavatum*, and C = the annelid worm family, Oligochaeta. Standard errors are shown. 'n' indicates the invertebrates were not found at that time.

We found no significant relationships between invertebrate densities and nitrate conversion rates in our study. Other studies which have shown such effects measured denitrification rates in sediment cores under controlled laboratory conditions. In such laboratory experimental situations, the water headspace in the cores was generally minimised and so was the turbulent energy input to the cores. In contrast, in our *in situ* enclosures, we retained the full water column above the sediments and allowed for turbulent energy from the highly energetic lake environment to propagate into the enclosures. Thus, in our experiments, these realistic conditions may have reduced the impact of the invertebrate infauna on denitrification. The literature clearly indicates the significance of these benthic invertebrates in supporting not only the health of the sediments, but also the stimulation of denitrification through immobilizing nitrate to deeper layers, and supporting the breakdown of organic matter. There are two possible reasons why

our results didn't link infaunal densities with nitrate conversion rates. Chironomid densities at the time of our studies were unusually low in the lake, while their chironomid tubes seemed to be intact within the sediment. Further studies will be required to more fully understand the role of infauna in denitrification in Te Waihora/Lake Ellesmere.



**Figure 5.12.** A sediment sample from Te Waihora/Lake Ellesmere showing oxidised zones around chironomid burrows.

### **Comparison of measurements of denitrification potential and nitrate conversion rates**

The *in situ* nitrate conversion rates measured in summer 2015 and summer 2016 were positively correlated (Fig. 5.13), indicating that the *in situ* rates we measured were robust over time. Similarly, the rates of denitrification potential measured *in vitro* were robust because the rates measured when amended with glucose and nitrate correlated with the rates measured when only nitrate was added. These independent checks lend credibility to these measurements.

The *in situ* rates of nitrate conversion and the *in vitro* rates of denitrification potential, however, did not correlate among the sites we studied. This is not surprising due to the fact that one method aimed to retain the biogeochemical structure of the sediment core while the other homogenised the sediment from the top 4 cm of the sediment cores. The higher rates measured *in vitro* can be attributed to the addition of labile carbon (glucose), the homogenisation of sediment which mixes the solutes in the sediment pore waters stimulating





In addition, our observations indicate that polysaccharide secretions from benthic macroinvertebrates and bacteria are also abundant in sediments at many sites and these materials may also fuel microbial activities including denitrification. Further research into labile carbon dynamics within the lake could provide valuable insights to potential temporal “hot moments” of denitrification (McClain *et al.* 2003).

Apart from the rate measured in one core, nitrate conversion rates recorded in Te Waihora/Lake Ellesmere are within the range of previously published denitrification rates in aquatic sediments ecosystems (Table 5.6). Our highest recorded rate (one replicate enclosure from site 19, which was over 10-fold higher than any other measurement) lies well outside the reported range measured using flexible enclosures. The sediment at this site had high organic matter content and oxygen was rapidly depleted within this core during the incubation, declining to  $1.72 \text{ mg L}^{-1}$ , and such hypoxic conditions may have enhanced the rate of nitrate conversion.

**Table 5.6.** Previously published denitrification rates measured in aquatic ecosystems using a type of *in situ* enclosure.

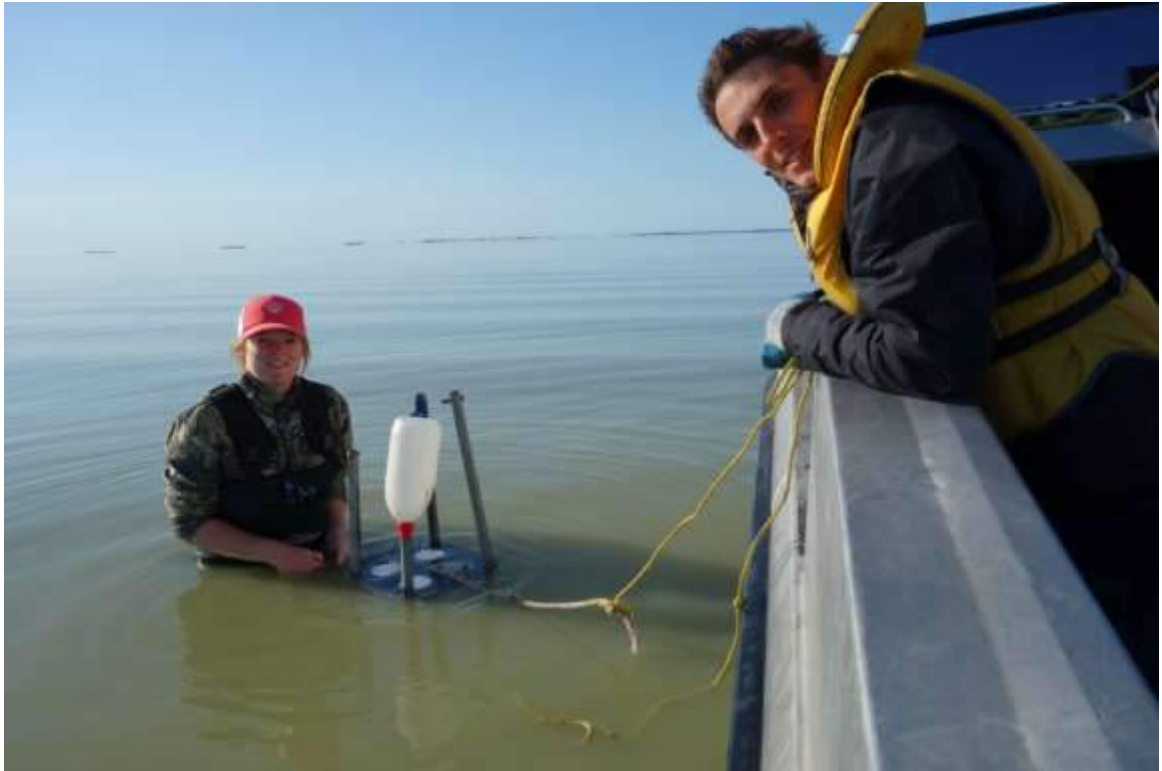
	Incubation chamber	Study System	Denitrification measurement	Denitrification rate ( $\mu\text{mol m}^{-2} \text{h}^{-1}$ )	Added/ambient nitrate ( $\mu\text{mol L}^{-1}$ )
<b>Our Study</b>	<b>Flexible enclosure</b>	<b>Shallow eutrophic lake</b>	$^{15}\text{N}$ Isotope	<b>0 – 4227</b>	<b>90 - 200</b>
Risgaard-Petersen <i>et al.</i> (1999)	Flexible enclosure	Shallow hypertrophic lake	$^{15}\text{N}$ Isotope	63 - 146	30 - 100
Tomaszek and Czerwieniec (2000)	<i>In situ</i> chamber	Reservoirs	$\text{N}_2$ flux	25 – 1102	31 - 138
Mengis <i>et al.</i> (1997)	Benthic chamber	Eutrophic lake	$^{15}\text{N}$ Isotope	179	230
Nielsen and Glud (1996)	Benthic chamber	Ocean	$^{15}\text{N}$ Isotope	15 - 19	35-50
(Smith <i>et al.</i> 2009)	Incubation chamber	Stream	$^{15}\text{N}$ Isotope	390 - 1145	34-1192
(An and Joye 2001)	Benthic chamber	Shallow estuary	$\text{N}_2$ flux	58 - 154	1.6 - 23
(Macreadie <i>et al.</i> 2006)	Incubation chamber	Harbour	$\text{N}_2:\text{Ar}$	10 - 33	0.5
(Kreiling <i>et al.</i> 2011)	Incubation chamber	Shallow lake	$^{15}\text{N}$ flux	870	179 - 536
(Tomaszek <i>et al.</i> 1997)	Incubation chamber	Freshwater wetland	$\text{N}_2$ flux	300 - 1200	0.93 - 313

## Nitrogen budgets of the enclosures

In our experiments, the majority of nitrate that was removed from the water column was not measured as N<sub>2</sub> gas by the end of the incubations. We originally hypothesised that denitrification could be a mechanism for the removal or shedding of substantial amounts of nitrate in the lake. Table 5.6 presents the amount of nitrate converted to N<sub>2</sub> gas at each site over the duration of the summer 2015/2016 experiments. Apart from one of the enclosures at Site 19, which apparently transformed more nitrate than was added, the percentages of added nitrate that was converted to N<sub>2</sub> ranged from 0.002 to 30% of the added nitrate (mean = 10%). This is likely to be an underestimate of the total nitrate converted because it is likely that some nitrate that had diffused into the sediment was yet to be converted to N<sub>2</sub> in the sediment and that some N<sub>2</sub> that had been produced in the sediment had not yet diffused into the water column at the end of the experiment. Our study does however present compelling evidence that the microbial conversion of nitrate to N<sub>2</sub> is substantial at some sites in the lake during the warmer months and that on a lake-wide basis the processes involved are likely to be at least a moderate sink for nitrate in the summer time. Nitrate conversion is very likely to be minor and unimportant in the winter due to temperature limitation of microbial activity.

**Table 5.7.** The nitrogen budget of the *in situ* enclosures using summer 2016 data (except site 5 which is 2015 summer data).

Site	Added nitrate (µmol/L)	Denitrified nitrate (µmol/L)	Remaining nitrate (µmol/L)	Missing nitrate (µmol/L)	Nitrate denitrified (%)
1	105-124	0.02-0.40	0.39-11	104-140	0.01-0.38
2	81-101	0.01	0.57-0.68	80-99.9	0.01
3	99-126	0.84-36	0.53-37	44-124	0.67-30
5	90-201	0.001-0.14	0.68-4	73-201	0.0005-0.16
6	95-125	5-27	0.45-7	86-105	4-22
14	96-124	0.003-0.02	0.5-3	96-122	0.002-0.02
19	185-393	27-502	4-29	-168 - 330	9-149



Sampling water from the *in situ* enclosure.

## DISCUSSION AND CONCLUSIONS

---

Our results indicate that nitrate removal through microbial denitrification may not directly convert the major proportion of nitrate entering Te Waihora/Lake Ellesmere. This may be due to competition for nitrate with the high biomass of phytoplankton in the water column, which are apparently able to rapidly absorb large pulses of nitrate. The greater the phytoplankton biomass, the greater the phytoplankton uptake capacity is and the less nitrate there will be immediately available for denitrification and conversion to  $N_2$ .

This raises the possibility that the lake may support higher rates of nitrate conversion than we were able to measure because recycled (as opposed to influent) nitrate may drive a substantial amount of denitrification. The nitrate taken up by phytoplankton can subsequently be mineralised to ammonium, which can then undergo nitrification and eventually denitrification in the sediments. Our methods were unable to measure the contribution of recycled nitrogen to

denitrification in the lake. Further work would be needed to quantify the contribution of recycled nitrate to the pool of denitrified N.

Temperature has been clearly shown to impose a strong influence on nitrate conversion rates, and this indicates that nitrate conversion is essentially shut down in winter, the time when most of the pulsed loads of nitrate arrive in the lake. Nitrate additions to the lake during the colder months will be mostly available for assimilation by the high phytoplankton biomass in this lake (Hamill and Schallenberg 2013).

The spatial patterns of nitrate conversion were difficult to attribute to any specific variables. This was partly due to the very high within-site variability in nitrate conversion rates, which has also been reported in an Australian coastal embayment (Berelson *et al.* 1998). This may be due to high within site variability in sediment characteristics (particularly infaunal density and activity and burrow density). Variations in infaunal density between the sites did not correlate with nitrate conversion rate and this may also be due to the high within site variability in infaunal density and burrow density, which appeared to be decoupled in our study due to unusually low numbers of chironomids present in the lake.

As has been reported in a coastal embayment (Berelson *et al.* 1998), denitrification in Lake Ellesmere is seasonally and spatially highly variable. When nitrate was available, organic carbon supply was the most significant variable supporting denitrification rates within our *in situ* experiments, accounting for some of the spatial variation in denitrification rates. Lag periods were exhibited in finer grained sediments, likely due to the slow rates of nitrate and gas diffusion, influencing competition between sediment denitrifiers and phytoplankton for nitrate. Nitrogen fixation was recorded in summer 2016 at most sites, reducing net nitrogen removal by conversion to N<sub>2</sub>. It is not known whether this apparent N-fixation was due to the activity of cyanobacteria in the water column, or sulphate reducing bacteria in the sediment. Sediment invertebrate communities were not significantly related to denitrification rates in this study, however their high abundances in the littoral margins probably stimulate denitrification through their bioturbation activities. Denitrification does provide a sink for nitrate in Lake

Ellesmere, however this is seasonally limited to the warmer months and is enhanced in shallow zones of the lake.



Attaching the flexible tubing to the enclosure after measuring the water depth.

---

## Section 6

---

### 6 SUMMARY OF N AND P DYNAMICS IN TE WAIHORA/LAKE ELLESMERE AND RELEVANCE FOR MANAGEMENT

---



Foam produced by phytoplankton exudate, blown on shore at Timberyard Point, April 2015.



## THE RELATIONSHIP BETWEEN NUTRIENT AND PHYTOPLANKTON DYNAMICS

---

Previous studies have suggested that both N and P concentrations can at times be saturating and limiting to the growth of phytoplankton in Te Waihora/Lake Ellesmere. Measurements and experiments by Hawes and Ward (1996) indicated that additions of both N and P could stimulate phytoplankton growth in lake water samples incubated at saturating light intensities, but that in the lake itself, light availability in the water column was the primary factor restraining phytoplankton growth. In their experiments, Hawes and Ward (1996) found that additions of N stimulated phytoplankton growth more frequently than additions of P.

Using the rates of phytoplankton productivity from Hawes and Ward (1996), Sorrell *et al.* (1998) estimated rates of N and P uptake by the phytoplankton in the lake and concluded that rate of nutrient uptake by phytoplankton probably exceeded the rate of nutrient supply from external sources, except during winter. They also concluded that the estimated rate of nutrient uptake by phytoplankton could fully account for the conversion of dissolved forms of N and P (which dominate the flows) to particulate forms (that dominate within the lake).

Furthermore, based on records of the absolute and relative concentrations of dissolved inorganic nitrogen and total phosphorus in the lake over the period 1983-2005, Larned and Schallenberg (2006) inferred that the phytoplankton in the lake were probably equally limited by N and P availability throughout the time period, but that low nutrient availability only constrained phytoplankton growth around 10 percent of the time due to extreme light attenuation in the water column. The severe restriction of light penetration into the lake was confirmed by Stephens and Hawes (2002) who calculated that the typical depth to which 1% of surface light penetrates in the lake is generally between 20 and 60 cm, with occasional, transient penetration depths of up to 1 m. When compared to the mean (1.4 m) and maximum (2.3 m) depths of Te Waihora/Lake Ellesmere, these calculations also imply that light availability is often low enough to be the main constraining factor to phytoplankton growth.

This general picture of the drivers of phytoplankton growth was supported by a modelling exercise, based on input data from January 2000 to January 2001, which estimated that phytoplankton growth in the lake was limited by light 51% of the

time, by N availability 37% of the time and by P availability 12% of the time (Hamilton 2009).

Schallenberg *et al.* (2010) and Hamill and Schallenberg (2013) examined nutrient concentrations and ratios in the inflows and lake to infer the nutrient status of phytoplankton in the lake. In-lake nutrient concentrations and ratios confirmed earlier analysis indicating that phytoplankton growth in the lake is more likely to be constrained by N availability than P availability, but that concentrations of available forms of both N and P in the lake were often high enough to imply that other factors must also often constrain phytoplankton growth. However, Schallenberg *et al.* (2010) found that chlorophyll *a* concentrations in the lake were weakly positively correlated with catchment DRP loading rates and not with N loading rates, implying that DRP loading from the tributaries could be an important factor driving phytoplankton biomass.

In summary, generally, previous studies have shown that while light and other factors also constrain algal blooms in Te Waihora/Lake Ellesmere, when the conditions of these other factors are suitable for phytoplankton growth, the availability of nitrogen is more likely to constrain and fuel production than the availability of phosphorus, although either or both can drive/limit production at certain times (Table 6.1). Only the external load of DRP was weakly correlated with chlorophyll *a* (no other nutrient loads were correlated), so any links between external N and P loading and in-lake phytoplankton production and biomass are complex and mediated by other factors.

**Table 6.1.** Summary of findings of studies linking nutrient availability to phytoplankton biomass and production in Te Waihora/Lake Ellesmere.

Study	Phytoplankton growth	Time period of inference
Hawes & Ward (1996)	Bioassays indicated N additions stimulated more often limiting than P.	1996
Larned & Schallenberg (2006)	Analysis of in-lake nutrient ratios indicated light limitation was most prevalent and nutrient shortages limited production for < 10% of the record (N and P limitation was equally prevalent in the lake).	1983 to 2005
Hayward & Ward (2009)	Phytoplankton growth was generally not N limited because chlorophyll a did not decline during 1993-2007 despite decreases in TN and DIN observed in the lake and tributaries.	1993 to 2007
Hamilton (2009)	Phytoplankton growth was constrained by light availability 51% of the year, N availability 37% of the year and P availability 12% of the year.	January 2000 to January 2001
Schallenberg <i>et al.</i> (2010)	Based on nutrient ratios in the lake and in the absence of other limiting factors such as light, temperature and grazing, phytoplankton growth is most likely to be constrained by N availability. However, chlorophyll <i>a</i> concentrations increased linearly with rates of DRP loading from the tributaries, not with rates of DIN loading.	1996 to 2007
Hamill & Schallenberg (2013)	Light, temperature and salinity may be more important than nutrients in constraining phytoplankton growth, but, based on nutrient ratios, N-limitation is would be more common than P limitation.	1992 to 2013
This study	Based on changes in dynamics of in-lake dissolved inorganic nutrient concentrations both prior to, and during, phytoplankton blooms, both N and P availability appeared to influence the formation and persistence of numerous phytoplankton blooms in the lake. Not all blooms seemed to be directly related to nutrient dynamics.	1992 to 2013

In this study, we examined the relationship between nutrient availability and phytoplankton dynamics in a novel way - by identifying discrete phytoplankton blooms and then examining the dynamics of available nutrients in the lake immediately prior to, and during, the blooms. This approach identifies potential interactions between phytoplankton blooms and nutrient availability, allowing the identification of blooms that were potentially fuelled by nutrient availability and blooms which eventually exhausted nutrient availability.

We identified 14 discrete phytoplankton blooms in the chlorophyll *a* record from the mid-lake site spanning the years 1992 to 2013 (Table 1.1). **Unlike the blooms in Wairewa/Lake Forsyth, the blooms in Te Waihora/Lake Ellesmere were not regular, discrete, seasonal blooms, but often persisted for more than one year and sometimes skipped years. Although blooms most often occurred in spring and summer, they sometimes persisted for more than one year.** This confirms that a complex set of factors regulates phytoplankton dynamics in Te Waihora/Lake Ellesmere.

Our analysis showed that phytoplankton blooms were often preceded by spikes in available N and/or P, suggesting that concentrations of available nutrients in the lake were often low enough to constrain phytoplankton production, especially in spring and summer and that the sudden availability of nutrients in the lake at these times often precedes phytoplankton blooms. **Therefore, despite the inconsistent and complex nature of phytoplankton dynamics in Te Waihora/Lake Ellesmere, our analysis supports previous work suggesting that nutrient availability plays a role in regulating phytoplankton blooms in the lake and that both N and P availability are important at times, especially during spring and summer.**

## THE ROLE OF DENITRIFICATION IN NITROGEN CYCLING

---

A key question of our research concerns the potential role of denitrification in Te Waihora/Lake Ellesmere. The dynamic Te Waihora/Lake Ellesmere model of Hamilton (2009) suggested that the lake lost  $8.1 \text{ mg N m}^{-2} \text{ d}^{-1}$ , when averaged over one year (2000 to 2001). Denitrification is just one microbial mechanism that can convert nitrate to  $\text{N}_2$  gas. When ammonium and nitrite co-exist under the right conditions, microbial anaerobic ammonium oxidation can also result in the

production of N<sub>2</sub> gas. However, denitrification is the most commonly studied mechanism and is probably the most important mechanism in estuarine systems.

Denitrification generally proceeds when nitrate diffuses across an oxic-anoxic boundary in the presence of heterotrophic denitrifying bacteria which require carbon substrates to accomplish the denitrification process. In turbulent, aerobic aquatic systems, denitrification will most likely occur in the sediments where an oxygen gradient exists some distance below the sediment water interface. In such environments, denitrification should also be dependent on the rate of diffusion of nitrate into the sediments, which will be dependent on the porosity, cohesiveness, organic matter concentration and infaunal density of the sediment, which will influence the depth and steepness of the oxygen gradient within the sediment.

We attempted to measure the rate of conversion of nitrate in the water column to N<sub>2</sub> gas in the water column. Because Te Waihora/Lake Ellesmere is such a turbulent system, we designed *in situ* experimental enclosures that enclosed the water column and sediments, but allowed the transfer of turbulent wave energy through the flexible walls of the enclosure into the experimental system. Nitrate was added to the enclosures to final concentrations that were similar to episodic peaks of nitrate recorded in the ECAN dataset for the mid-lake site. The nitrate was spiked with <sup>15</sup>N and this tracer was measured in N<sub>2</sub> gas released within the enclosures over a period of approximately 48 h. These experiments were able to measure the short term loss of nitrate from the water column and the subsequent increase in N<sub>2</sub> in the water column over the time course of the experiments.

Nitrate was always rapidly depleted from the water column and our results indicated that it was mostly taken up by phytoplankton, supporting the findings of Sorrell *et al.* (1998) who calculated that the phytoplankton in the water column of the lake were abundant and productive enough to account for the conversion of the large nitrate loads of the inflows into the high levels of particulate N measured in the water column of the lake. Thus, the large nitrate pulses that sometimes enter the lake (especially in winter) are rapidly taken up by phytoplankton and this represents a process that competes with the sediment denitrification process for nitrate in the water column. We undertook denitrification experiments in winter and summer, but were only able to measure significant nitrate conversion

rates in summer (January and March), suggesting that the colder temperatures in winter inhibit denitrification. **Thus, there is a disconnect between the timing of major inputs of nitrate to the lake (which tend to happen in winter) and the period of activity of denitrifying bacteria.**

Rates of conversion of nitrate to N<sub>2</sub> gas measured in our enclosures also varied markedly at different spatial scales, as has been reported for a coastal embayment (Berelson *et al.* 1998). Sometimes, replicate enclosures showed different rates of conversion as did the different sites. We found that the organic matter content of the sediment correlated positively with nitrate conversion rates, but organic matter content was also correlated to numerous other sediment characteristics. Generally, sediments richer in organic matter also had finer sediment grain sizes (i.e. lower sand content) and higher porosity, so this general gradient probably is the key gradient driving denitrification in the lake. We measured *in vitro* sediment denitrification potentials at all 18 sites in the lake and the general pattern observed was that the shallower sites showed greater denitrification potentials than the deeper sites in the middle of the lake.

Apart from one anomalous measurement, *in situ* rates of nitrate conversion to N<sub>2</sub> gas varied between 0 and 135 mg N m<sup>-2</sup> d<sup>-1</sup> and these rates are within the range reported in the literature for aquatic ecosystems. One replicate measurement made at the site where Hart's Ck. flows into the lake was around 10-fold greater than the maximum conversion rate recorded among all other enclosure measurements and we consider this to be an anomaly in our dataset, possibly related to the hypoxia that occurred in the enclosures at this site because of the very shallow water depth and high organic matter content of the sediment. When comparing our measured rates with the average lake-wide loss rate of N averaged over 1 year calculated by (Hamilton 2009) which was 8.1 mg N m<sup>-2</sup> d<sup>-1</sup>, it is apparent that at some of our sites, the measured summer conversion rates were much higher than this estimated lake-wide annual average (e.g. up to 135 mg N m<sup>-2</sup> d<sup>-1</sup>). However, our experiments involved spiking the enclosures with high concentrations of nitrate, which could be expected to generate a maximum conversion rate under nitrate-saturating conditions. In contrast, no nitrate conversion to N<sub>2</sub> gas was recorded during winter due to low temperatures. So,

given these caveats, our measurements appear to be roughly supportive of the annual N losses estimated by the dynamic model for the lake.

Although the measured rates of nitrate conversion were often substantial in relation to other rates of denitrification published in the literature, the proportion of the N load spiked into the enclosures that was converted to N<sub>2</sub> was usually small (the summer average was around 10%). This probably reflects some of the limitations of our experimental approach, which necessitated short experimental incubations because phytoplankton usually took up most of the nitrate very rapidly. Because of the short-term experimental time frame, we could not measure the potential conversion of N to N<sub>2</sub> that could occur once phytoplankton senesce at the sediment-water interface, releasing ammonium and dissolved organic N, which could be nitrified in the sediments, followed by denitrification. So, the eventual re-processing of nitrate initially taken up into phytoplankton is a longer-term denitrification pathway that we were unable to quantify using our approach and which may be an important indirect denitrification pathway in Te Waihora/Lake Ellesmere. Much more detailed measurements of N transformations between organic forms and N<sub>2</sub> in the lake sediments would need to be carried out over longer time scales to quantify such potentially important processes.

Organic matter availability to the heterotrophic microbial denitrifying bacteria appeared to influence both the measurements of *in vitro* denitrification potential (where the addition of glucose stimulated denitrification) and the *in situ* measurements of nitrate conversion (which were positively correlated with sediment organic matter content). In both cases, carbon stimulation was an important secondary stimulant of the microbial process, increasing rates once nitrate had been added to the systems. The indication that the supply of labile carbon limits the rate of denitrification suggests that increasing the supply of labile organic carbon to the sediments could enhance denitrification in the lake. However, before organic carbon amendments are considered as a potential management action, the findings of Berelson et al. (1998) in Port Phillip Bay, Australia, should be considered. These researchers found that the denitrification efficiency (denitrification vs. N cycling) in the sediments decreased as the amounts

of labile organic carbon in the sediments increased. This suggests the existence of an optimum carbon supply rate, and further studies in Te Waihora/Lake Ellesmere would need to be undertaken to ascertain the relationship between denitrification rate and organic matter supply rate so as to optimise the supply rate and to avoid overloading the sediments with organic carbon.

Both methods suggested that the shallower sites around the northern and eastern lake margins were the sites with the highest rates of nitrate conversion/denitrification rates. In addition, a site in the Hart's Creek estuary showed high rates of nitrate conversion to N<sub>2</sub> gas during summer 2016 (the only time this site was studied).

## THE POTENTIAL FOR INTERNAL P LOADING

---

### Sediment P pools and exchange rates

The amount of P in various fractions within the sediments of Te Waihora/Lake Ellesmere is considerable and similar to other lakes in the South Island for which these fractions have been measured. In this lake, the largest P fractions are bound to calcium, organic matter and aluminium, but these fractions are not readily and rapidly exchangeable with pore water under normal conditions in the lake. The smallest fractions, including pore water P, loosely-bound P and metal oxyhydroxide-bound P, are the most readily exchanged with the pore water and hence the water column, particularly if the sediment were to become anoxic. The aluminium-bound fraction would be exchangeable under conditions of high pH (e.g. > 9), but we didn't study the release rates of this fraction of sediment P.

The redox-exchangeable fraction of P, measured as the increase in pore water P resulting from a shift to anoxic state, was weakly positively correlated to the P fraction bound to metal oxyhydroxides. The redox-exchangeable fraction was somewhat lower than the metal oxyhydroxide-bound fraction (as measured by chemical extraction), but this may have been due to changes in P fractions as a result of the sequential P fraction analysis methodology. **The spatial pattern of redox-exchangeable P in the sediments indicated that sediments releasing the largest amounts of P under anoxic conditions are those near the Selwyn River inflow and those in the northern part of Kaituna Lagoon.** Sites closer to the Kiorete Spit



and to the barrier bar opening site have little redox-exchangeable P and this may be due to sediment sulphur levels which may bind iron in the form of iron sulphide, preventing iron oxyhydroxides from participating in P binding. Overall, the results show that the sediments of Te Waihora/Lake Ellesmere contain a pool of P which is either dissolved in pore water, loosely-bound to sediment and colloids or is redox exchangeable (available under anoxic conditions).

Interestingly, our study also showed that small amounts of redox-exchangeable N were also released under anoxic conditions from sediments collected from most of the sites in the lake and this N was likely to be in the form of ammonium, which is available to phytoplankton. However, these relatively small releases of N are unlikely to be important to the phytoplankton except during periods when dissolved inorganic N concentrations are low in the lake.

#### **Water column anoxia and the release of sediment bound P**

Our study examined oxygen depletion in the bottom waters of Te Waihora/Lake Ellesmere which could facilitate internal loading of P from the sediments into pore water and consequently into the water column of the lake, potentially fuelling phytoplankton blooms. ***In situ* dissolved oxygen sensors recorded transient periods of bottom water deoxygenation lasting up to only a few hours and only during calm periods in summer and autumn.** Such periods of oxygen depletion at the sediment-water interface could dissolve redox-exchangeable P and N, allowing them to diffuse into the water column. **Transient episodes of complete anoxia were only found to occur in the mid-lake site (not near the Taumutu lake opening site) during summer and autumn.** Saline intrusions from lake openings and barrier bar splash-over events did not result in vertical density stratification leading to bottom water anoxia during the study period, but the role of saline intrusions as potential drivers of bottom water anoxia merit further study.

*In vitro* measurements of sediment oxygen depletion showed that these rates did not vary greatly among sites within the lake. Sites with the highest sediment chemical and biological oxygen demands tended to be the deeper sites with higher clay and silt contents. This is consistent with measured *in situ* bottom water

deoxygenation, which occurred at ECAN's mid-lake site and not at the shallower Taumutu site.

Sediment oxygen penetration depths were highly variable both within and among sites, largely due to the burrowing activities of infauna such as oligochaetes. It is likely that the densities of infaunal sediment irrigators in the sediment influence conversion rates of nitrate to N<sub>2</sub> gas, but we found no evidence of such a correlation. The lack of a correlation between infauna and nitrate conversion rates in our data contrasts with findings from other published studies and may be due to the unusually low chironomid densities we observed in the lake during our study, while many unoccupied chironomid tubes were obviously still present in the sediments. Measurements of chironomid tube densities at the sites might have shown a stronger correlation with nitrate conversion rates than chironomid densities did.

Our findings suggest that transient anoxic events occur at the sediment-water interface in this lake, principally during summer and autumn and in the deep water zones. These events, which are precipitated by calm conditions, probably release small amounts of dissolved reactive phosphorus into sediment pore waters and subsequently into the water column while anoxia persists. Subsequent wind-induced turbulent mixing will entrain released P into the mixed layer where it can be rapidly taken up by phytoplankton. Increased sulphate concentrations, related to saline intrusions, probably reduces the pool of redox-exchangeable P in the sediment by binding iron as FeS, but in the process of scavenging Fe, this process may also facilitate the release of some P into the water column.

To date, episodes of anoxic P release have not been measured in the lake, but our evidence of transient anoxic episodes indicates that P releases should be measurable in the bottom waters during calm periods in summer and autumn within the deeper, profundal zone of the lake. Both anoxic releases and frequent sediment resuspension by winds probably regularly equilibrate the surface sediment pore water P with the water column, but sediment regeneration of P from the decomposition of organic matter probably provides a continual supply of redox-exchangeable P and porewater P, especially during summer and autumn.

Our studies have provided evidence that internal nutrient processing with Te Waihora/Lake Ellesmere contributes to the dynamics of available nutrients in the water column of the lake and that these nutrients, in turn, are important drivers/regulators of phytoplankton blooms. However, the relationships between nutrient processing, nutrient availability and phytoplankton blooms are complex and variable, both in space and time. **Strong seasonality of both nutrient inputs and nutrient processing/cycling can couple internal anoxic sediment P releases with the major summer period of phytoplankton blooms. However strong seasonal decoupling between the periods of high nitrate inputs to the lake in winter and the time of microbial conversion of nitrate to N<sub>2</sub> in summer and autumn, means that much of the nitrate load entering the lake from the catchment is mainly available to phytoplankton, without much competition for nitrate by denitrifiers. Denitrification proceeds in summer, but at that time it is probably mainly driven by nitrate supplied indirectly, after the mineralisation of dead phytoplankton biomass and subsequent microbial nitrification phytoplankton-derived ammonium within the sediments. Thus, nitrification within the sediments of organic N probably also plays an important role in nitrogen cycling and denitrification within the lake.**

## RELEVANCE OF FINDINGS FOR MANAGEMENT

---

This report contributes to a programme of work undertaken by Whakaora Te Waihora and Environment Canterbury to investigate a range of potential restoration options for Te Waihora/Lake Ellesmere. This work also contributes to the Zone Committee Regional Planning Process which has identified a range of pathways and actions to explore to restore Te Waihora/Lake Ellesmere to help give effect to the Canterbury Water Management Strategy. In addition, the findings of this report contribute to an updating of the Te Waihora/Lake Ellesmere dynamic ecological model (Dada et al. 2016), which is being used to test future land use and climate change scenarios for the lake.

The findings of our investigations into in-lake nutrient cycling and processing support many of the pathways and actions outlined by the Selwyn Waihora Zone Committee (SW ZIP 2013) (Table 6.2). Te Waihora/Lake Ellesmere is one of the most eutrophic lakes in New Zealand and while in-lake interventions to reduce

nutrient availability to phytoplankton are likely to provide some benefits (e.g., Table 6.2), returning the lake back to a condition where water clarity supported macrophyte beds and more diverse aquatic communities will ultimately rest on success in reducing the external nutrient loads to the lake (MacKenzie 2016; Schallenberg et al. 2016).

**Table 6.2.** Relevance of findings of the present study to lake restoration pathways and actions identified by the Selwyn Waihora Zone Committee (SW ZIP 2013).

<b>Pathways and Actions</b>	<b>Implications of the present study</b>
<b>Water quality actions</b>	
Restrict N load	This study suggests that in-lake denitrification competes for inflowing nitrate with phytoplankton, especially during the colder months when pulses of nitrate often enter the lake. Our results indicate that denitrification rates are significant but not substantial, compared to phytoplankton uptake. In light of the moderate magnitude of whole-lake denitrification inferred from our study, restricting the external N load will probably have a large impact on nitrogen availability to algae.
Restrict P load	This study shows that the sediments of the lake contain exchangeable phosphorus and probably recycle significant amounts of this phosphorus, especially in summer. In addition to restricting the availability of new phosphorus to algae, restricting the P load to the lake will, over time, also reduce the pool of recyclable phosphorus in the sediment.
Manage sediment losses	Fine sediments in the lake are a key factor reducing light penetration. They also contain sediment-bound phosphorus, which contributes to the amount of P that can be recycled in the lake. Reducing the input of fine sediment should improve light penetration (for potential macrophyte recovery) and also reduce the amount of recyclable P in the lake.
<b>Lake interventions</b>	
Lake level and lake margin	Changes to the management of lake level and artificial openings would be expected to have substantial effects on

management (opening management)	nutrient cycling within the lake. Our study showed transient vertical stratification and periods of anoxia in the open water of the lake. Lowering the water levels could inhibit stratification from occurring, increasing the advection and diffusion of dissolved oxygen from the atmosphere to the lake bed. This could consequently result in less internal P release from the sediment. However, the reduction of water levels would likely also increase wind-induced sediment resuspension, reducing water clarity. During our study, we also observed the profound negative effect of high salinity associated with an extended lake opening on the chironomid density in the lake bed. The sediment irrigation and oxygenation provided by chironomids probably enhances sediment denitrification, although we were unable to find evidence of this during our study, which was affected by reduced chironomid abundance.
Addressing legacy phosphorus	This study has shown that there is a pool of phosphorus in the lake sediment that can be recycled into the water column either by anoxia or by organic matter degradation. Interventions to reduce these potentially available pools of legacy phosphorus would be expected to reduce the amount of phosphorus available to algae.
Restoring macrophyte beds	Macrophytes profoundly influence nutrient cycling in lakes. By oxygenating the rhizosphere in lake sediments, macrophytes can increase rates of nitrification (and ultimately denitrification) and improve sediment P binding. Biofilms growing on macrophytes are also able take up available nutrients from the water column and in some cases increase denitrification. Although we weren't able to directly measure the beneficial effect of macrophytes on sediment denitrification in the lake (due to a lack of macrophytes at our study sites), we expect that restoring macrophyte beds would increase denitrification and nutrient uptake, reducing the amount of nitrate and phosphate that would be available for algae.
Constructing floating wetlands and enhancing lake margin wetlands	Wetlands are habitats which can exhibit high rates of denitrification. Therefore, efforts to develop floating and marginal wetlands would be expected to enhance overall denitrification rates in the lake, reducing the amount of nitrate available for phytoplankton growth.

---

# Section 7

---

## REFERENCES

---

Ahlgren, I., Sorensson, F., Waara, T. & Vrede, K. 1994. Nitrogen budgets in relation to microbial transformation in lakes. *Ambio*, 23, 367-377.

Aller, R. C. 1998. Benthic fauna and biogeochemical processes in marine sediments: the role of burrow structure. *In: BLACKBURN, T. H. & SØRENSEN, J. (eds.) Nitrogen Cycling in Coastal Marine Environments*. Chichester: John Wiley & Sons Ltd.

An, S. & Joye, S. B. 2001. Enhancement of coupled nitrification-denitrification by benthic photosynthesis in shallow estuarine sediments. *Limnology and Oceanography*, 46, 62-74.

Banks, J. L., Ross, D. J., Keough, M. J., Macleod, C. K., Keane, J. & Eyre, B. D. 2013. Influence of a burrowing, metal-tolerant polychaete on benthic metabolism, denitrification and nitrogen regeneration in contaminated estuarine sediments. *Marine Pollution Bulletin*, 68, 30-37.

Berelson, W.M, Heggie, D., Longmore, A. Kilgore, T., Nicholson, G., Skyring, G. 1998. Benthic nutrient recycling in Port Phillip Bay, Australia. *Estuarine and Coastal Shelf Science*, 46, 917-934.

Bertics, V. J., Sohm, J. A., Treude, T., Chow, C. E. T., Capone, D. G., Fuhrman, J. A. & Ziebis, W. 2010. Burrowing deeper into benthic nitrogen cycling: the impact of bioturbation on nitrogen fixation coupled to sulfate reduction. *Marine Ecology Progress Series*, 409, 1-15.

Biswas, J. K., Ranaa, S., Bhakta, J. N. & Jana, B. B. 2009. Bioturbation potential of chironomid larvae for the sediment–water phosphorus exchange in simulated

pond systems of varied nutrient enrichment. *Ecological Engineering*, 35, 1444–1453.

Braak, C. t. & Smilauer, P. 2002. CANOCO reference manual and CanoDraw for Windows user's guide: software for canonical community ordination (version 4.5), Microcomputer power, Itaca, www.canoco.com.

Bruesewitz, D., Hamilton, D. & Schipper, L. 2011. Denitrification Potential in Lake Sediment Increases Across a Gradient of Catchment Agriculture. *Ecosystems*, 14, 341-352.

Carpenter, E. J. & Capone, D. G. 1983. *Nitrogen in the marine environment*, New York, Academic Press INC.

Chatarpaul, L., Robinson, J. B. & Kaushik, N. K. 1979. Effects of Tubificid Worms on Denitrification and Nitrification in Stream Sediment. *Canadian Journal of Fisheries and Aquatic Sciences*, 37, 656-663.

Colt, J. 2012. 2 - Solubility of Atmospheric Gases in Brackish and Marine Waters. In: COLT, J. (ed.) *Computation of Dissolved Gas Concentration in Water as Functions of Temperature, Salinity and Pressure (Second Edition)*. London: Elsevier.

Dada, A. C., McBride, C., Cho, E., Lehman, M. K., Hamilton, D. P. 2016. Water Quality Modelling of Te Waihora/Lake Ellesmere. Report of the Environmental Research Institute, University of Waikato, Hamilton.

Dodla, S. K., Wang, J. J., DeLaune, R. D. & Cook, R. L. 2008. Denitrification potential and its relation to organic carbon quality in three coastal wetland soils. *Science of The Total Environment*, 407, 471-480.

Downing, J. A. & McCauley, E. 1992. The nitrogen:phosphorous relationship in lakes. *Limnology and Oceanography*, 37, 936-945.

Dunn, R. K., Welsh, D., Jordan, M., Teasdale, P. & Lemckert, C. 2009. Influence of natural amphipod (*Victoriopisa australiensis*) (Chilton, 1923) population densities on benthic metabolism, nutrient fluxes, denitrification and DNRA in sub-tropical estuarine sediment. *Hydrobiologia*, 628, 95-109.

- Eyre, B. D. & Ferguson, A. J. P. 2005. Benthic metabolism and nitrogen cycling in a subtropical east Australian estuary (Brunswick): Temporal variability and controlling factors. *Limnology and Oceanography*, 50, 81-96.
- Fulweiler, R. W., Brown, S. M., Nixon, S. W. & Jenkins, B. D. 2013. Evidence and a conceptual model for the co-occurrence of nitrogen fixation and denitrification in heterotrophic marine sediments. *Marine Ecology Progress Series*, 482, 57-68.
- García, r., Pattinson & Whitton 1998. Denitrification in river sediments: relationship between process rate and properties of water and sediment. *Freshwater Biology*, 39, 467-476.
- Gerbeaux, P. 1993. Potential for re-establishment of aquatic plants in Lake Ellesmere (New Zealand). *Journal of Aquatic Plant Management*, 31, 122-128.
- Gibbs, M., Norton, N. 2013. Te Waihora/Lake Ellesmere: water quality remediation and ecosystem restoration opportunities. NIWA Client Report CHC2012-138. Prepared for Environment Canterbury, Christchurch. 82 p.
- Gilbert, F., Aller, R. C. & Hulth, S. 2003. The influence of macrofaunal burrow spacing and diffusive scaling on sedimentary nitrification and denitrification: An experimental and model approach. *Journal of Marine Research*, 61, 101-125.
- Golterman, H. L. 2007. The chemistry of phosphate and nitrogen compounds in sediments. Heidelberg: Springer.
- Gongol, C. L. 2010. Denitrification, oxygen consumption, and anaerobic ammonium oxidation in sediments of four New Zealand estuaries. Doctor of Philosophy PhD, University of Otago.
- Gooderham, J. & Tsyrlin, E. 2002. The waterbug book: A guide to the freshwater macroinvertebrates of temperate Australia, Australia, CSIRO Publishing.
- Groffman, P. M. & Tiedje, J. M. 1989. Denitrification in north temperate forest soils: Spatial and temporal patterns at the landscape and seasonal scales. *Soil Biology and Biochemistry*, 21, 613-620.
- Groffman, P. M. & Tiedje, J. M. 1991. Relationships between denitrification, CO<sub>2</sub> production and air-filled porosity in soils of different texture and drainage. *Soil Biology and Biochemistry*, 23, 299-302.



- Hamersley, M. R. & Howes, B. L. 2005. Evaluation of the N<sub>2</sub> flux approach for measuring sediment denitrification. *Estuarine, Coastal and Shelf Science*, 62, 711-723.
- Hamill, K. D. & Schallenberg, M. 2013. Mechanisms that drive in-lake nutrient processing with Te Waihora/Lake Ellesmere: Inter-annual water quality variability. Whakatane, New Zealand: River Lake Ltd.
- Hamilton, D. P. 2009. Brief of evidence for Te Runanaga O Ngai Tahu in the matter of the proposed Central Plains Water Enhancement Scheme. Environment Canterbury and Selwyn District Council.
- Hamilton, D. P. & Mitchell, S. F. 1997. Wave-ensued shear stresses, plant nutrients & chlorophyll in seven shallow lakes. *Freshwater Biology*, 38, 159-168.
- Hamilton, S. K. & Ostrom, N. E. 2007. Measurement of the stable isotope ratio of dissolved N<sub>2</sub> in <sup>15</sup>N tracer experiments. *Limnology and Oceanography: Methods*, 5, 233-240.
- Hawes, I. & Ward, J. C. 1996. The factors controlling the growth and abundance of phytoplankton in Lake Ellesmere. NIWA Client Report CRC 60506 prepared for Environment Canterbury, Christchurch: Environment Canterbury.
- Haywood, S. & Ward, J. C. , 2009. Water quality in the Ellesemere Catchment. Pp. 21-31 In: Hughey, K. F. D. & Taylor, K. J. W. (eds) Te Waihora/Lake Ellesmere - the 2007 state of the lake and management futures report.
- Holdren, G. C. & Armstrong, D. E. 1980. Factors affecting phosphorus release from intact lake sediment cores. *Environmental Science & Technology*, 14, 79-87.
- Howarth, R. W. 1988. Nutrient limitation of net primary production in marine ecosystems. *Annual Review of Ecology and Systematics*, 19, 89-110.
- Howarth, R. W., Marino, R. & Lane, J. 1988. Nitrogen fixation in freshwater, estuarine, and marine ecosystems. 1. Rates and importance. *Limnology and Oceanography*, 33, 669-687.
- Hughes, H. R., McColl, R. H. S. & Rawlence, D. J. 1974. Lake Ellesmere, Canterbury, New Zealand. A review of the lake and its catchment. New Zealand Department of

- Scientific and Industrial Research Information Series No. 99. DSIR, Wellington. 27 p.
- Inwood, S., Tank, J. & Bernot, M. 2007. Factors Controlling Sediment Denitrification in Midwestern Streams of Varying Land Use. *Microbial Ecology*, 53, 247-258.
- James, K. R., Cant, B. & Ryan, T. 2003. Responses of freshwater biota to rising salinity levels and implications for saline water management: a review. *Australian Journal of Botany*, 51, 703-713.
- Jellyman, D. J. 2012. Fish recruitment into Te Waihora/Lake Ellesmere. A consideration of the requirements of key species. NIWA Report CHC2001-094 prepared for Environment Canterbury. Environmental Canterbury, Christchurch. 75 p.
- Jia, Z., Liu, T., Xia, X. & Xia, N. 2016. Effect of particle size and composition of suspended sediment on denitrification in river water. *Science of The Total Environment*, 541, 934-940.
- Jones, C. G., Lawton, J. H. & Shachak, M. 1994. Organisms as Ecosystem Engineers. *Oikos*, 69, 373-386.
- Jones, M. B. & Marsden, I. D. 2005. *Life in the estuary : illustrated guide and ecology*, Christchurch, New Zealand, Canterbury University Press.
- Kalff, J. 2002. *Limnology: Inland water ecosystems.* , New Jersey, Prentice Hall.
- Kelly, D. J. & Jellyman, D. J. 2007. Changes in trophic linkages to shortfin eels (*Anguilla australis*) since the collapse of submerged macrophytes in Lake Ellesmere, New Zealand. *Hydrobiologia*, 569, 161-173.
- Kitto, S. G. 2010. The environmental history of Te Waihora - Lake Ellesmere. MSc thesis, University of Canterbury, Christchurch. 270 p.
- Knuth, M. L. & Kelly, J. R. 2011. Denitrification rates in a Lake Superior coastal wetland. *Aquatic Ecosystem Health & Management*, 14, 414-421.
- Kreiling, R. M., Richardson, W. B., Cavanaugh, J. C. & Bartsch, L. A. 2011. Summer nitrate uptake and denitrification in an upper Mississippi River backwater lake: the role of rooted aquatic vegetation. *Biogeochemistry*, 104, 309-324.

- Kristensen, E. 2008. Mangrove crabs as ecosystem engineers; with emphasis on sediment processes. *Journal of Sea Research*, 59, 30-43.
- Larned, S. & Schallenberg, M. 2006. Constraints on phytoplankton production in Lake Ellesmere/Te Waihora NIWA.
- Laverman, A. M., Canavan, R. W., Slomp, C. P. & Cappellen, P. V. 2007. Potential nitrate removal in a coastal freshwater sediment (Haringvliet Lake, The Netherlands) & response to salinization. *Water Research*, 41, 3061-3068
- Livingstone, M. W., Smith, R. V. & Laughlin, R. J. 2000. A spatial study of denitrification potential of sediments in Belfast and Strangford Loughs and its significance. *Science of The Total Environment*, 251-252, 369-380.
- MacKenzie, E.M. 2016. The role of nutrients and light in the growth of phytoplankton in Te Waihora/Lake Ellesmere, New Zealand. Unpublished Masters of Resource Management thesis. University of Canterbury. Christchurch.
- Macreadie, P. I., Ross, D. J., Longmore, A. R. & Keough, M. J. 2006. Denitrification measurements of sediments using cores and chambers. *Marine Ecology Progress Series*, 326, 49-59.
- McClain, M. E., Boyer, E. W., Dent, C. L., Gergel, S. E., Grimm, N. B., Groffman, P. M., Hart, S. C., Harvey, J. W., Johnston, C. A., Mayorga, E., McDowell, W. H. & Pinay, G. 2003. Biogeochemical Hot Spots and Hot Moments at the Interface of Terrestrial and Aquatic Ecosystems. *Ecosystems*, 6, 301-312.
- McCrackin, M. L. & Elser, J. J. 2010. Atmospheric nitrogen deposition influences denitrification and nitrous oxide production in lakes. *Ecology*, 91, 528-539.
- Mengis, M., Gachter, R. & Wehrli, B. 1997. Nitrogen elimination in two deep eutrophic lakes. *Limnology and Oceanography*, 42, 1530-1543.
- Moore, S. C. 1997. A photographic guide to the freshwater invertebrates of New Zealand, Otago Regional Council.
- Nielsen, L. P., Christensen, P. B., Revsbech, N. P. & Sørensen, J. 1990. Denitrification and oxygen respiration in biofilms studied with a microsensor for nitrous oxide and oxygen. *Microbial Ecology*, 19, 63-72.

- Nielsen, L. P. & Glud, R. N. 1996. Denitrification in a coastal sediment measured in situ by the nitrogen isotope pairing technique applied to a benthic flux chamber. *Marine Ecology Progress Series*, 137, 181-186.
- Nielson, S. L., Banta, G. T. & Pedersen, M. F. 2004. *Estuarine nutrient cycling: The influence of primary producers*, Dordrecht, The Netherlands, Kluwer Academic Publishers.
- Nizzoli, D., Bartoli, M., Cooper, M., Welsh, D. T., Underwood, G. J. C. & Viaroli, P. 2007. Implications for oxygen, nutrient fluxes and denitrification rates during the early stage of sediment colonisation by the polychaete *Nereis* spp. in four estuaries. *Estuarine, Coastal and Shelf Science*, 75, 125-134.
- Nizzoli, D., Welsh, D., Longhi, D. & Viaroli, P. 2014. Influence of *Potamogeton pectinatus* and microphytobenthos on benthic metabolism, nutrient fluxes and denitrification in a freshwater littoral sediment in an agricultural landscape: N assimilation versus N removal. *Hydrobiologia*, 737, 183-200.
- Nogaro, G. & Burgin, A. J. 2014. Influence of bioturbation on denitrification and dissimilatory nitrate reduction to ammonium (DNRA) in freshwater sediments. *Biogeochemistry*, 120, 279-294.
- Norton, N., Allan, M., Hamilton, D., Horrell, G., Sutherland, D., Meredith, A. 2014. Technical report to support the water quality limit setting process in the Selwyn Waihora Catchment. Predicting the consequences of future scenarios: Te Waihora/Lake Ellesmere. Report R14/14. Environment Canterbury, Christchurch. 114 p.
- Olafsson, J. S. & Paterson, D. M. 2004. Alteration of biogenic structure and physical properties by tube-building chironomid larvae in cohesive sediments. *Aquatic Ecology*, 38, 219-229.
- Pattinson, S. N., García-Ruiz, R. & Whitton, B. A. 1998. Spatial and seasonal variation in denitrification in the Swale–Ouse system, a river continuum. *Science of The Total Environment*, 210–211, 289-305.
- Pelegri, S. P. & Blackburn, T. H. 1995. Effects of *Tubifex tubifex* (Oligochaeta: Tubificidae) on N-mineralization in freshwater sediments, measured with <sup>15</sup>N isotopes *Aquatic Microbial Ecology*, 9, 289-294.

- Pelegrí, S. P. & Blackburn, T. H. 1994. Bioturbation effects of the amphipod *Corophium volutator* on microbial nitrogen transformations in marine sediments. *Marine Biology*, 121, 253-258.
- Piña-Ochoa, E. & Álvarez-Cobelas, M. 2006. Denitrification in Aquatic Environments: A Cross-system Analysis. *Biogeochemistry*, 81, 111-130.
- Poulsen, M., Kofoed, M. V. W., Larsen, L. H., Schramm, A. & Stief, P. 2014. *Chironomus plumosus* larvae increase fluxes of denitrification products and diversity of nitrate-reducing bacteria in freshwater sediment. *Systematic and Applied Microbiology*, 37, 51-59.
- Psenner, R., Boström, B., Dinka, M., Pettersson, K., Pucsko, R. & Sager, M. 1988. Fractionation of phosphorus in suspended matter and sediment. *Arch Hydrobiol Beih Ergebn Limnol* 30, 83-112.
- Rasmussen, H. & Jorgensen, B. B. 1992. Microelectrode studies of seasonal oxygen uptake in a coastal sediment: role of molecular diffusion *Marine Ecology Progress Series*, 81, 289-303.
- Risgaard-Petersen, N., Skarup, S. & Nielsen, L. P. 1999. Denitrification in a soft bottom lake: evaluation of laboratory incubation. *Aquatic Microbial Ecology*, 17, 279-287.
- Santmire, J. A. & Leff, L. G. 2007. The effect of sediment grain size on bacterial communities in streams. *Journal of the North American Benthological Society*, 26, 601-610.
- Saunders, D. L. & Kalff, J. 2001. Denitrification rates in the sediments of Lake Memphremagog, Canada-USA. *Water Research*, 35, 1897-1904.
- Schallenberg, M. & Burns, C. W. 2001. Tests of autotrophic picoplankton as early indicators of nutrient enrichment in an ultra-oligotrophic lake. *Freshwater Biology*, 46, 27-37.
- Schallenberg, M. & Burns, C. W. 2004. Effects of sediment resuspension on phytoplankton production: teasing apart the influences of light, nutrients and algal entrainment. *Freshwater Biology*, 49, 143-159.

- Schallenberg, M., Larned, S. T., Hayward, S. & Arbuckle, C. 2010. Contrasting effects of managed opening regimes on water quality in two intermittently closed and open coastal lakes. *Estuarine, Coastal and Shelf Science*, 86, 587-597.
- Schallenberg M, Hamilton, D.P., Hicks, A.S., Robertson, H.A., Scarsbrook, M., Robertson, B., Wilson, K., Whaanga, D., Jones, H.F.E., & Hamill K. 2017. Multiple lines of evidence determine robust nutrient load limits required to safeguard a threatened lake/lagoon system. *New Zealand Journal of Marine and Freshwater Research*, DOI: 10.1080/00288330.2016.1267651
- Scheffer, M. 2004. Ecology of shallow lakes. Springer. 357 p.
- Scheffer, M., Hosper, S. H., Meijer, M.-L., Moss, B. & Jeppesen, E. 1993. Alternative equilibria in shallow lakes. *Trends in Ecology and Evolution*, 8, 275-293.
- Shang, J., Zhang, L., Shi, C. & Fan, C. 2013. Influence of Chironomid Larvae on oxygen and nitrogen fluxes across the sediment-water interface (Lake Taihu, China). *Journal of Environmental Sciences*, 25, 978-985.
- Smith, K. A., Ball, T., Conen, F., Dobbie, K. E., Massheder, J. & Rey, A. 2003. Exchange of greenhouse gases between soil and atmosphere: interactions of soil physical factors and biological processes. *European Journal of Soil Science*, 54, 779-791.
- Smith, R. L., xh, hlke, J. K., Repert, D. A. & Hart, C. P. 2009. Nitrification and Denitrification in a Midwestern Stream Containing High Nitrate: In Situ Assessment Using Tracers in Dome-Shaped Incubation Chambers. *Biogeochemistry*, 96, 189-208.
- Solomon, C. T., Hotchkiss, E. R., Moslemi, J. M., Ulseth, A. J., Stanley, E. H., Hall, R. O. & Flecker, A. S. 2009. Sediment size and nutrients regulate denitrification in a tropical stream. *Journal of the North American Benthological Society*, 28, 480-490.
- Sorrell, B., Hawes, I., Woods, R. & Coffey, W. 1998. Lake Ellesmere water quality investigations. Report prepared for Environment Canterbury by NIWA. Christchurch: Environment Canterbury.
- Steingruber, S. M., Friedrich, J., Gachter, R. & Wehrli, B. 2001. Measurement of Denitrification in Sediments with the <sup>15</sup>N Isotope Pairing Technique. *Applied and Environmental Microbiology*, 67, 3771-3778.

- Stephens, S. & Hawes, I. 2002. Suspended sediment concentrations in Lake Ellesmere: effect of wind on resuspension at different lake depths and implications for lake clarity. *In*: NIWA (ed.). Christchurch: Environment Canterbury.
- Stief, P. 2013. Stimulation of microbial nitrogen cycling in aquatic ecosystems by benthic macrofauna: mechanisms and environmental implications. *Biogeosciences*, 10, 7829–7846.
- Stief, P., Poulsen, M., Nielsen, L. P., Brix, H. & Schramm, A. 2009. Nitrous oxide emissions by aquatic macrofauna. *PNAS*, 106, 4296-4300.
- Svensson, J. M. 1997. Influence of *Chironomus plumosus* larvae on ammonium flux and denitrification (measured by the acetylene-blockage and the isotope pairing-technique) in eutrophic lake sediment. *Hydrobiologia*, 346, 157–168.
- Svensson, J. M., Enrich-Prast, A. & Leonardson, L. 2001. Nitrification and denitrification in a eutrophic lake sediment bioturbated by oligochaetes. *Aquatic Microbial Ecology*, 23, 177–186.
- SW ZIP (2013). Selwyn Waihora ZIP Addendum. Christchurch City Council and Environment Canterbury Report R13/92. Christchurch.
- Teixeira, C., Magalhães, C., Boaventura, R. A. R. & Bordalo, A. A. 2010. Potential rates and environmental controls of denitrification and nitrous oxide production in a temperate urbanized estuary. *Marine Environmental Research*, 70, 336-342.
- Tomaszek, J. A. & Czerwieniec, E. 2000. *In situ* chamber denitrification measurements in reservoir sediments: an example from southeast Poland. *Ecological Engineering*, 16, 61-71.
- Tomaszek, J. A., Gardner, W. S. & Johengen, T. H. 1997. Denitrification in sediments of a Lake Erie Coastal Wetland (Old Woman Creek, Huron, Ohio, USA). *Journal of Great Lakes Research*, 23, 401-415.
- Unisense. 2014. *Oxygen sensor user manual* [Online]. Available: <http://www.unisense.com/files/PDF/Manualer/Oxygen%20Sensor%20Manual.pdf>.
- Vance-Harris, C. & Ingall, E. 2005. Denitrification pathways and rates in the sandy sediments of the Georgia continental shelf, USA. *Geochemical Transactions*, 6, 12.

- Veraart, A. J., de Klein, J. J. M. & Scheffer, M. 2011. Warming Can Boost Denitrification Disproportionately Due to Altered Oxygen Dynamics. *PLoS ONE*, 6, e18508.
- Wang, C., Shan, B., Zhang, H. & Rong, N. 2014. Analyzing sediment dissolved oxygen based on microprofile modeling. *Environmental Science and Pollution Research*, 21, 10320-10328.
- Wilks, T. 2010. Response of benthic invertebrate fauna to fluctuating lake levels and salinity concentrations in Lake Ellesmere/Te Waihora. Unpublished thesis (MSc), University of Canterbury.
- Winterbourn, M. J., Gregson, K. L. D. & Dolphin, C. H. 2006. *A guide to the aquatic insects of New Zealand*, Bulletin of the Entomological Society of New Zealand.
- Wood, H. 2008. An investigation into the benthic invertebrate communities of Te Waihora. MSc thesis. University of Canterbury. Christchurch.
- Xu, K., Zhang, L. & Zou, W. 2009. Microelectrode Study of Oxygen Uptake and Organic Matter Decomposition in The Sediments of Xiamen Western Bay. *Estuaries and Coasts*, 32, 425-435.
- Zhang, L., Wang, S. & Wu, Z. 2014. Coupling effect of pH and dissolved oxygen in water column on nitrogen release at water-sediment interface of Erhai Lake, China. *Estuarine, Coastal and Shelf Science* 149, 178-186.
- Zhong, J., Fan, C., Liu, G., Zhang, L., Shang, J. & Gu, X. 2010. Seasonal variation of potential denitrification rates of surface sediment from Meiliang Bay, Taihu Lake, China. *Journal of Environmental Sciences*, 22, 961-967.



## 7 APPENDIX A: SPATIAL SEDIMENT SURVEY

---

### SITE GPS LOCATIONS

---

**Table 7.1** GPS locations of the 18 sediment coring sites around Lake Ellesmere.

Locations are in NZGD 2000.

Site No.	NZGD 2000	
	Latitude	Longitude
E1	-43.725895	172.416428
E2	-43.748827	172.449359
E3	-43.728116	172.466425
E4	-43.761805	172.415959
E5	-43.761955	172.465757
E6	-43.762262	172.515553
E7	-43.762412	172.602356
E8	-43.787333	172.627041
E9	-43.798591	172.602120
E10	-43.789411	172.552485
E11	-43.789261	172.515214
E12	-43.798044	172.465440
E13	-43.797625	172.415741
E14	-43.794051	172.368931
E15	-43.833454	172.365663
E16	-43.847326	172.384423
E17	-43.833715	172.415395
E18	-43.816209	172.502446

### SITE SEDIMENT CHARACTERISTICS

---

#### 2013 survey sediment characteristics

**Table 7.2.** Sediment characteristics of the 18 sampled sites in Lake Ellesmere in 2013.

					0-2.0 µm	2-63 µm	63-2000 µm
Site	Redox (mV)	Depth (m)	Porosity (kg m <sup>-2</sup> )	Organic matter (kg m <sup>-2</sup> )	Clay %	Silt %	Sand %
E1	-2	0.85	6.85	1.21	9.6	51.97	38.44
E2	-151	1.5	7.78	1.32	13.3	83.76	2.94
E3	-307	0.48	5.62	0.79	2.88	14.94	82.18
E4	30	1.5	7.55	1.2	11.81	85.24	2.95
E5	-345	1.6	7.75	1.47	11.62	84.99	3.39
E6	93	0.58	4.67	0.56	0.88	2.48	96.64
E7	-124	0.75	6.03	1.49	4.86	23.61	71.53
E8	-83	0.58	5.24	1.82	13.65	63.09	23.27
E9	-80	1.1	6.68	1.04	9.32	78.53	12.16
E10	-240	2.1	7.65	1.5	15.9	78.33	5.77
E11	-247	2.1	8.06	1.53	17.97	76.08	5.95
E12	-63	1.2	7.38	1.43	11.48	88.07	0.45
E13	-41	1.5	7.06	1.19	8.82	71.54	19.64
E14	0	0.8	6.79	0.95	7.48	39.55	52.97
E15	-10	0.75	6.63	1.17	8.31	57.81	33.88
E16	154	0.8	5.95	0.98	7.58	39.12	53.3
E17	63	0.65	6.19	1.35	8.1	57.73	34.18
E18	-55	0.92	6.62	1.38	6.2	77.8	16.01

## 2014 survey sediment characteristics

Table 7.3. Sediment characteristics of the 18 sampled sites in Lake Ellesmere in 2014.

					0-2.0 $\mu\text{m}$	2-63 $\mu\text{m}$	63-2000 $\mu\text{m}$
Site	Redox (mV)	Depth (m)	Porosity ( $\text{kg m}^{-2}$ )	Organic matter ( $\text{kg m}^{-2}$ )	Clay %	Silt %	Sand %
E1	-380	0.88	6.75	1.28	5.85	48.69	45.46
E2	-40	1.04	4.91	0.72	2.42	13.22	84.36
E3	-400	0.62	5.65	0.97	2.67	17.71	79.62
E4	-315	1.92	7.62	1.29	9.24	88.56	2.2
E5	-310	1.93	8.11	1.37	10.11	87.14	2.75
E6	-20	0.87	5.04	0.53	0.54	1.78	97.68
E7	-185	0.53	5.92	1.31	2.64	15.47	81.89
E8	-368	1.52	6.98	1.37	7.12	67.36	25.52
E9	-325	1.4	7.47	1.29	7.22	84.74	8.05
E10	-355	2.37	8.77	1.43	12.99	83.86	3.15
E11	-332	2.27	8.55	1.45	11.52	84.15	4.34
E12	-333	1.69	7.88	1.33	8.62	86.69	4.69
E13	-315	1.8	7.64	1.41	9.29	76.04	14.67
E14	-360	1.2	6.86	1.22	5.7	42.11	52.18
E15	-100	1.13	8.54		7.94	69.2	22.87
E16	-160	1.34	6.01	1.24	5.69	44.77	49.54
E17	-275	1.03	6.54	1.26	5.84	56.79	37.37
E18	-325	1.33	6.71	1.03	5.98	77.2	16.82

## Invertebrate locations

**Table 7.4.** Presence/absence of invertebrate species recorded in sediment cores at 18 sites in Lake Ellesmere in 2014. A cross indicates presence.

Site Number	<i>Chironomid</i>	<i>Potamopyrgus antipodarum</i>	Sphaeriidae	<i>Potamopyrgus estuarinus</i>	<i>Austridotea annectens</i>	<i>Paracorophium excavatum</i>	<i>Cyclomactra ovata</i>	<i>Tenagomysis chiltoni</i>	Oligochaeta	Spionidae	Neridae
E1	x	x				x		x	x		x
E2		x		x	x	x		x	x		x
E3		x				x		x	x		x
E4		x				x		x	x		
E5		x				x					
E6		x				x		x	x		x
E7		x				x		x	x		x
E8		x				x			x		x
E9		x				x		x	x		x
E10		x						x	x		
E11		x				x		x	x		
E12		x				x					
E13		x				x			x		
E14		x				x			x		x
E15		x		x		x			x	x	x
E16		x	x			x	x		x	x	
E17		x		x		x			x	x	x
E18		x		x		x			x		x

## SITE PHYSICO-CHEMICAL CONDITIONS

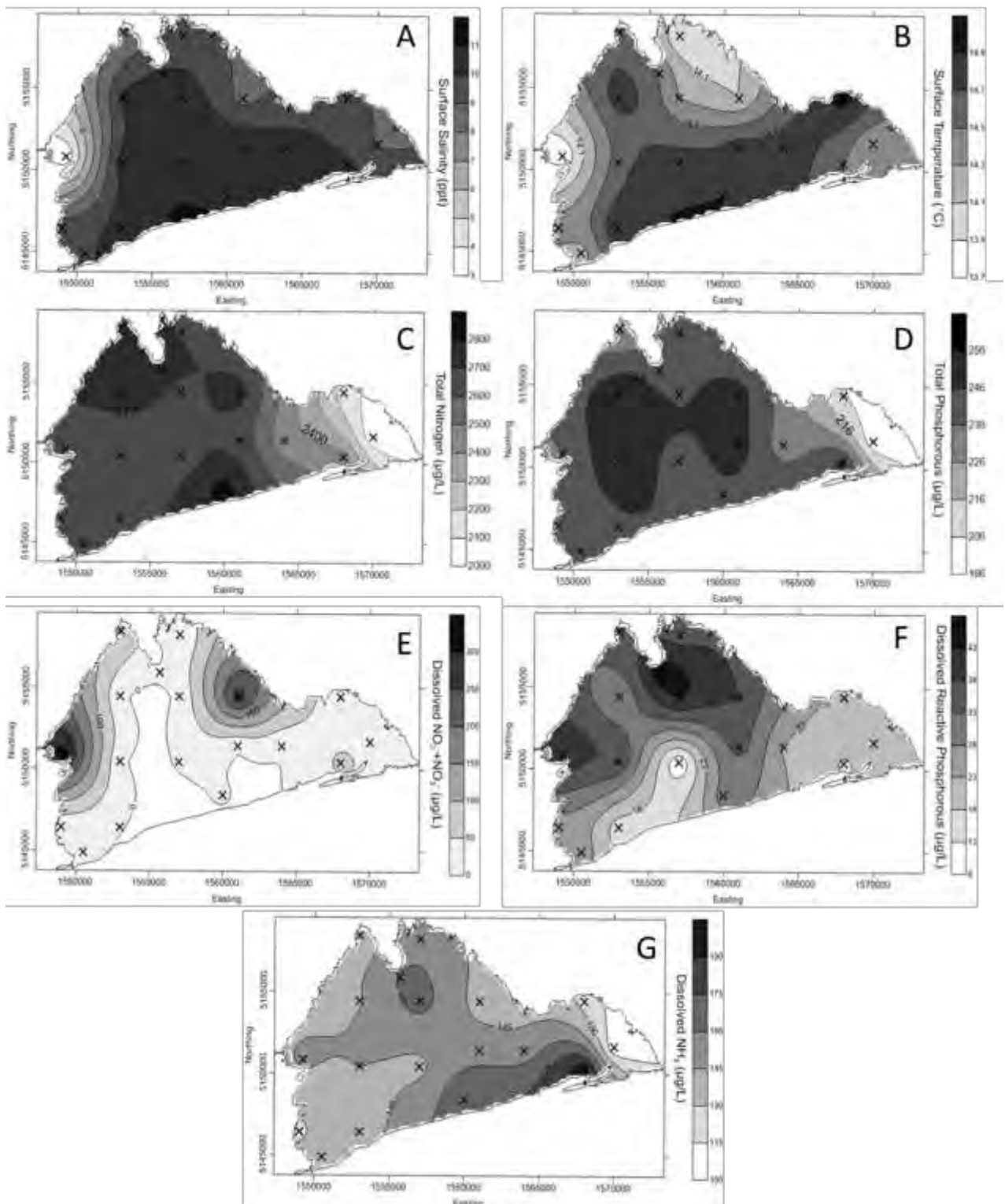


**Figure 7.1.** Spatial patterns of surface salinity (A), surface temperature (B), total nitrogen (C), total phosphorus (D), dissolved  $\text{NO}_2^- + \text{NO}_3^-$  (E), dissolved reactive phosphorus (F), and  $\text{NH}_3$  (G), across the 18 sites in Lake Ellesmere in April 2014.

# 8 APPENDIX B: OXYGEN DYNAMICS

## OXYGEN PROFILES SUMMER 2015

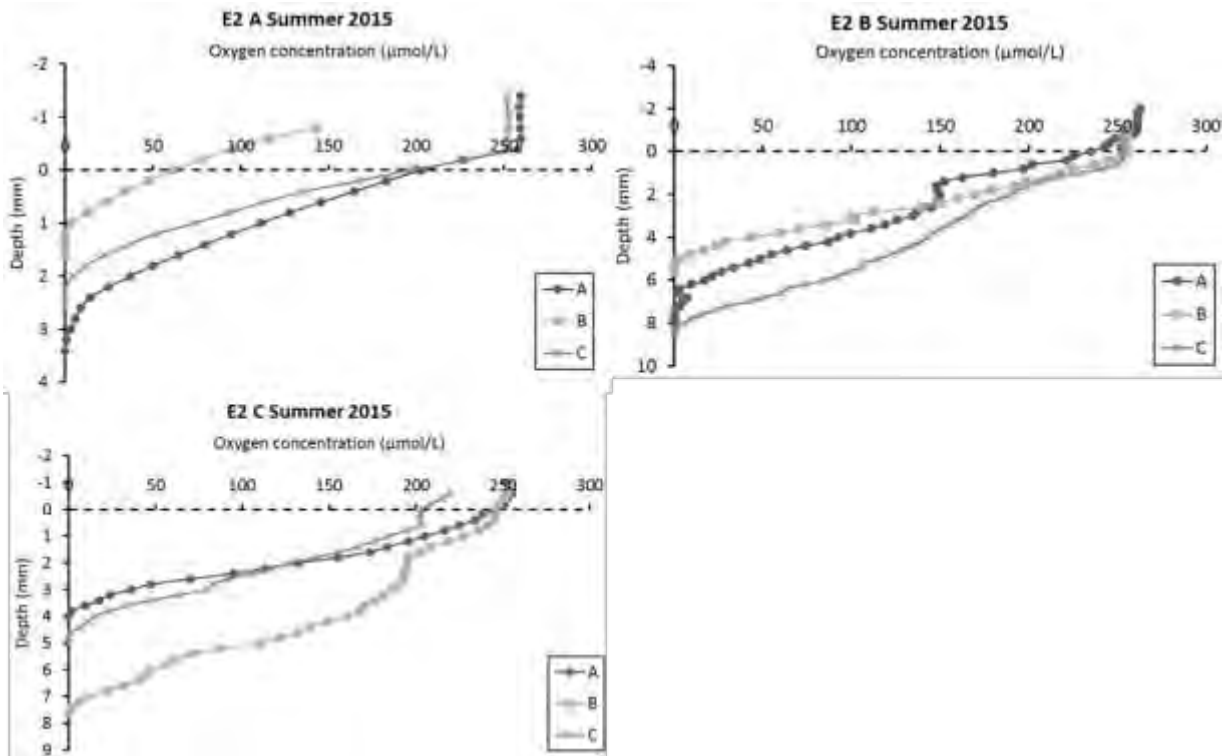


Figure 8.2. Sediment oxygen micro-profiles measured at site E2 in summer 2015.

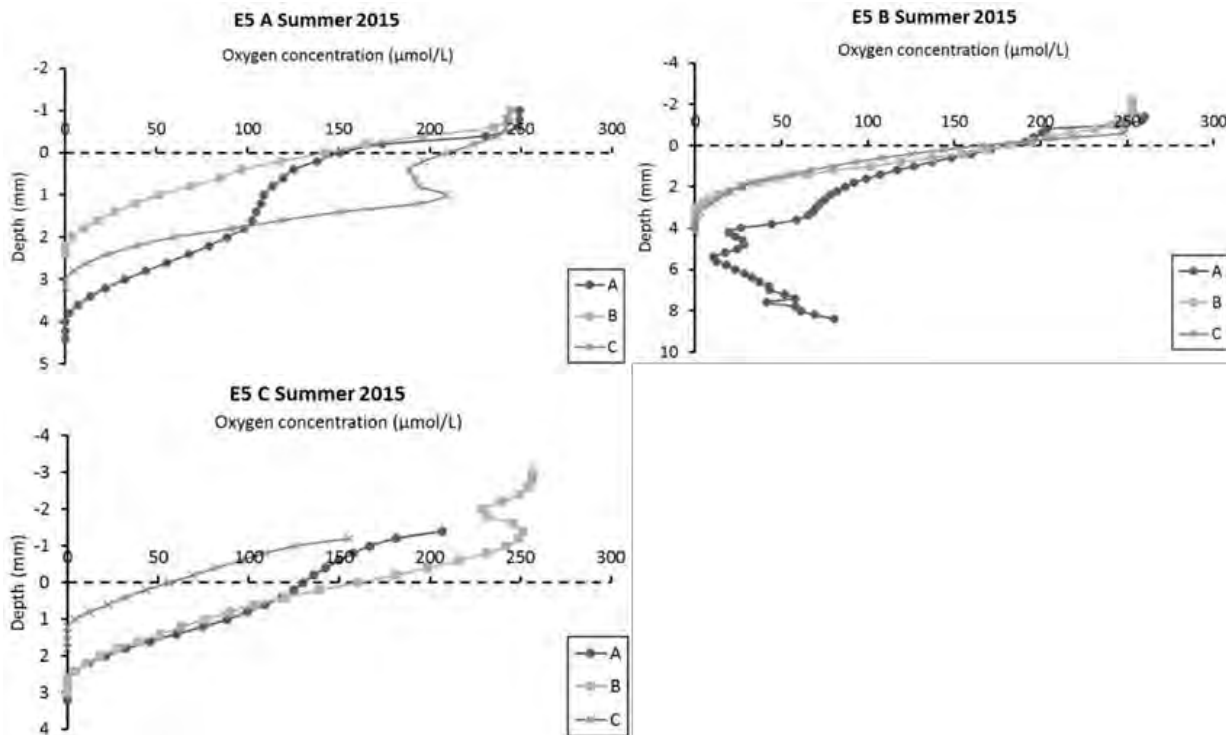
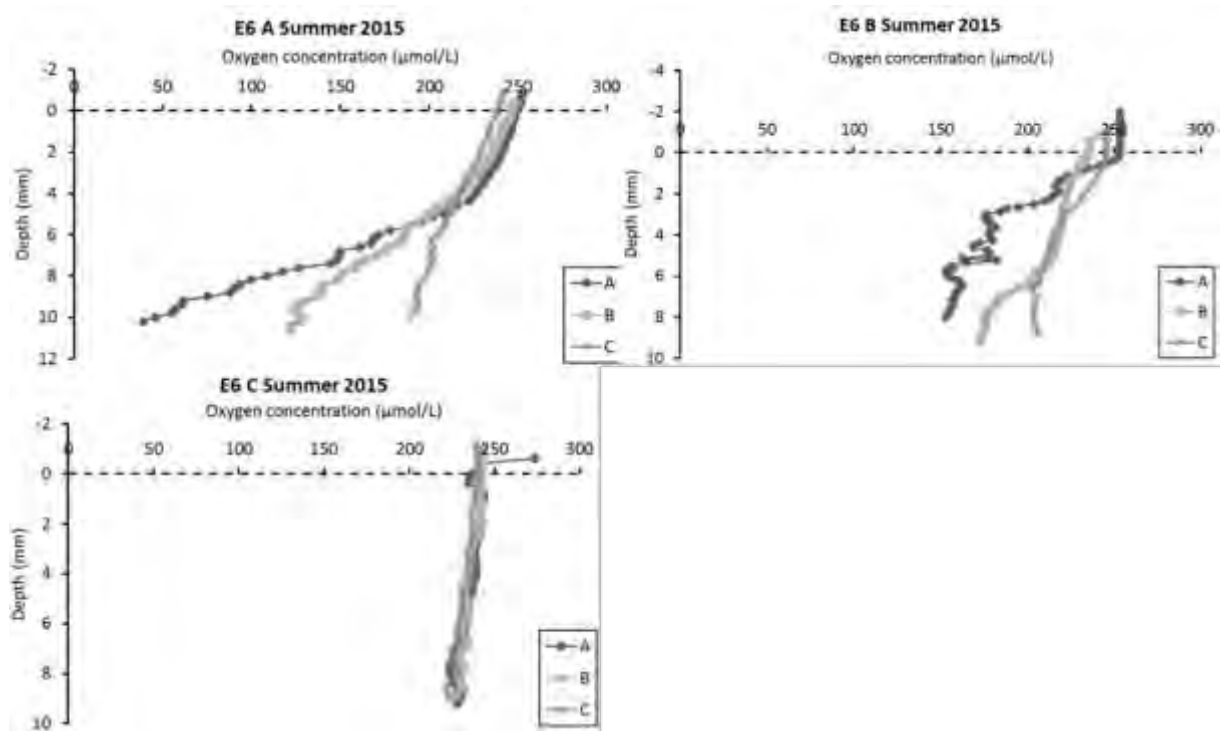


Figure 8.1. Sediment oxygen microprofiles measured at site E5 in summer 2015



**Figure 8.3.** Sediment oxygen micro-profiles measured at site E6 in summer 2015.

## OXYGEN PROFILES WINTER 2015

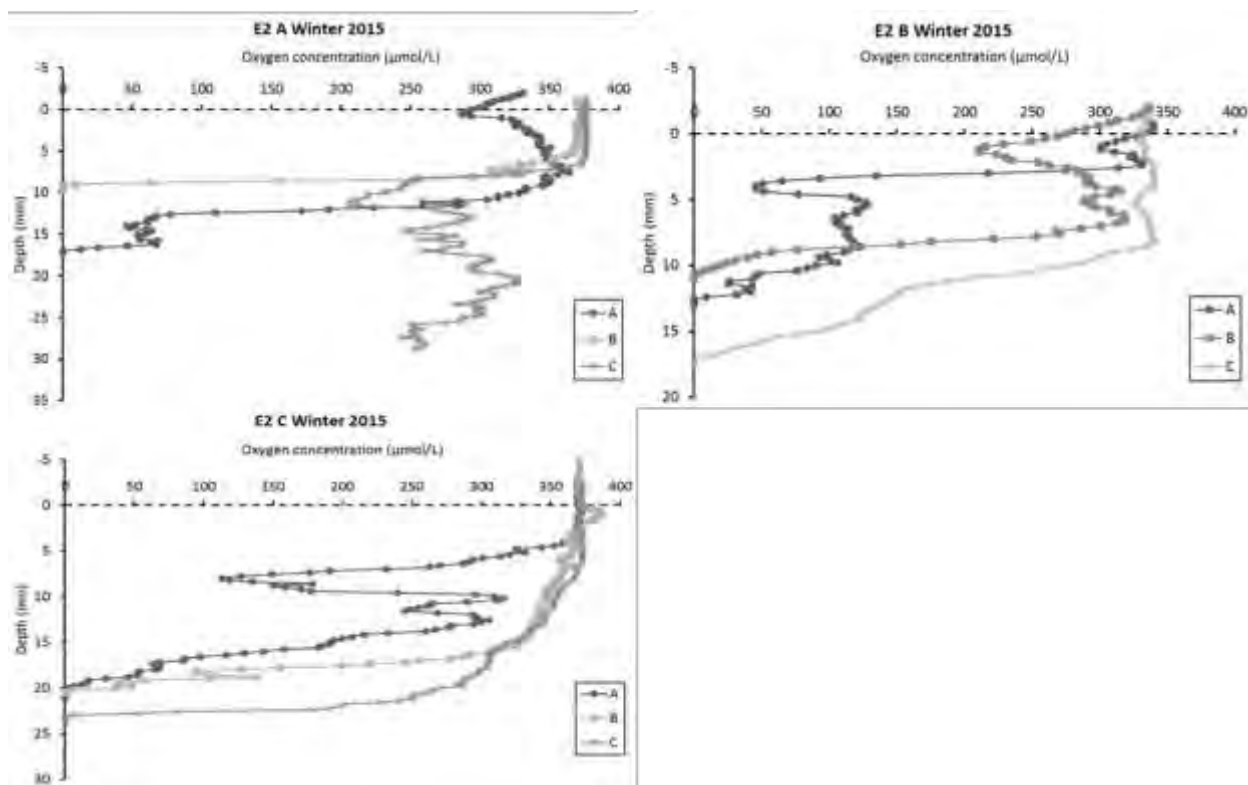


Figure 8.5. Sediment oxygen micro-profiles measured at site E2 in winter 2015.

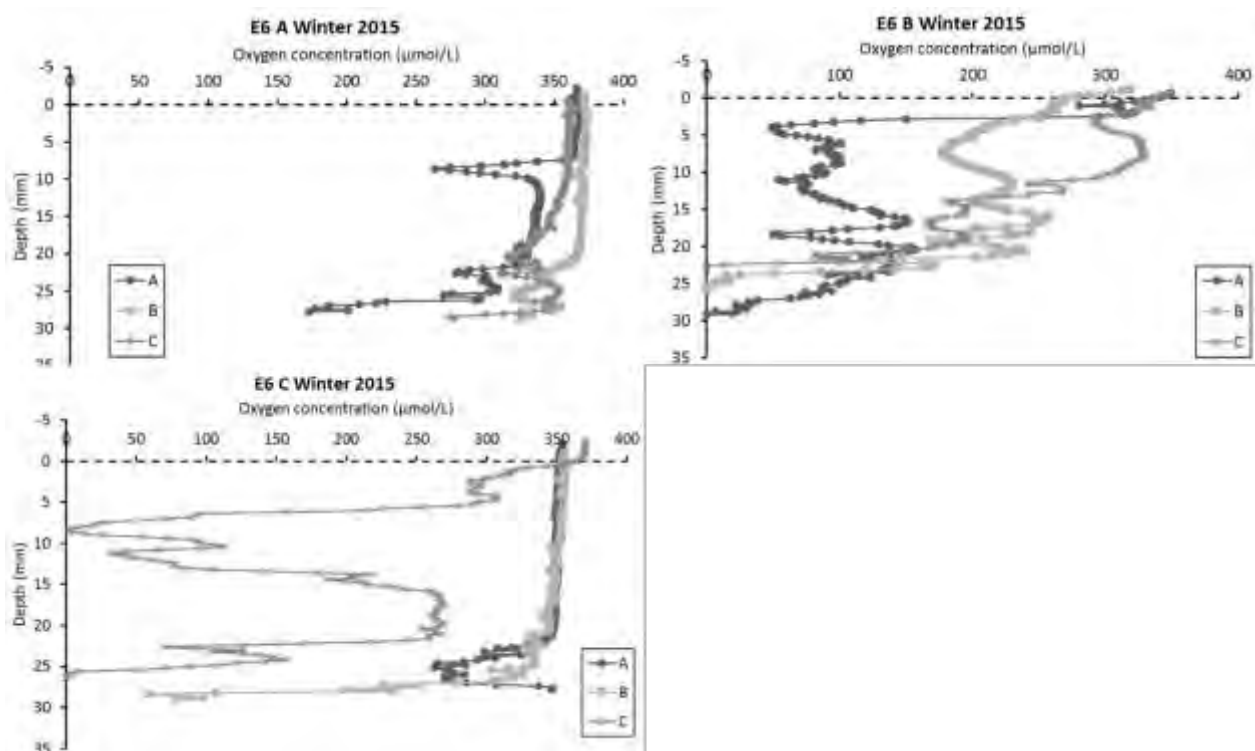
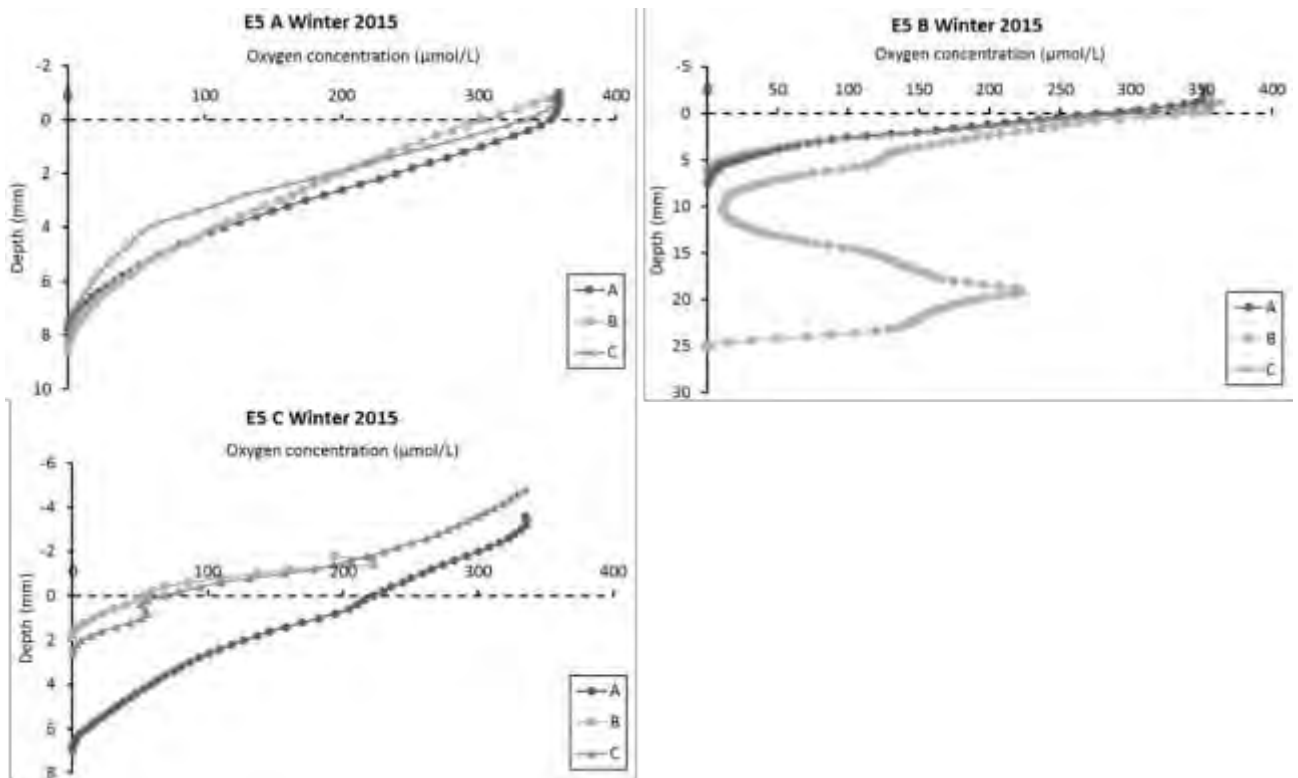


Figure 8.4. Sediment oxygen micro-profiles measured at site E6 in winter 2015.





**Figure 8.6.** Sediment oxygen micro-profiles measured at site E5 in winter 2015.

## OXYGEN PROFILES SUMMER 2016

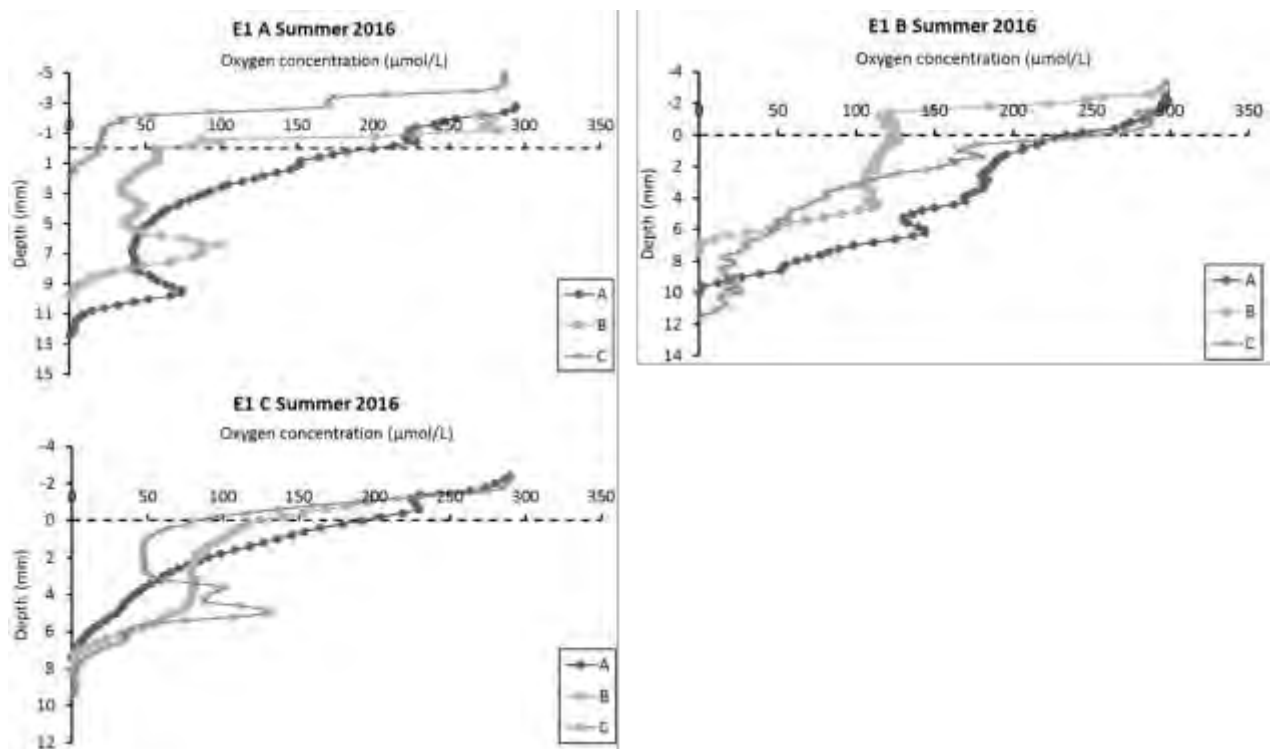


Figure 8.7. Sediment oxygen micro-profiles measured at site E1 in summer 2016.

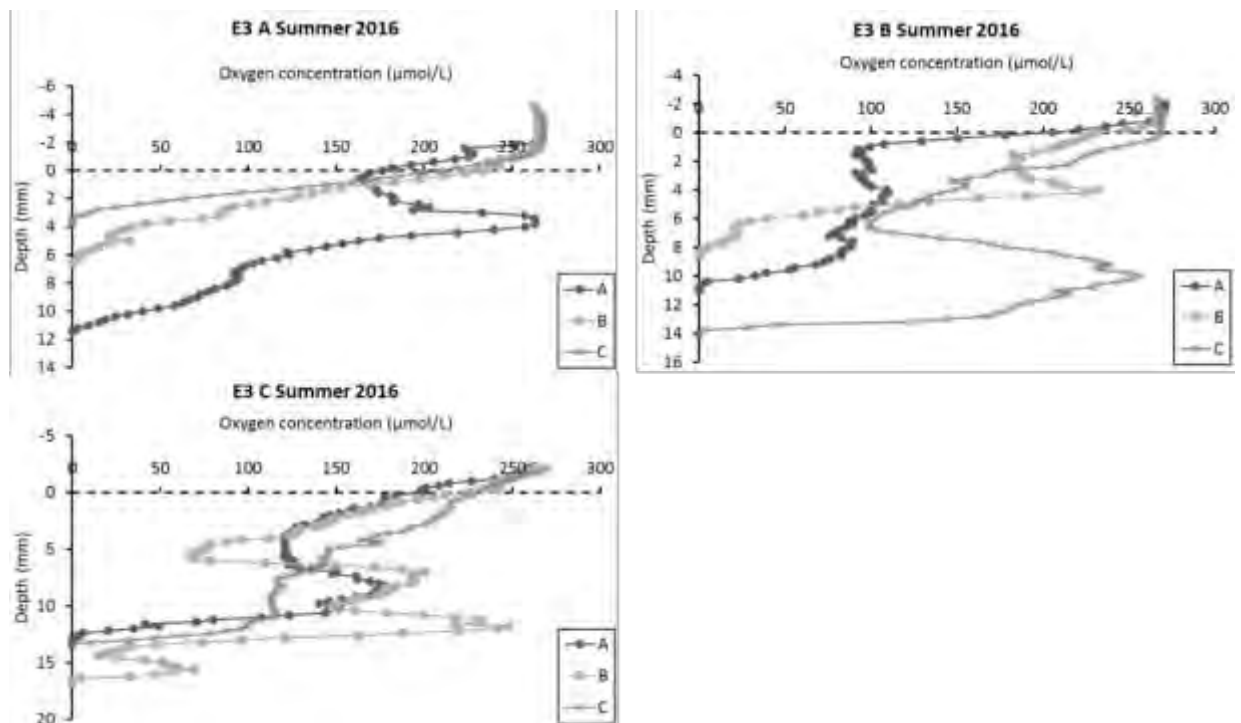


Figure 8.8. Sediment oxygen micro-profiles measured at site E3 in summer 2016.

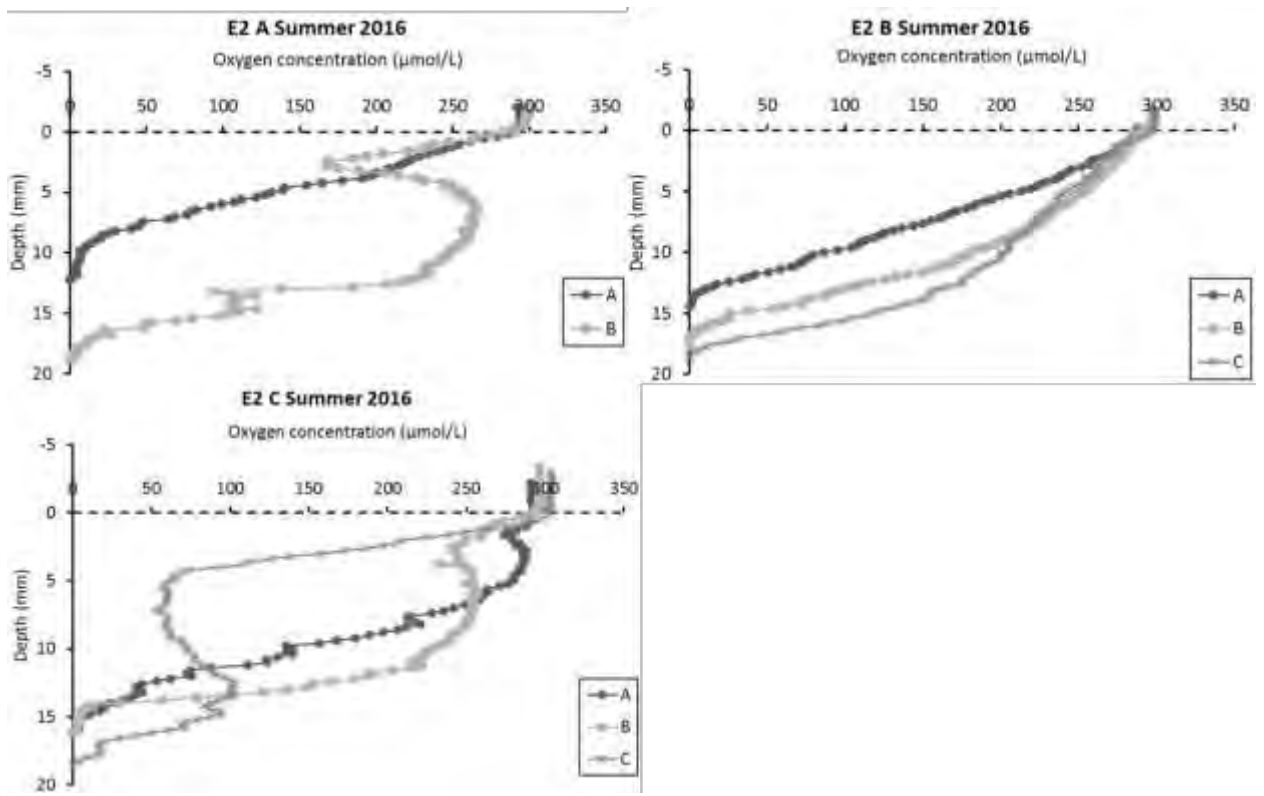


Figure 8.9. Sediment oxygen micro-profiles measured at site E2 in summer 2016.

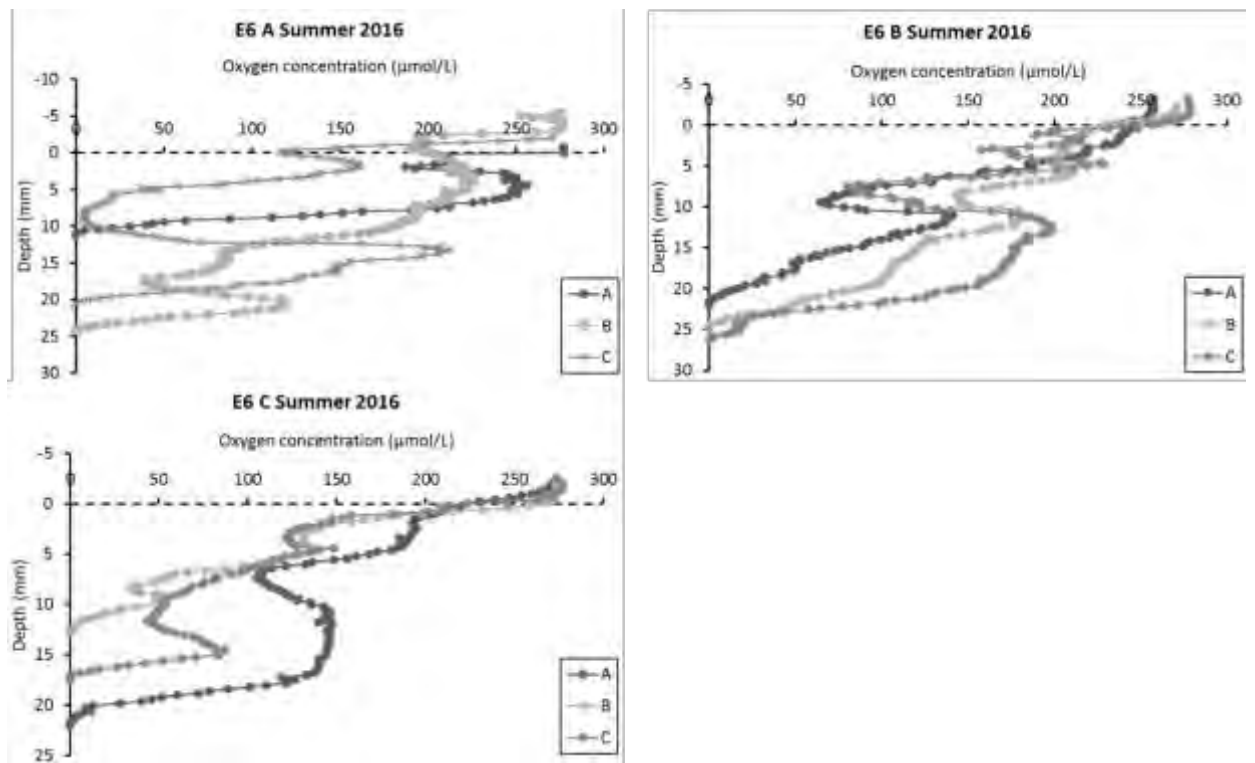
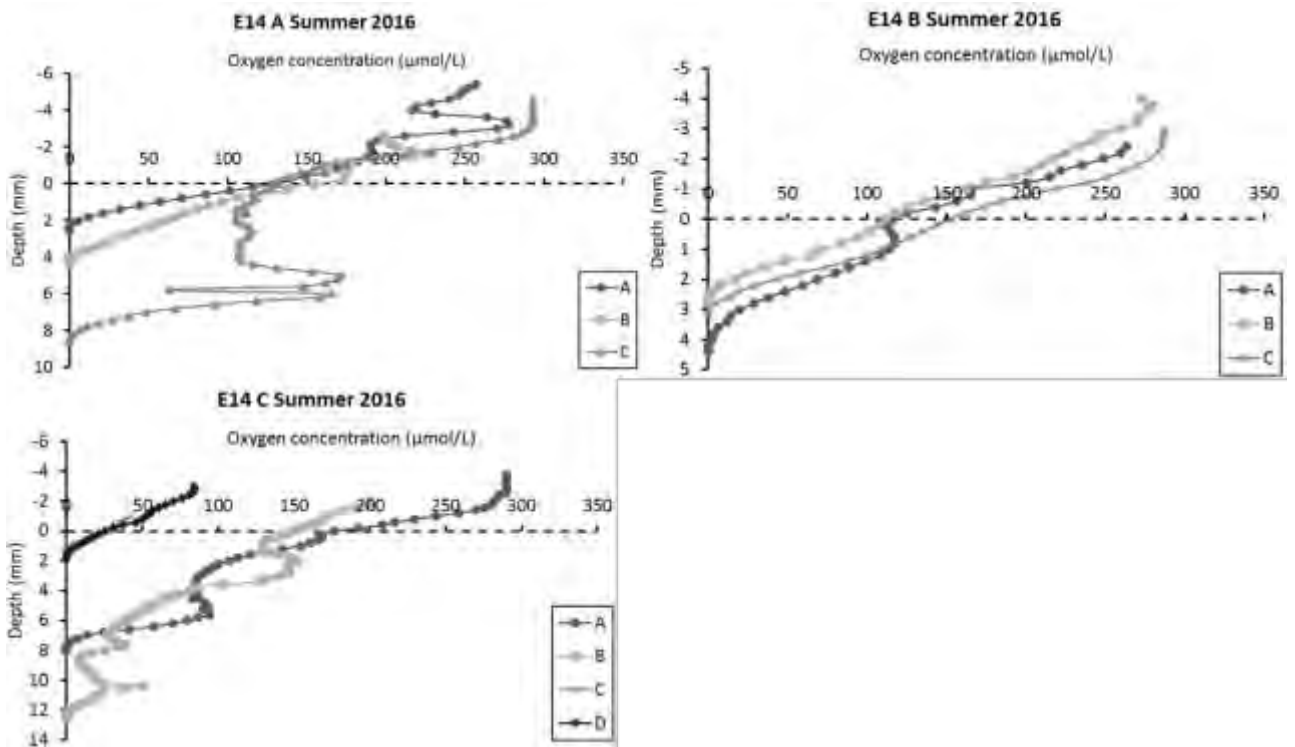
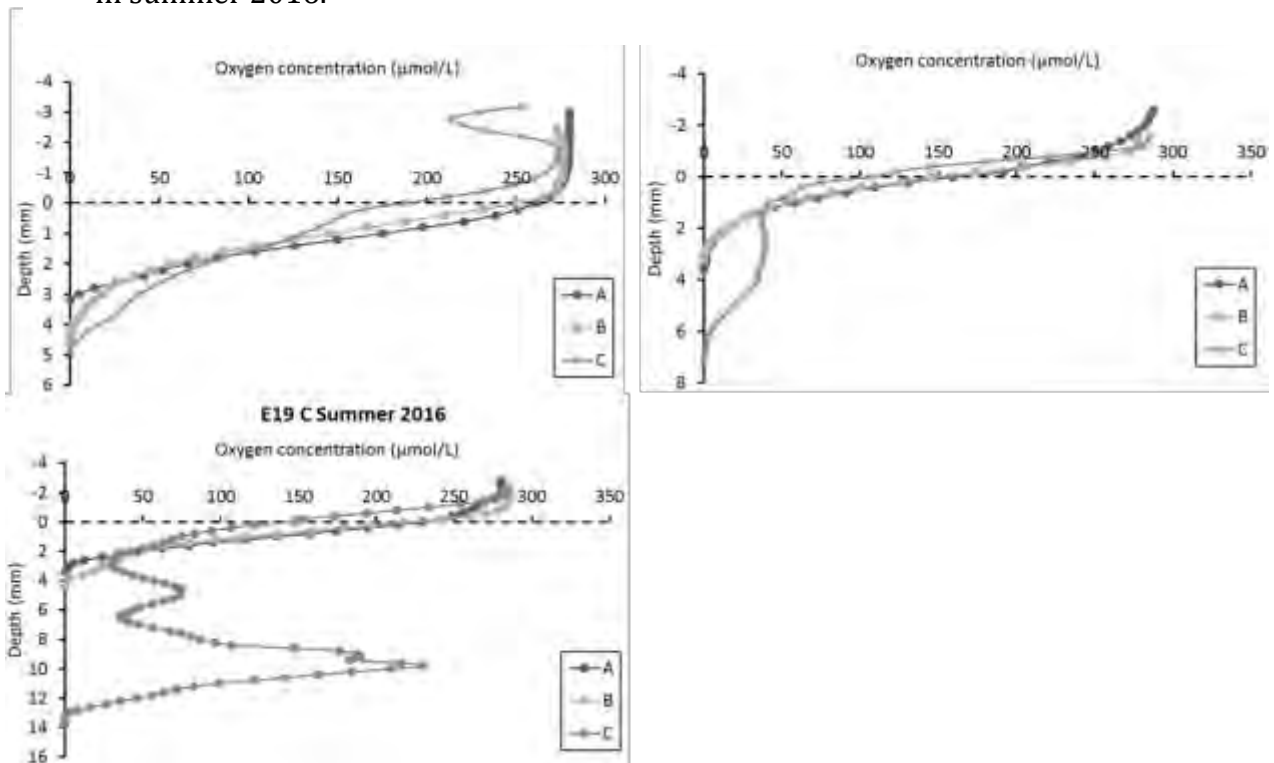


Figure 8.10. Sediment oxygen micro-profiles measured at site E6 in summer 2016.



**Figure 8.12.** Sediment oxygen micro-profiles measured at site E19 (Hart's Creek estuary) in summer 2016.



**Figure 8.11.** Sediment oxygen micro-profiles measured at site E14 in summer 2016.

## 9 APPENDIX C: DENITRIFICATION

### LONG-TERM NITRATE PULSE ANALYSIS

The water column concentration of nitrate in Lake Ellesmere is recorded at two sites as part of Environment Canterbury’s monitoring regime, one taken from a mid-lake monitoring station, and one from the mouth of the Selwyn River. Figure 10.1 shows the frequency of different concentration nitrate pulses, using the data from 1993 to 2013. Nitrate is most often ranges from detection levels (<0.005) to 0.1 mg L<sup>-1</sup>. However, there appears to be occasional “pulses” of larger concentrations. Nitrate concentration data plotted over time shows the pulse nature of nutrients in Lake Ellesmere (Fig. 10.2). We have defined a pulse as a nitrate reading above 0.3 mg L<sup>-1</sup>. Pulses occur almost annually, with the exception of a few intermittent years between 1993 and 2013. The pulses generally begin during late Autumn, with high readings continuing throughout winter and into

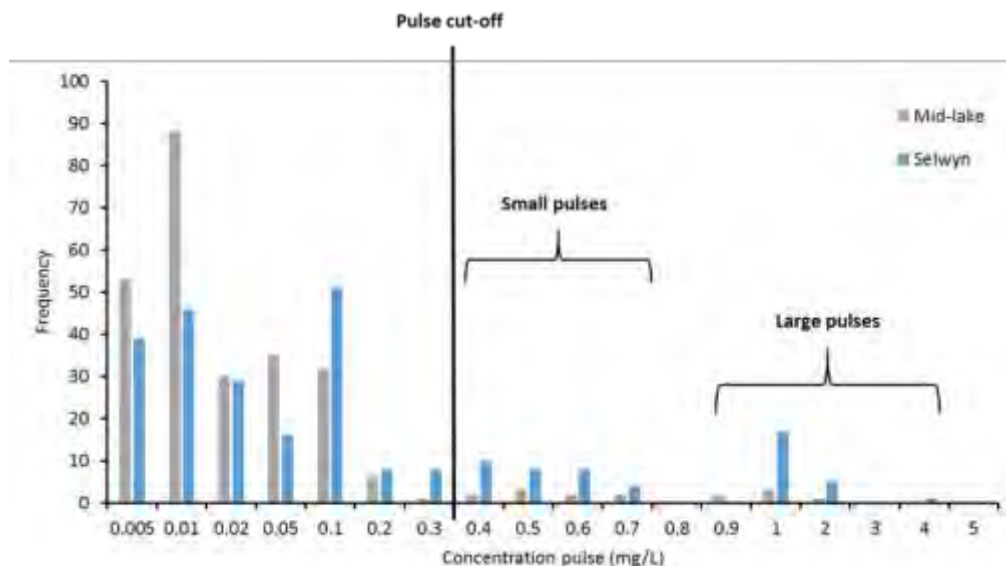


**Figure 9.1.** Frequency of nitrate concentration pulses (mg L<sup>-1</sup>) from measurements taken between 1993 and 2013. Data is split into measurements taken at the two sites, mid-lake and at the mouth of the Selwyn River.

Spring, and decreasing below the threshold in Summer. Table 10.1 compares the frequency and season of the pulse occurrences between the two sites.

**Table 9.1.** Frequency of nitrate concentration pulses ( $\text{mg L}^{-1}$ ) from measurements taken between 1993 to 2013, showing the seasons they occurred in. Data is split into measurements taken at the two sites, mid-lake and at the mouth of the Selwyn River.

Concentration pulse	Selwyn		Mid-lake	
	Occurrences	Season	Occurrences	Season
0.005	39	All	53	All
0.01	46	All	88	All
0.02	29	All	30	All
0.05	16	All	35	All
0.1	51	All	32	All
0.2	8	All	6	Winter/Spring/Summer
0.3	8	Autumn/Winter/Spring	1	Winter
0.4	10	Autumn/Winter/Spring	2	Winter/Spring
0.5	8	Spring/Winter	3	Winter
0.6	8	Autumn/Winter/Summer	2	Winter
0.7	4	Winter/Spring	2	Winter/Spring
0.8	0	-	0	-
0.9	0	-	2	Spring
1	17	Winter/Spring	3	Winter/Spring
2	5	Winter/Spring	1	Spring
3	0	-	0	-
4	1	Spring	0	-
5	0	-	0	-

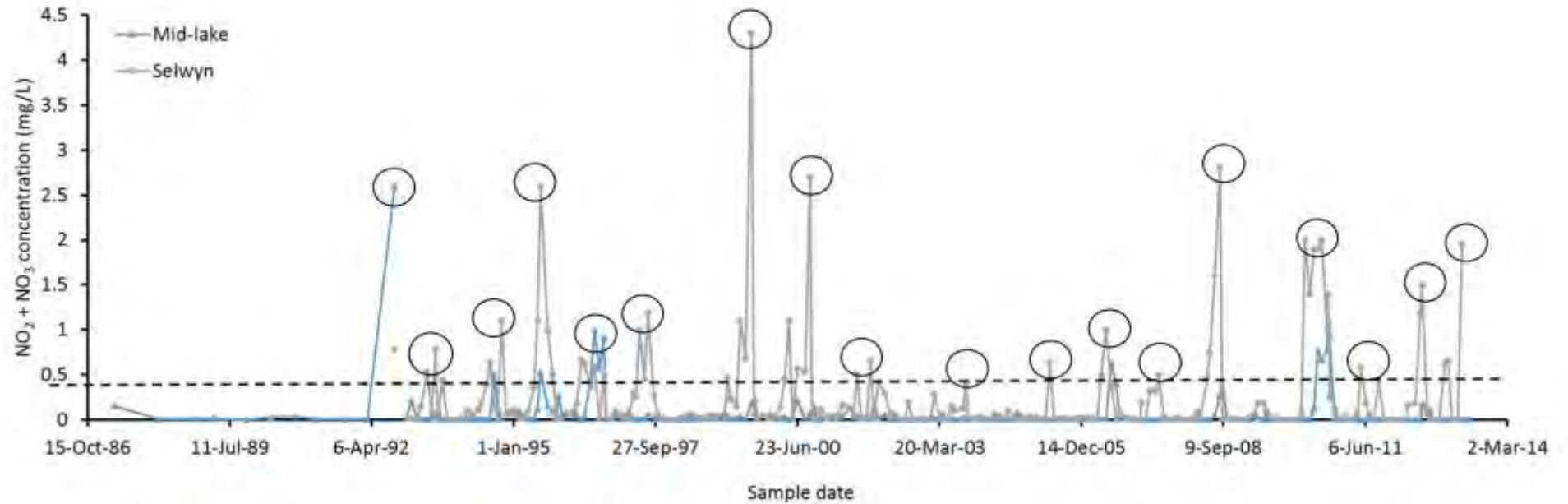


**Figure 9.2.** Long-term nitrate concentration data ( $\text{mg L}^{-1}$ ) taken at the ECAN mid-lake site and at the Selwyn River mouth. Black dotted line indicates  $0.3 \text{ mg L}^{-1}$  marking the spike definition. Black circles show the maximum peak within the seasonal sustained high concentrations

## METHODS

---

### Denitrification enzyme assay methods

For full method details, please refer to (Bruesewitz *et al.* 2011). Briefly, 15 mL of sediment was homogenized with 15 mL of unfiltered lake water. Four treatments were set up in order to look at possible nutrient limitations of denitrification in the sediment. These included sediment only, and the additions of 10 mg of potassium nitrate (+N), 12 mg of glucose (+C) and a combination of both. Lake water only was used as a control. 30 mL of the sediment-water mixtures were transferred to 45 mL glass bottles, with gas-tight silicon septa at the top. Anoxic conditions were created by purging the bottle headspace with pure N<sub>2</sub>. Ten mL of acetylene (C<sub>2</sub>H<sub>2</sub>) were added to block the conversion of N<sub>2</sub>O to N<sub>2</sub>, and to maintain over-pressurised conditions in the bottle. Incubation was performed at 22°C. Eight mL of gas sample was collected hourly for 4 hours after the addition of C<sub>2</sub>H<sub>2</sub>. To maintain a constant pressure in the bottle, C<sub>2</sub>H<sub>2</sub> was added to replace the collected gas samples. N<sub>2</sub>O samples were analysed using a Varian CP 3800 gas chromatogram equipped with a Hayesep D column and an ECD detector. N<sub>2</sub>O production was calculated using the following equations:

N<sub>2</sub>O production was calculated using the ideal gas law:

$$PV = nRT$$

Where P = pressure of the gas, V = volume of the gas, n = moles of the gas, R = universal gas constant (6.022 x 10<sup>23</sup>), and T = temperature of the gas (K).

This was then converted to an areal basis (m<sup>-2</sup>) using the sediments bulk density.

### *In situ* core methods

#### *Core structures*

Nutrient fluxes and nitrate conversion rates were measured in custom built *in situ* enclosures which included both sediment and overlying water (henceforth called “enclosures”), which promoted the transfer of in-lake turbulence to the enclosures - potentially a key driver of nitrate supply to the sediment microbial community (Risgaard-Petersen *et al.* 1999). The sets of 4 enclosures were anchored in the lake



bed by four poles. The enclosure inner diameter was 6.4 cm and they penetrated to a sediment depth of 15 cm. The flexible enclosure height was adjusted for the depth of the water column across sites. The tops of the enclosures were sealed below the surface of the lake to exclude air. The enclosures were spiked with  $K^{15}NO_3^-$ , to a final concentration of 1.0 mg/L. A final enrichment of 30 to 50 atom % of  $^{15}N$  in the  $NO_3^-$  pool was achieved by additionally spiking the enclosures with unlabelled  $NaNO_3^-$  to a concentration of 1.0 mg/L.

The incubation was run for 48 hours, with 50 mL samples taken at 0, 4, 24, 30 and 48 hours for dissolved nutrients and labelled  $N_2$  pairs. After gas removal, the samples were then filtered through Microscience MS GF 47 mm filters (nominal pore size = 0.7  $\mu m$ ), into 50 mL acid-washed falcon tubes and frozen at  $-18^\circ C$  until analysis of dissolved nutrients ( $NO_2^-+NO_3^{2-}$ , DRP,  $NH_3^+$ ). The dissolved oxygen concentration of the samples was also measured a calibrated YSI ProODO Optical Dissolved Oxygen meter (Yellow Springs, Ohio, USA). At the end of the experiment the sediment enclosures were retrieved and sieved through a 500  $\mu m$  mesh, into a bucket collecting the sediment. All infauna retained were preserved in 99% ethanol until identification was carried out.

At each site ambient physicochemical measurements were taken with an YSI Professional Plus Multiprobe (Yellow Springs, Ohio, USA) (temperature, salinity, dissolved oxygen, conductivity and pH), and water clarity with a Secchi disk. A water sample was also collected to measure the ambient total nitrogen and phosphorus concentrations.

### *Water Sampling*

To sample the enclosures, a 50 mL screw-end plastic syringe with a 3-way luer valve, is attached to the lids 2-way luer valve, and the valves are opened, and two volumes of the syringe are slowly drawn and re-expelled into the enclosure to mix the water column before drawing a final 40 ml sample. The stopcock is closed, and the syringe held upright for bubbles to collect at the top, then 5 mL of water is expelled (to have a final, bubble free sample of 35 mL). The syringe is then stored under site water at *in situ* temperature until gas removal back at the lab (within 5 hours).

### *Core retrieval*

At the end point of the experiment, a final water sample was taken, then the lids were removed, and each core was bunged *in situ* using a long pole with the bung attached. Once all four cores in a structure are bunged, the whole structure is pulled up using a rope attached in the middle of the structure. Once the cores are just below the water's surface, the bottoms of the cores were capped to contain the sediment. The cores were removed from the structure, labelled and stored for later collection of infauna and sediment characteristics (within 12 hours). Each core was sieved through a 500 µm mesh, into a bucket collecting the sediment. All infauna retained was preserved in 99% ethanol until identification to the lowest possible group.

The sediment in the bucket was well mixed, then 200 mL of sediment was then collected for analysis of particle size, organic matter and porosity. Sediment samples were frozen until analysis.

### *Exetainer evacuation*

Special gas vials called exetainers were used for storage of the gases before measurement. These consist of a 12 mL glass vial, with a rubber septum (Labco, High Wycombe, UK). Exetainers needed to be evacuated under a month prior to sample collection, to eliminate N<sub>2</sub> contamination. A custom-built vacuum manifold was used, which consisted of 20 ports with stopcocks. The exetainers were fitted to the vacuum line using BD PrecisionGlide needles, and left on the vacuum line for 12 hours to ensure that a sufficient vacuum level is achieved (10<sup>-6</sup> Torr). The exetainers were kept submerged in milli-Q water freshly sparged with helium gas while the needles were being removed from the septa, to ensure that air does not enter the punctured septum. This was achieved using 50 mL centrifuge tubes. Exetainers are stored this way to decrease the potential of air contamination, by taking advantage of the slower gas diffusion rates in water than in air.

### *N<sub>2</sub> extraction*

<sup>28</sup>N<sub>2</sub>, <sup>29</sup>N<sub>2</sub> and <sup>30</sup>N<sub>2</sub> were extracted from the water in the syringes, by introducing a 15 ml helium headspace into the syringe. A constant stream of helium (He) is supplied to a line, with an open end with constant He overflow into a water filled beaker (to visually assess flow, and prevent air being sucked into the line once the

syringe valve was opened), and another open-ended tubing with a female luer hose valve connector fitted into the hose to allow connection with a male luer valve. The water filled syringe was attached to the He tubing, and the 3-way valve turned to allow purging of the valve for 10 seconds, before turning to open the water filled syringe to the helium. 15 mL of helium was introduced to the valve, before closing the valve off to the helium and disconnecting.

Each syringe was then shaken vigorously for three minutes, after which more than 98% of the N<sub>2</sub> will be in the headspace (Hamilton and Ostrom 2007). After equilibrium, at least 85% of the headspace (~13 ml) was transferred into an evacuated 12 ml exetainer with a chlorobutyl rubber septum, taking the following precautions to minimize contamination with air. A needle extender was used, that consisted of 15 cm of a 21 G 1 ½ (0.80 x 38 mm) needle with its point filed off that is inserted tightly into a 9 cm long polyetheyne tube (1.27 mm external diameter, 0.86 mm internal diameter). The tubing was connected to a Chemfluor miniature fluid flow fitting that is fitted to a 26 G ½ (0.45 x 13 mm) needle. This flexible needle extender allows the gas headspace in the syringe to be injected downwards into an exetainer, which will sit within a water filled falcon tube holding the syringe upright. The septum of the exetainer were kept submerged in distilled water freshly sparged with helium to avoid atmospheric N<sub>2</sub> contamination. The point where the needle punctures the exetainer septum was maintained underwater, thereby avoiding introduction of air. Before inserting the needle into the exetainer septum, water in the needle extender and a few milliliters of headspace gas from the syringe was expelled into the water beside the exetainer. Next, the needle was quickly moved over and into the septum, while avoiding contact with overlying air. The remainder of the headspace (~ 13 mL) was then injected into the exetainer, and the needle quickly withdrawn. The exetainers were stored at room temperature in water filled falcon tubes until gas analysis. The water left inside the syringe was filtered through a Microscience MS GF 47mm filters into a 50 mL acid washed falcon tube, and frozen until analysis of dissolved nutrients.

### *Gas analysis*

The isotopic composition of N<sub>2</sub> in the headspace is then determined by mass spectrometry. The exetainers are placed in an auto sampler in line with a gas chromatograph and a mass spectrometer. The 2015 summer samples were processed at Lincoln University, and the winter 2015 and summer 2015 samples analysed at Isotrace, University of Otago.

### *Nitrate conversion calculations*

The <sup>29</sup>N and <sup>30</sup>N ratios provided were converted to molar volumes using computed concentrations of nitrogen expected in the water at time of sampling, given the temperature and salinity of the sampled water, using tables by Colt (2012).

The production of each ratio (<sup>29/28</sup>N<sub>2</sub> and <sup>30/28</sup>N<sub>2</sub>) at each time point was calculated as the sample ratio minus the ratio at time 0. This was used rather than the air standard due to seasonal variation in the ambient ratios in gases dissolved in the lake water.

The molar amounts of <sup>29</sup>N<sub>2</sub> and <sup>30</sup>N<sub>2</sub> were then calculated using the following equation:

$$AM_{xx} (\mu\text{mol}) = (R_{xx} * {}^{28}\text{N}_2) * \text{Sample Volume}$$

Where:

$AM_{xx}$  = the amount of <sup>xx</sup>N<sub>2</sub> present in the core structure ( $\mu\text{mol}$ )

$R_{xx}$  = the ratio of 29:28 N provided by mass spectrometry

${}^{28}\text{N}_2$  = the concentration of <sup>28</sup>N<sub>2</sub> ( $\mu\text{mol L}^{-1}$ ) expected in the water calculated from nitrogen diffusion tables (Colt 2012)

Sample Volume = the volume of water the gas was extracted from (0.035L)

The production of N<sub>2</sub> was then measured as:

$$p({}^{xx}\text{N}_2) (\mu\text{mol m}^{-2} \text{h}^{-1}) = \frac{\alpha_{xx}}{A} \times V$$

Where:

$P({}^{xx}\text{N}_2)$  ( $\mu\text{mol m}^{-2} \text{h}^{-1}$ ) = the production rate of <sup>xx</sup>N<sub>2</sub>

$\alpha_{xx}$  = slope of the regression line of the amount of <sup>xx</sup>N<sub>2</sub> ( $\mu\text{mol N L}$ ) versus time (h)

A = area of the sediment surface in core structure (m<sup>2</sup>)

V = the water volume of the core structure (L)

Nitrate conversion rates were then calculated from the production rates of <sup>15</sup>N isotopes (Nielsen 1992):

$$D_{15} = p(^{29}\text{N}_2) + 2p(^{30}\text{N}_2)$$

$$D_{14} = D_{15} \frac{p(^{29}\text{N}_2)}{2p(^{30}\text{N}_2)}$$

Where:

D<sub>15</sub> = rate of nitrate conversion of <sup>15</sup>NO<sub>3</sub><sup>-</sup> (μmol N m<sup>-2</sup> h<sup>-1</sup>)

D<sub>14</sub> = rate of nitrate conversion of <sup>14</sup>NO<sub>3</sub><sup>-</sup> (μmol N m<sup>-2</sup> h<sup>-1</sup>)

The total rate of nitrate conversion is then:

$$D_{\text{Tot}} = D_{15} + D_{14}$$

Where:

D<sub>Tot</sub> = total rate of nitrate conversion in core (μmol N m<sup>-2</sup> h<sup>-1</sup>)

Because nitrate conversion occurs in the sediment, all units were expressed on an areal basis, which also accounted for differences in enclosure volumes at the different sites.

## IN SITU NITRATE CONVERSION EXPERIMENT – SUPPLEMENTAL DATA

---

**Table 9.2.** Ambient dissolved nutrient concentrations ( $\text{NO}_3^-$ ,  $\text{NH}_4^+$ , DRP) at the time of the three *in situ* denitrification experiments (summer 2015, winter 2015 and summer 2016).

Site	$\text{NO}_3^-$ ( $\mu\text{mol L}^{-1}$ )			$\text{NH}_4^+$ ( $\mu\text{mol L}^{-1}$ )			DRP ( $\mu\text{mol L}^{-1}$ )		
	S 15	W 15	S 16	S 15	W 15	S 16	S 15	W 15	S 16
1	-	-	2.56	-	-	2.29	-	-	0.28
2	6.16	9.61	0.64	0.54	1.00	2.05	3.92	2.16	0.29
3	-	-	1.07	-	-	3.11	-	-	0.54
5	5.21	0.60	-	0.45	2.25	-	3.45	2.93	-
6	3.20	0.94	0.61	0.53	2.22	2.79	3.95	3.29	0.29
14	-	-	1.22	-	-	2.61	-	-	0.47
19	-	-	16.37	-	-	2.47	-	-	0.97
Average	4.86	3.72	3.75	0.51	1.82	2.55	3.77	2.79	0.47

**Table 9.3.** Pearson correlation matrix showing the relationships between the denitrification rates recorded in summer 2016, and sedimentary characteristics and invertebrate species. \* =  $p < 0.05$ , \*\* =  $p < 0.01$ , \*\*\* =  $p < 0.001$ .

	D15	Redox	OM	Porosity	Clay	Silt	Sand	<i>P.ant</i>	<i>P.exc</i>	<i>Olig</i>	<i>Chiro</i>	<i>Neridae</i>
D15												
Redox	0.28											
OM	0.58*	0.11										
Porosity	0.35	-0.16	0.83***									
Clay	0.25	-0.23	0.82***	0.90***								
Silt	0.41	-0.21	0.87***	0.97***	0.86***							
Sand	-0.4	0.22	-0.87***	-0.97***	-0.87***	-1.00***						
<i>P.ant</i>	-0.14	-0.28	0.21	0.44	0.60*	0.3	-0.32					
<i>P.exc</i>	-0.25	-0.14	-0.32	-0.03	0.11	-0.21	0.2	0.69**				
<i>Olig</i>	0.01	0.33	-0.38	-0.29	-0.44	-0.33	0.34	-0.41	-0.07			
<i>Chiro</i>	0.4	-0.11	0.84***	0.87***	0.95***	0.84***	-0.85***	0.56*	0.13	-0.35		
<i>Neridae</i>	-0.16	0.38	-0.43	-0.35	-0.44	-0.47	0.47	-0.05	0.35	0.07	-0.51*	
<i>Mysid</i>	0.19	0.26	0.66**	0.68**	0.45	0.69**	-0.68**	-0.09	-0.39	0.06	0.47	-0.21